Preparation of nanotubes and nanofibers from silicon carbide precursor polymers by using polymer blend and spinning techniques

Zormy Correa

Gunma University

Graduate School of Engineering

Department of Nano-Material Systems

Japan

2007

Abstract

Many potential applications have been proposed for silicon carbide (SiC) nanostructures, including high-strength composites, nanosensors and nanodevices. Limitations in processing are an important barrier that has to be overcome in order to develop these applications.

The aim of this study is to explore the possibility of fabricating SiC nanotubes and to improve the elaboration process of SiC nanofibers prepared by using polymer blend and spinning techniques.

In the general introduction, the structure of SiC and the recent uses of polycarbosilane (PCS) as a SiC precursor for nanofibers are discussed. A review of the synthesizing methods for SiC nanotubes and nanofibers and their possible applications are presented.

The present work proposes the use of polymer blend technique in order to prepare the SiC nanotubes and nanofibers. Due to the versatility of the polymer blend industrially, it could be used to mass-production of nanostructures. The polymer blend technique presented is based on the use of a precursor polymer with a ceramic residue and a thermally decomposable polymer without carbon residue after heating.

Chapter 1 presents an attempt to prepare nanotubes from core/shell particles by using polymer blend and wet-spinning techniques. Polystyrene (PS) was used as a core decomposable polymer and polydimethylsilylvinylacetylene (PDMSVA) as the shell silicon carbide precursor polymer. The core/shell particles were prepared by emulsion polymerization. They were subjected to wet-spinning, stretched mechanically

six times their original length, stabilized by UV and also in air, and finally heat-treated in an inert atmosphere. Nanotubes were prepared although the silicon carbide precursor polymer (PDMSVA) was insufficiently stabilized.

Preparation of nanotubes from poly(methyl methacrylate) / polycarbosilane (PMMA/PCS) and poly(methyl methacrylate) / polyacrylonitrile / polycarbosilane (PMMA/PAN/PCS) core/shell particles by the aforementioned techniques is presented in Chapter 2. The core/shell particles were prepared by the spray drying method. They were subjected to wet-spinning, stretched, stabilized and heat-treated. Few nanotubes were obtained from the PMMA/PAN/PCS heat-treated sample because the stretching technique was not efficient in order to elongate all the core/shell particles.

Recently, SiC fibers have found many applications in composites at higher temperatures in oxidizing environments. One of the most important factors related to the chemical composition of these fibers is the oxygen content because it decreases the mechanical properties of the fibers used for such applications.

In this study, how to improve the preparation process in order to obtain SiC nanofibers with low oxygen content was sought.

Chapter 3 refers to preparation and study of the oxidation behavior of nanofibers derived from polycarbosilane by using polymer blend and melt-spinning techniques. Polycarbosilane (PCS) and novolac-type phenol-formaldehyde resin (PF) were dissolved in tetrahydrofuran (THF) and after removal of THF, the polymer blend was melt-spun. The polymer blend fibers were soaked in an acid solution in order to

cure the phenolic matrix. The stabilized polymer blend fibers were heated at 1000 ^{o}C under a nitrogen atmosphere and kept in nitric acid solution to remove the matrix carbon. The oxidation behavior was characterized. A part of the nanofibers was further heated at 1500 ^{o}C. Nanofibers of several 100 nm in diameter were prepared. A large amount of oxygen was introduced into the nanofibers during the oxidation process. After heating at 1500 ^{o}C, the nanofibers changed from an amorphous phase to β-SiC.

In Chapter 4, the microstructural changes of nanofibers were examined. The preparation procedure was the same as that of Chapter 3, but the nanofibers were heated to two different temperatures, 1000 ^{o}C and 1200 ^{o}C. The nanofibers heated at 1200 ^{o}C were straight, longer and had a smoother surface compared with the nanofibers heated at 1000 ^{o}C. The nanofibers heated at 1200 ^{o}C had higher resistance to oxidation by nitric acid treatment than the nanofibers heated at 1000 ^{o}C, revealing the importance of the heat treatment temperature.

Finally, the general conclusions are presented.

General Introduction

Background

The Si-C bond

The silicon-carbon bond is thermodynamically nearly as strong as a single C-C bond. The value for dissociation energy of the silicon-carbon bond has been reported as 318 kJ/mol and for the C-C bond as 345.6 kJ/mol [1]. Silicon carbide, the simplest silicon-carbon compound, is especially stable. The most well-known allotolopic form of SiC is β-SiC. This compound has a diamond structure, that is, each Si atom is surrounded by four C atoms, and each carbon atom is surrounded by four Si atoms [2].

SiC is commonly referred to as ‘carborundum’. This term is a commemorative word used by Edward G. Acheson in 1892 to describe a crystal that he synthesized. He aimed to make a diamond-like crystal from carbon and alundum and succeeded to make SiC by using a primitive electric furnace designed by himself. However, Acheson is not the first person to prepare SiC. Just a small quantity of SiC had been made already by Despretz in 1849; Marsden in 1880; and Colson in 1882.

SiC has a closed-packed crystal structure. It is divided into cubic form (ABCABC…) and hexagonal form (ABAB…) depending on the stacking order. It is known that SiC has numerous polytypes. Using the notation developed by Ramsdell in 1947, the most common SiC polytypes are 3C (cubic or β phase), 4H, 6H, 15R and 27R [3]. The 3C and 4H polytypes are shown in Figure 1.

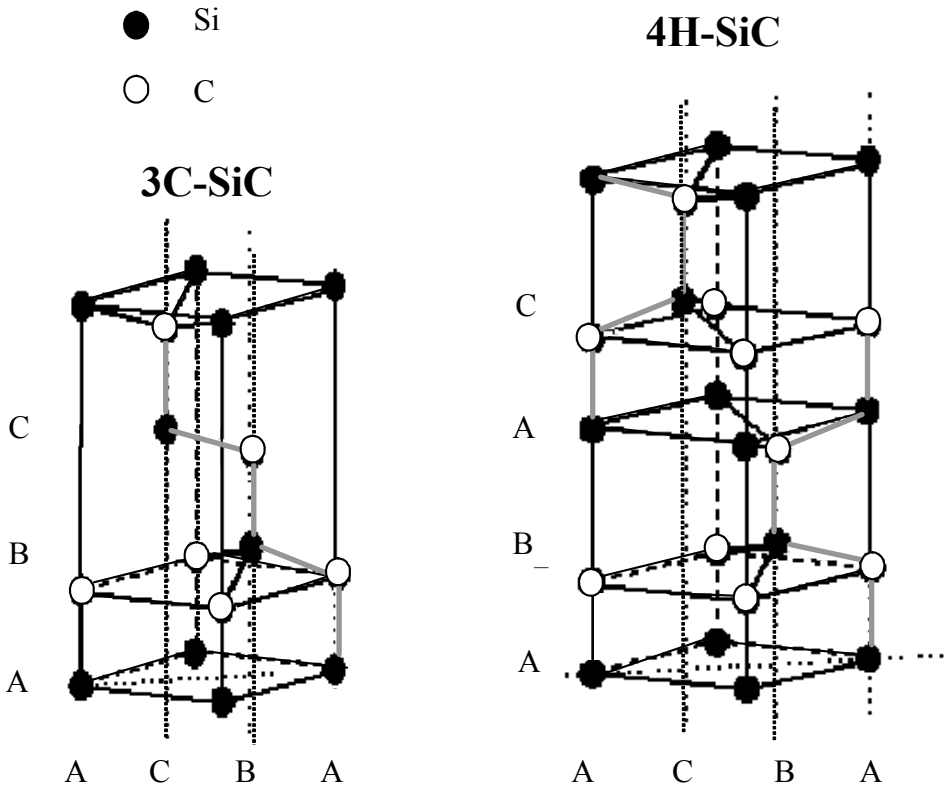

Fig.1. 3C and 4H polytypes for SiC.

There are now many non-oxide ceramics and they are used industrially in many application fields. Among them, SiC is the most important material because it has many attractive properties as follows: high strength and high Young's modulus, high chemical stability and so on. However, it was quite difficult to prepare fine products. SiC products were prepared by using sintering of SiC powder prior to an invention of unique preparation method using polymer precursor by S. Yajima [4]. The polymer precursor used by Yajima was polycarbosilane. The molecular structure is shown in Figure 2.

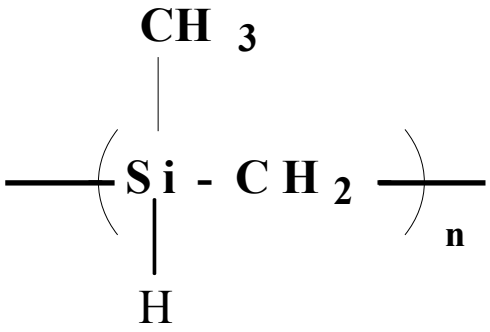

Fig.2. Molecular structure of polycarbosilane.

Polycarbosilanes as SiC Precursors

A major motivation to synthesize and to investigate polycarbosilane (PCS) is that PCS can be used to prepared fine SiC products, particularly in the form of continuous fibers. The following requirements are asked for a ceramic precursor used practically:

(1) low cost

(2) ability to be fabricated under the required shape

(3) a high residual yield after heat treatment

(4) easiness to control chemical composition of the resulting material

(5) easiness to control microstructure of the resulting material

In the preparation process by using polymer as a precursor, the polymer has to be stabilized (changed into a fusible state) after shaping. The stabilization is proceeded by formation of cross-linkages [5]. Therefore, a precursor polymer must be stabilized easily. Polycarbosilane satisfies these requirements considerably.

Synthesis of SiC nanotubes

A nanotube can be defined as a tube (hollow structure) with nanoscale dimensions of nanometers (1nm = 10^{-9} m). Since the discovery of carbon nanotubes (CNT) by Iijima *et al*. [6] there has been a great interest in developing new materials with unique shapes. The successful synthesis of boron nitride nanotubes [7-9] showed the possibility to prepare tubular non-carbon (or part carbon) materials. SiC nanotubes were also attempted to prepare eagerly and succeeded by using so-called "template method" using CNT as a template. In the method, SiO gas is decomposed thermally to deposit Si on CNT surface, and the resulting CNT is heated to convert into SiC nanotube according to the equation 1. This method is also called "shape memory synthesis", where nanotube is used as template. A history of the preparation of SiC nanotubes is reviewed briefly.

$$SiO\ (gas) + 2C\ (nanotubes) \longrightarrow SiC\ (nanotubes) + CO\ (gas) \qquad (1)$$

Pham-Huu *et al.* reported the first preparation of SiC nanotubes with various internal and external diameters [10]. They obtained these nanotubes through the template method stated above. Keller *et al.* prepared SiC nanotubes with an average outer diameter of 100 nm and a length up to several tens of micrometers by the gas-solid reaction between carbon nanotubes and SiO vapor under vacuum at 1200 ºC [11]. Sun *et al.* obtained SiC nanotubes and C-SiC coaxial nanotubes (carbon nanotubes sheated with a SiC layer) by the reaction of carbon nanotubes with silicon powder at 1200 ºC [12]. Various shapes of nanostructural SiC were obtained by decomposing SiO

on multiwalled carbon nanotubes as a templates in different temperature zones in a tube furnace. They prepared β-SiC nanowires, biaxial SiC-SiO_x nanowires and a new type of multi-walled SiC nanotubes with interlayer spacing between 3.5 Å and 4.5 Å. The outer layer of the multi-walled CNT was transformed into multi-walled SiC nanotube, while the inner part remained unchanged as carbon nanotube. SiC was formed layer by layer via surface diffusion of Si atoms into CNT.

A thermally induced template synthesis was used by Rümmeli *et al.* for SiC nanotubes and nanofibers. Here vaporized Si was carried by ammonia (NH_3) or N_2 gas [13]. The bundles of SWCNT were used as a carbon source and as a template. Various SiC nanostructures were obtained by changing the reaction period, the temperature, the carrier gas and the gas pressure. They obtained SiC nanorods coated with C, SiC nanorods, SiC nanotubes and SiC nanocrystals. When NH_3 was used as a carrier gas, it decomposed at a reaction temperature to N and H and was responsible for the transformation of SiC nanorods into porous nanorods and further into nanotubes.

The NASA Glenn Research Center has been collaborating with Rensselaer Polytechnic Institute to realize the synthesis of SiC nanotubes. Several methodologies, including the template method and direct SiCNT growth on a catalyst were explored. In the template method, chemical vapor deposition into the template resulted in polycrystalline/amorphous uniform tubes [14]. Cheng *et al.* prepared SiC nanotubes and bamboo-like nanofibers by using CVD and infiltration of liquid precursor into alumina templates [15]. SiCNTs by the CVD method were consistent of a nanocrystalline β-SiC or β-SiC/C, while in the case of the infiltration method single crystal SiC bamboo-like

nanofibers and small particles were observed.

However, some of the SiC nanotubes produced by these methods are thermally unstable, and the layers were bent or transformed into SiC particles on heating. It was not easy to control the wall thickness which affects the thermal stability of the SiCNTs. In other cases the nanotubes were composed of SiC grains formed on the walls of the CNTs, and the grains grew by heating. That's why it is very important to find a more simple preparation method for the SiCNTs.

Applications of SiC nanotubes

Hydrogen storage in silicon-carbon nanotubes (SiCNTs) has been investigated by Mpourmpakis *et al*. [16]. They concluded that SiCNTs absorb more hydrogen than carbon nanotubes (CNTs), particularly at low pressures around 1MPa. Morisada *et al*. prepared SiC-coated CNTs to apply as reinforcement filler for cemented carbides [17]. The SiC coating protects the nanotubes from the reaction with molten metal. Nanotubes form has some advantages. It offers a possibility to use as "nanoreactors" or "nanotests tubes" at a high temperature [18].

SiC: Precursor of SiC fibers

Continuous SiC fiber is mainly of interest as reinforcement filler for ceramic-based composites, because SiC fiber is thermally and chemically stable and has high mechanical properties. Yajima chose poly- (or cyclic) dimethylsilane as the starting point for his development of a SiC precursor, which are obtained ultimately from

dimethyldichlorosilane by Na coupling (equation 2). Although these polysilanes were not suitable for spinning, Yajima found that they are converted into a spinnable intermediate form by heating to 350-450 ˚C. The resulting material was polycarbosilane and is still now the most important precursor of SiC [19]. Polycarbosilane was first melt-spun by Yajima, followed by oxidative stabilization and heat treatment. The resulting material was an amorphous silicon oxycarbide fiber. The details are described below.

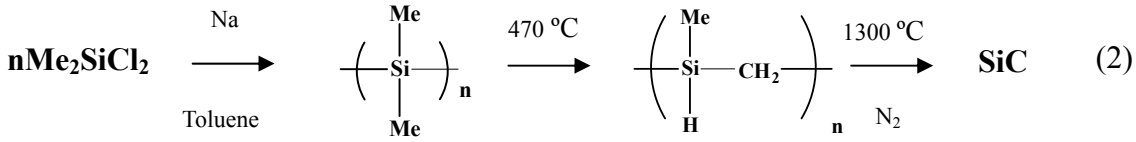

(2)

Synthesis of SiC fibers

Nanofibers are defined as fibers (continuous filaments similar to lengths of thread) with diameters of hundreds of nanometers. The first synthesis of continuous SiC fiber was reported by Yajima *et al.* [19]. They synthesized a polycarbosilane (PCS) as the precursor of continuos SiC fiber by thermal decomposition of polydimethylsilane. The PCS fibers were obtained by melt-spinning in a N_2 atmosphere. Then, the fiber was cured in air at 190-200 ˚C and finally heat-treated in a nitrogen atmosphere at 1300 ˚C. They divided the conversion process of PCS into SiC into three stages: the first stage is condensation of the polymers, the second stage is the thermal decomposition of the side chains such as hydrogen and methyl groups, and the third stage is the crystallization into β-SiC.

Recently, the electron beam curing method has been used to develop SiC fibers with low oxygen content (Hi-Nicalon) and oxygen-free SiC fibers (Hi-Nicalon type S). They have high oxidation resistance and mechanical properties. The fabrication process is fundamentally same as use for Nicalon with exception of the stabilization process.

The conventional Nicalon fiber is prepared by oxidative curing of the polycarbosilane fiber but Hi-Nicalon fiber is cure by radiation using an electron beam and Hi-Nicalon type S uses a modified "Hi-Nicalon" process [20]. Chollon *et al.* prepared a SiC-based fiber with low oxygen content from a polycarbosilane precursor. With a pyrolysis temperature of 1600 ºC, the resulted fiber consisted of SiC nanocrystals with mean size of 6-10 nm and free carbon [21].

SiC nanofibers were synthesized by Honda *et al.* on Si substrates covered by Ni thin films using high power microwave plasma chemical vapor deposition (CVD) under high concentration of H_2 gas [22]. The resultant fibrous material was identified as β-SiC with high crystallinity. The SiC nanofibers were also formed by the vapor liquid solid (VLS) mechanism in which SiC precipitated from the supersaturated Ni nanoparticle with Si and C.

Huczko *et al.* succeed in synthesizing β-SiC nanofibers via spontaneous dehalogenation of various alkyl and aryl halides with Si-containing reductants (Si elemental, FeSi, $CaSi_2$) [23]. The combustion process resulted in SiC nanofibers and also nanotubes ca. 20-100 nm in diameter with an aspect ratio higher than 1000. This method is simple and requires no catalyst or no template, but the growth mechanism of the SiC nanofibers was not fully understood.

Synthesis of SiC nanofibers (5-20 nm in diameter) by sol-gel and polymer blend techniques was achieved by Raman *et al.* [24]. Tetraethoxysilane and methyltriethoxysilane were used as a Si source and polycarbonate as a carbon source. A polymer solution containing alkoxide, water, and a suitable solvent was stirred and freeze-dried to get the polycarbonate incorporating the sol-gel derived silica. The dried precursor was pyrolyzed at 1400 ºC in an argon atmosphere to obtain the mixture of SiC, C and SiO_2. More recently, Hao *et al.* investigated the influence of various metal catalysts on the morphologies of SiC nanomaterials produced from sol-gel route, using lanthanum nitrate as an additive in the sol-gel process to prepare the xerogel [25]. The xerogel containing lanthanum resulted in the formation of bamboo-like SiC nanofibers. The nanofibers formed through the VLS (vapor-liquid-solid) mechanism had a diameter of 40-100 nm and a length of hundreds of micrometers.

SiC nanofibers by melt-spinning of polymer blend had been prepared from polycarbosilane as a SiC ceramic precursor and a novolac-type phenol-formaldehyde resin (PF) [26]. The phenolic resin and the polycarbosilane are mixed using a solvent, melt-spun, cured in an acid solution, oxidized in air and finally heat-treated at 1200 ºC in an argon atmosphere. After heating, the fibers were soaked in a nitric acid solution in order to remove the matrix carbon derived from phenolic resin and the released nanofibers were collected. These nanofibers were amorphous and were about 100 nm in diameter and more than 100 μm in length, but a significant amount of oxygen was included.

Applications of SiC fibers

SiC fiber is an attractive candidate as a reinforcement filler in metal-based and ceramic-based composites, because crystalline SiC has both high stiffness and good creep resistance in addition to high oxidation resistance. Hi-Nicalon hasn't sufficient creep and oxidation resistance to use as a temperature-structural material, because it mainly consists of SiC micro-crystals and excess carbon. Therefore, Hi-Nicalon type S with a stoichiometric SiC composition and high crystallinity has been developed. Hi-Nicalon S fiber has a high elastic modulus of 420 GPa, good oxidation resistance up to 1400 ºC, and excellent creep resistance [20].

Objectives and outline of the thesis

One of the objectives of this thesis is to show the possibility to prepare SiC nanotubes by using polymer blend technique. Another is to get a clue to improve the preparation process of nanofibers from polycarbosilane. Here polymer blend and spinning techniques are used.

In recent years, SiC nanotubes and nanofibers have gained great interest for various technological applications. SiC nanotubes can be used as catalyst supports and the excellent mechanical properties of SiC nanofibers make them good candidates for reinforcement. A new method for preparation of such nanomaterials must be sought. The polymer blend technique is conventionally used in the polymer industry. Thus, if this technique can be used to prepare nanomaterials, it may lead to their mass-production.

In Chapter 1, an attempt to prepare SiC nanotubes from core/shell polymer particles consisting of polystyrene core and polydimetylsilylvinylacetylene shell is described. Polydimethylsilylvinylacetylene is a unique SiC precursor synthesized by emulsion polymerization. Chapter 2 reports a method to prepare a novel double-layered or hybrid nanotube consisting of an inner carbon and an outer SiC layer. In this work, the spray-drying technique was used to prepare core/shell polymer particles. Chapter 3 is referred to preparation of nanofibers from polycarbosilane by using polymer blend and melt-spinning techniques. The resulting nanofibers contained a relatively large amount of oxygen introduced by treatment using nitric acid. The optimum condition to prepare highly purity nanofibers with less amount of oxygen was sought. In Chapter 4, the microstructure of the nanofibers was examined with various analytical techniques in detail. Finally, a series of works were concluded.

Chapter 1

Preparation of nanotubes from polystyrene/polydimethylsilylvinylacetylene core/shell particles by using polymer blend and wet-spinning techniques

1.1 Introduction

There has been an increasing interest in developing materials with a tubular structure since Iijima has discovered a tubular carbon material, so-called carbon nanotube (CNT) in 1991, because there are many possible applications [6]. Boron nitride nanotube was prepared successfully in 1995 [7]. One-dimensional silicon carbide (SiC) developed until now are nanorods [27,28], nanowires [29,30] and nanowhiskers [31,32]. SiC nanotube was also prepared but the process was very complex, namely, SiO gas was decomposed to coat CNT and then the resulting CNT was heated to convert into SiC nanotube [10,12].

SiC nanotube must exhibit different properties from those of CNT. Even if SiC nanotube has attractive properties or functions, its application will not extend without development of mass-production of this material. A unique preparation method of CNT by using polymer blend technique has been designed by the laboratory group [33]. The method is still now under development but thought to be suitable for mass-production of CNT after the completion. Therefore, the author thought to use this technique for preparation of SiC nanotube. An attempt to prepare SiC nanotube is described in chapter 1.

1.2. Experimental

1.2.1 Materials

Styrene monomer was purchased from Kanto Chemical Co. Inc. Polydimethylsilylvinylacetylene (abbreviation: PDMSVA) was supplied by Denki Kagaku Company. Figure 1.1 shows the molecular structure of styrene and dimethylsilylvinylacetylene.

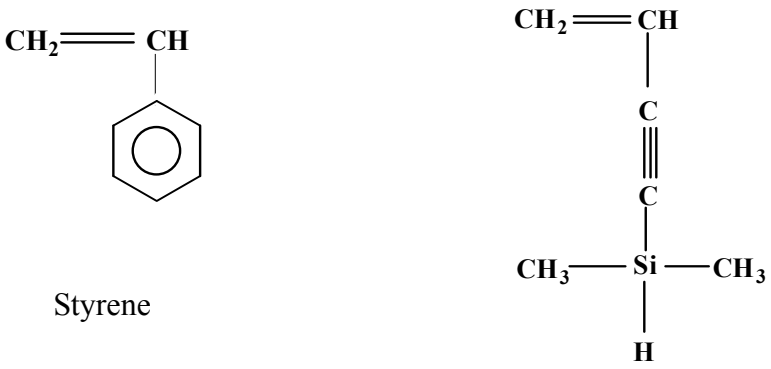

Styrene

Dimethylsilylvinylacetylene **(DMSVA)**

Fig.1.1 Molecular structures of styrene and dimethylsilylvinylacetylene.

1.2.2 Preparation Procedure

Figure 1.2 shows schematically the preparation process of SiC nanotubes by using polymer blend technique. Two kinds of polymers are used. One is a SiC precursor polymer (SiCPP) and another is a thermally decomposable polymer (TDP) with no carbon residue after heating. The core/shell polymer particle consisting of a TDP core and a SiC precursor shell is prepared. The resulting core/shell particle is subjected to wet-spinning, elongated six times their original length, stabilized and finally

heat-treated. After heat treatment, SiCNT is derived from the stabilized SiC precursor shell after the removal of the TDP core. Among the TDPs, PS and PMMA (polymethyl methacrylate) were selected. After SEM and TEM observations the PMMA/PDMSVA core/shell particles were not elongated and most of the sample was fused after heat treatment, as indicative of not good compatibility (elongation) and difficulty on the stabilization of the polymer blend. On the contrary, the PS/PDMSVA core/shell particles were more favorably elongated. Therefore, in the present work, polydimethylsilylvinylacetylene (PDMSVA) and polystyrene (PS) were used as a SiC precursor polymer and a TDP, respectively.

The core/shell particles were prepared as follows. First, fine PS particles were synthesized by soap-free emulsion polymerization. 35 ml of styrene was dissolved in 350 ml of water including a small amount of potassium persulfate (KPS) as a radical initiator. The solution was kept with stirring at 70-80 ^{o}C for 8 h in a flow of nitrogen. The emulsion of fine PS particles was sent to Denki Kagaku Company to coat the PS particles with PDMSVA.

Figure 1.3 shows the polymerization process for PDMSVA. 2,2-Azobis (2,4-dimethylvaleronitrile) was used as an initiator. The polymerization was carried out at 50 ^{o}C for 25 h. The residual monomer and low molecular weight polymer species were washed out with methanol and benzene, and finally the core/shell particles (PS core and PDMSVA shell) were obtained by freeze-drying.

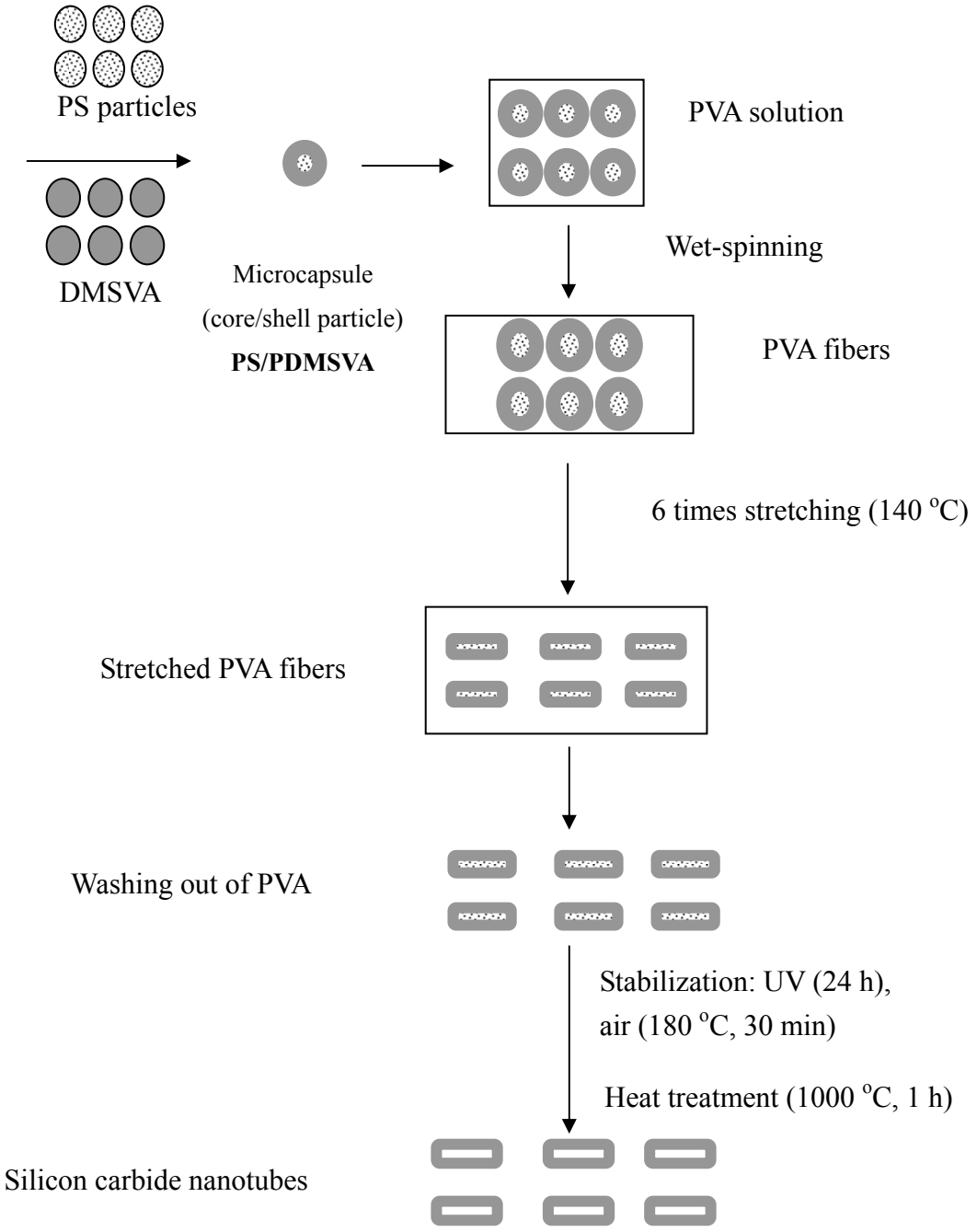

Fig.1.2. A schematic flow chart of the preparation of SiC nanotubes by using polymer blend and wet-spinning techniques.

The particles were suspended in poly (vinyl alcohol) (PVA) aqueous solution and subjected to wet-spinning using a saturated Na_2SO_4 aqueous solution as a solidification agent. The resulting PVA fibers including the core/shell particles were elongated (stretched) mechanically 6 times their original length at 140 °C. The fibers were treated with hot water to dissolve PVA and the non-dissolved fraction was recovered by filtration. The hot water treatment was repeated several times to obtain elongated particles with minimum PVA residue. The particles after drying were subjected to stabilization in which UV radiation for 1 day and heating in air at 180 ^oC for 30 minutes were used. Finally, the elongated particles were heated at 1000 ^oC for 1 h in a nitrogen atmosphere to obtain the SiC nanotubes. The wet-spinning and the stretching apparatuses are shown in Figure 1.4.

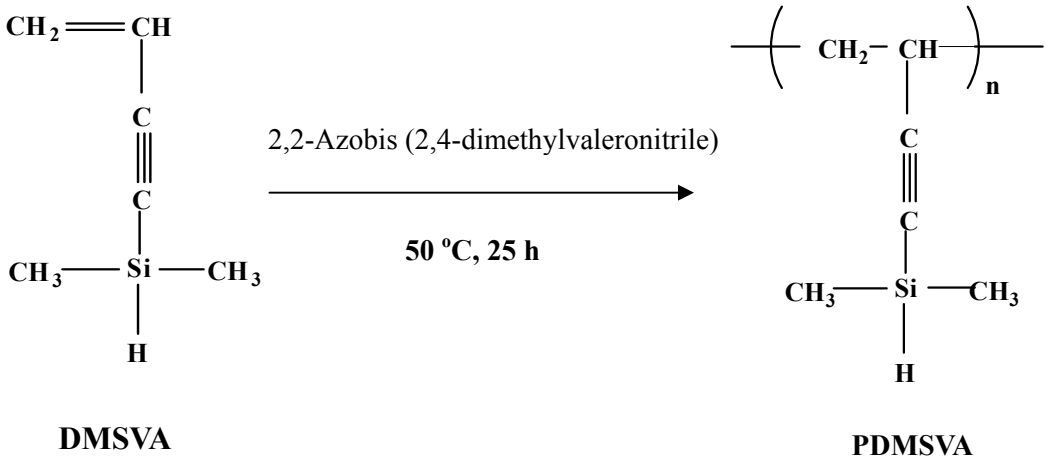

Fig.1.3. Polymerization process for PDMSVA.

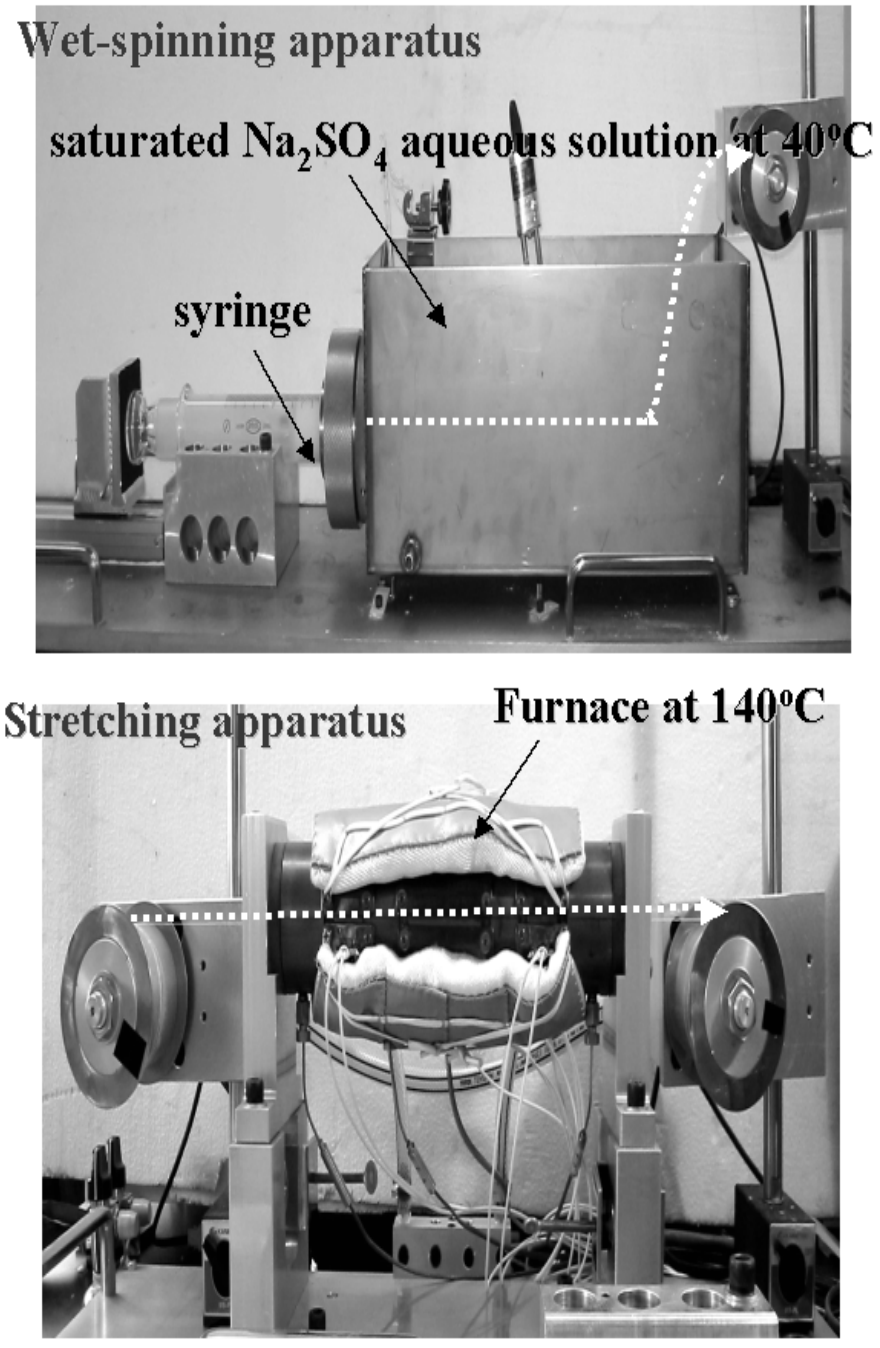

Fig.1.4. Wet-spinning and stretching apparatuses.

1.2.3. Measurements

1.2.3.1. Scanning electron microscopic (SEM) observation.

The surface morphology of the resulting materials was observed by a JEOL JSM-5300 scanning electron microscope.

1.2.3.2. Transmission electron microscopic (TEM) observation.

A transmission electron microscope JEOL JEM-2010 was used to observe the microstructure of the sample after heat treatment.

1.2.3.3. Thermogravimetric (TG) analysis.

TG was carried out in a nitrogen atmosphere with a heating rate of 10 ^{o}C/min by using a Rigaku Thermo plus TG8120 apparatus for the polystyrene and the PS/PDMSVA sample before and after stabilization.

1.2.3.4. Fourier transformation infrared spectroscopic (FT-IR) analysis.

FT-IR spectrum for the samples was taken by using a Nicolet Avatar 360 apparatus. The KBr method was used.

1.2.3.5. Chemical analysis.

Chemical analysis for the material after heat treatment was performed by use of an EDS apparatus (Oxford Instruments) attached to the TEM microscope. The beam

diameter was 10 nm.

1.3. Results and Discussion

Figure 1.5 shows the TG curves of PS, PS/PDMSVA before and after stabilization in a nitrogen atmosphere. PS disappeared completely below 500 ^{o}C after fusing. The weight loss of the PS/PDMSVA at 1000 ^{o}C was about 95%, leaving a ceramic residue, which was not changed by the stabilization treatment. The data in Figure 1.5 show clearly that both PS and PDMSVA can be used as a TDP and a SiC precursor polymer as shown in the preparation scheme.

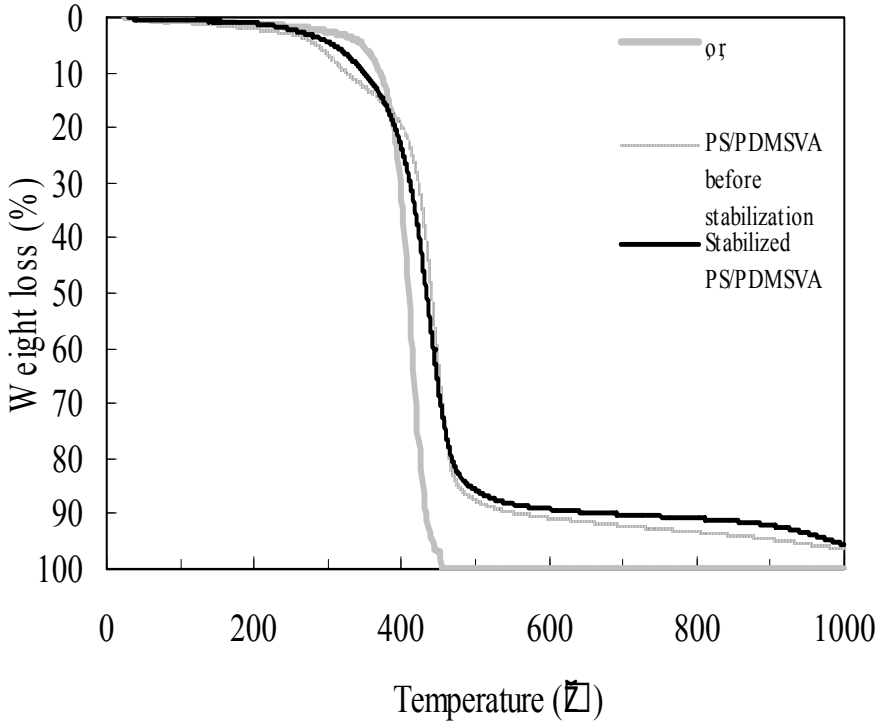

Fig.1.5. TG curves of PS and PS/PDMSVA before and after stabilization, in N_2 flow.

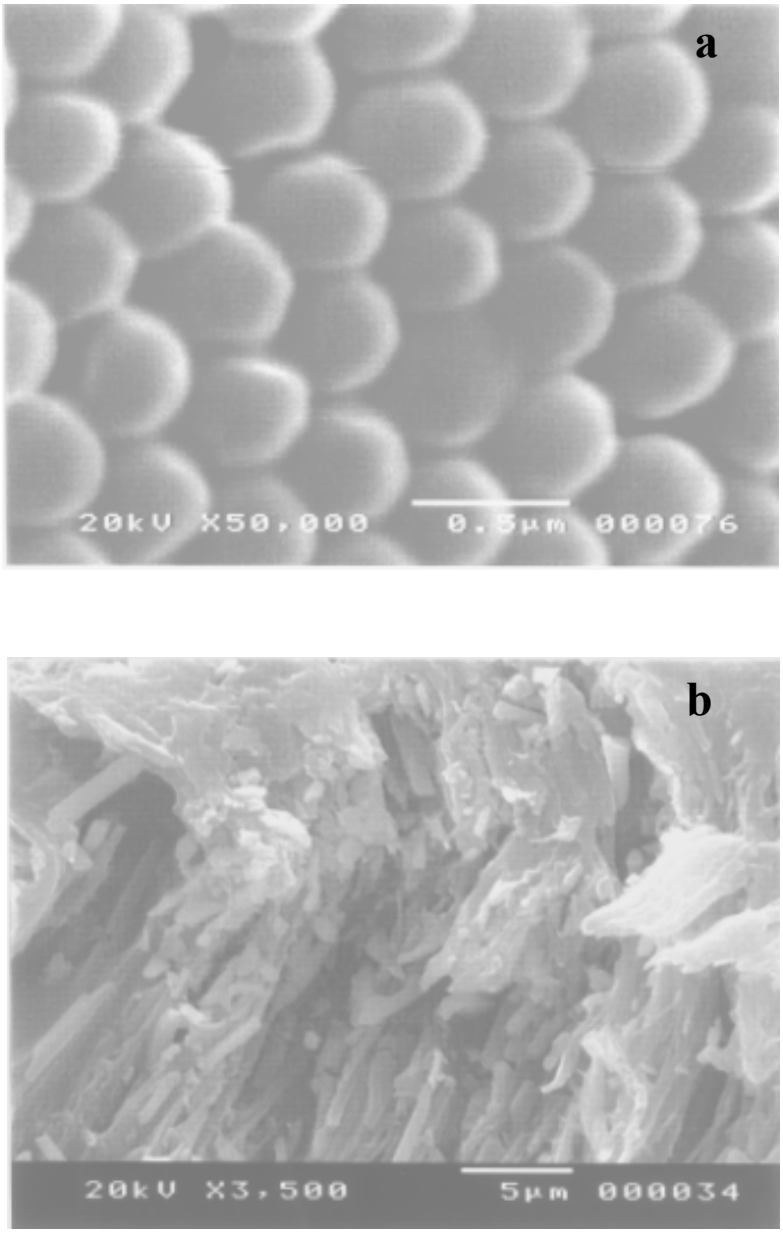

Fig.1.6. SEM photograph of the a) core/shell particles (PS/PDMSVA) and b) cross section of the stretched PVA fiber before stabilization.

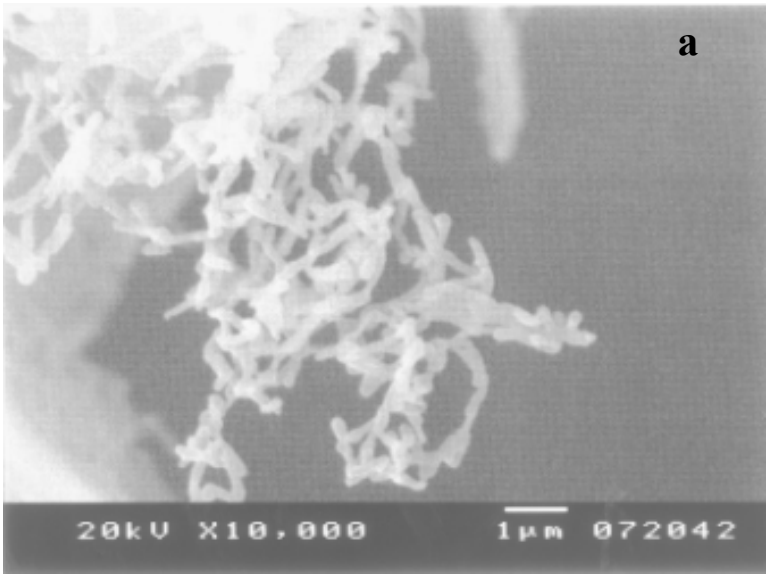

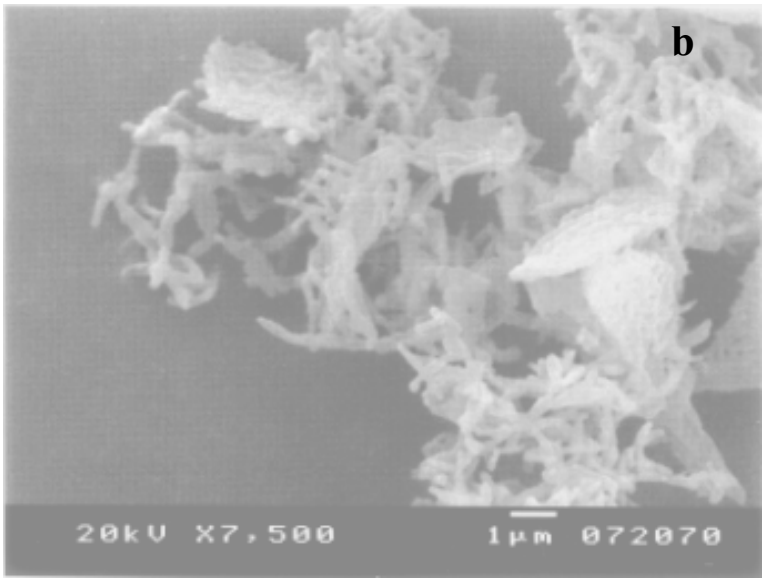

Fig.1.7. SEM photograph of the elongated core/shell particles a) after stabilization and b) after heat treatment.

Figure 1.6 (a) shows the SEM photograph of the core/shell (PS/PDMSVA) particles. They are quite uniform particles with ca. 0.5 μm in diameter as can be seen in the photograph. Figure 1.6 (b) shows a cross section of the stretched PVA fiber, including the particles, before the stabilization. The elongated core/shell particles aligned along the fiber axis are observed. Figure 1.7 (a) shows the elongated core/shell particles before the stabilization and Figure 1.7 (b) after heat treatment. Rod-like particles are seen. The diameter of the rods is about 200 nm.

PDMSVA has never used as a SiC precursor until now, because this polymer was developed by Denki Kagaku Company just recently. Therefore, the author is interested in a stabilization process of PDMSVA. The stabilization process is discussed below in somewhat detail.

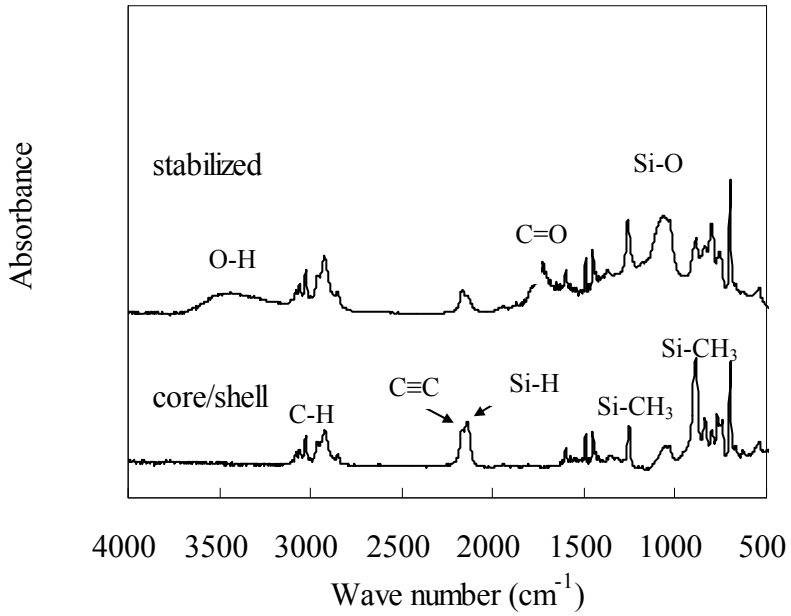

Fig.1.8. Infrared spectra of the core/shell particles (PS/PDMSVA) and the stabilized sample.

Figure 1.8 shows the infrared spectra of the core/shell particles and the stabilized sample. The characteristic absorption bands for the pristine core/shell particles (PS/PDMSVA) are: between 2900-3200 cm^{-1} due to C-H stretching, at 2150 cm^{-1} (C≡C stretching), at 2100 cm^{-1} due to Si-H stretching, at 1400 cm^{-1} (C-H deformation in CH_3), at 1250 cm^{-1} (Si-CH_3 deformation), at 820 cm^{-1} (Si-CH_3 rocking and Si-C stretching), and at 750 cm^{-1} (Si-CH_3 stretching).

After the stabilization process, intensities of the absorption bands due to C≡C, Si-H and Si-CH_3 (820 cm^{-1}) decreased, and absorption bands between 3200-3600 cm^{-1} due to O-H stretching and at 1710 cm^{-1} due to C=O stretching appeared instead. The band at 1100 cm^{-1} assigned to Si-O in Si-O-Si or Si-O-C was strengthened.

On the basis of above results, a possible stabilization mechanism as shown in Figure 1.9 is deduced. Si-H bond in PDMSVA is changed into Si-OH bond (silanol) by the oxidation in air, which is further changed into Si-O-Si by dehydration. In addition, a part of the Si-CH_3 bonds could be oxidized leading to formation of siloxane (Si-O). The details of the oxidation mechanism for Si-H and Si-CH_3 have been reported in the literature [34]. The absorption band of C=O appears due to oxidation of –CH_3 in PDMSVA.

The stabilization step is necessary in order to prevent re-melting of the material on heat treatment. For PDMSVA with the formation of a cross-linked structure by siloxane bonds and bonding to the C≡C.

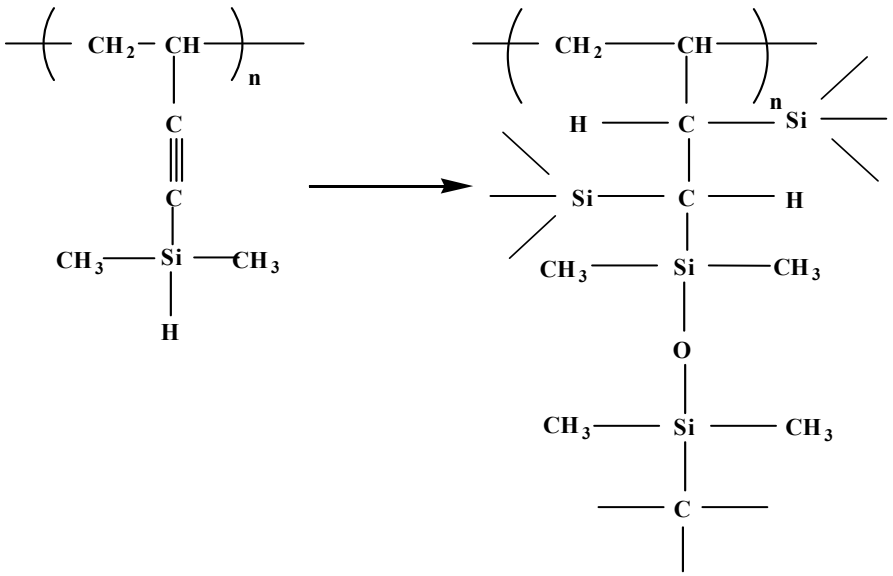

Fig.1.9. Possible chemical structure of PDMSVA after stabilization.

The next step is the heat treatment of the stabilized PDMSVA. At the initial of the heat treatment, the decomposition reactions of Si-H and C-H in Si-CH_3 are assumed to occur as follows:

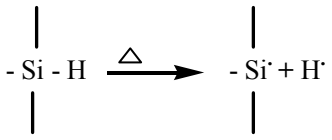

(1)

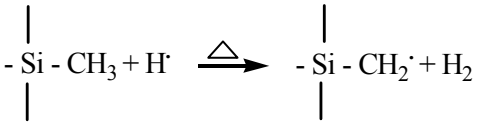

(2)

As heat treatment proceeds, the radicals produced in equations 1 and 2 should recombine to lead to the Si-CH_2-Si bond:

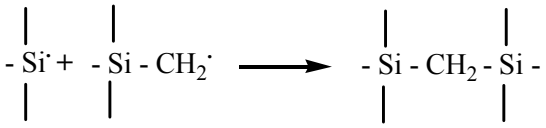

(3)

With increasing of the heat treatment temperature a SiC three-dimensional network structure forms by reaction as shown below.

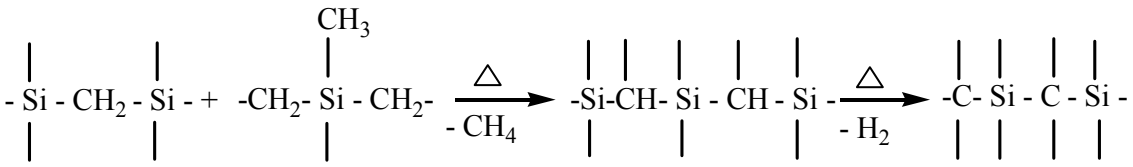

After the heat-treatment at 1000 ^{o}C, it appears that the organic polymer was not completely converted into the inorganic material, because absorption bands of C-H (broad band around 1400 cm^{-1}) and O-H band (between 3200-3600 cm^{-1}) are still present, as seen in Figure 1.10. The Si-O band at 1100 cm^{-1} is strong and the band assigned to Si-C (820 cm^{-1}) is small.

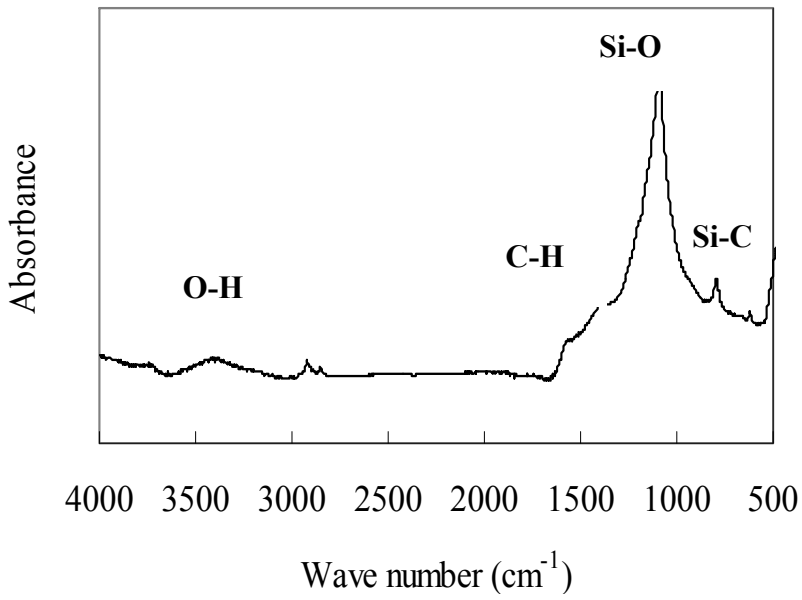

Fig.1.10. Infrared spectra of the heat-treated sample at 1000 ^{o}C.

The TEM photographs of Figure 1.11 show the sample after the heat treatment. Nanotubes were observed in Figures 1.11 (a) to (d), but rod-like materials are also observed in Figure 1.11 (e), possibly because of insufficient stabilization of PDMSVA. This idea will be supported by Figure 1.5, in which the samples (PS/PDMSVA) before and after the stabilization gave same ceramic yield.

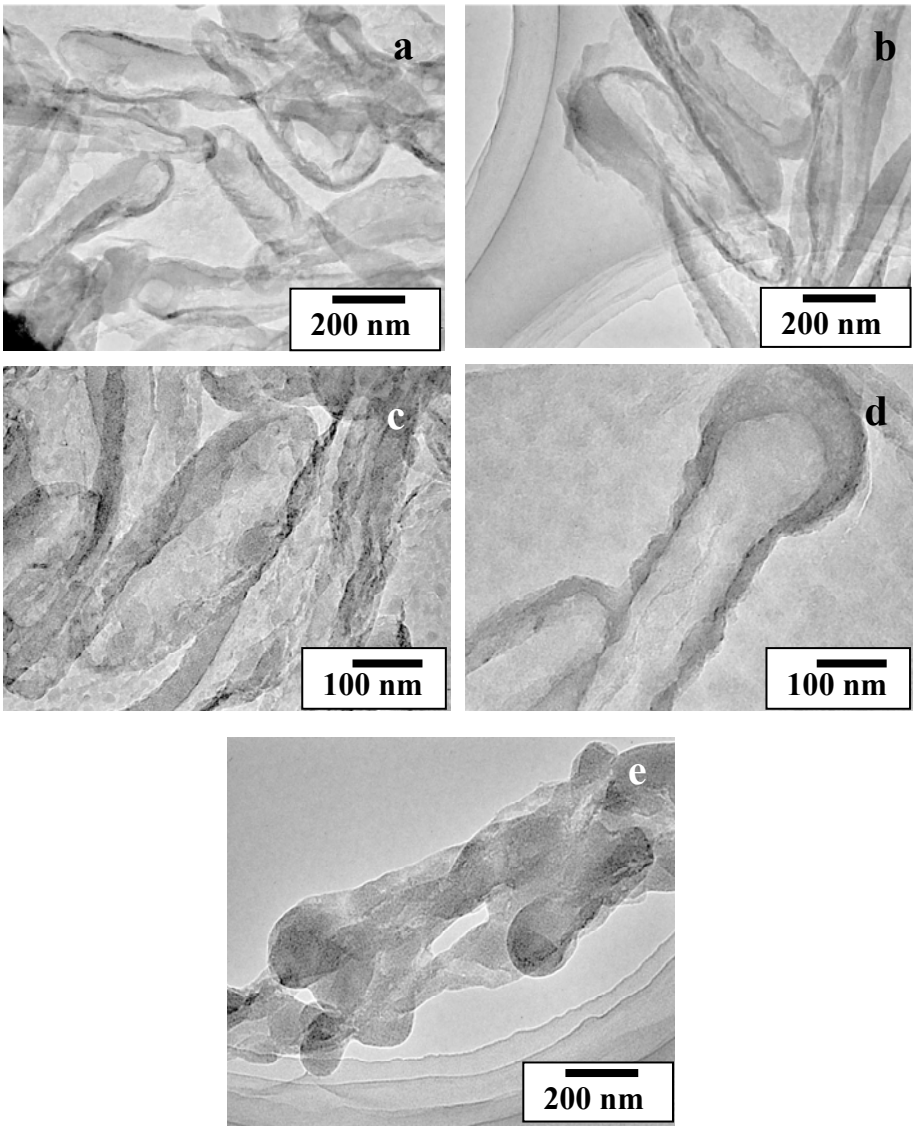

Fig.1.11 TEM photographs of the sample after heat treatment at 1000 ^{o}C.

In the formation of nanotubes using polymer blend technique, therefore, the key step is the initial cross-linking process to change PDMSVA into an infusible state.

Figure 1.12 shows a higher magnification TEM photograph of a resulting nanotube. The EDS profile at the site of the circle is shown in Figure 1.13 and the chemical composition of PDMSVA after heating at 1000 ^{o}C was compared with PCS filaments heated at 850 ^{o}C and Nicalon heated at 1200 ^{o}C (Table 1). Nicalon is a commercially available silicon carbide fiber derived from polycarbosilane produced by Nippon Carbon Co.

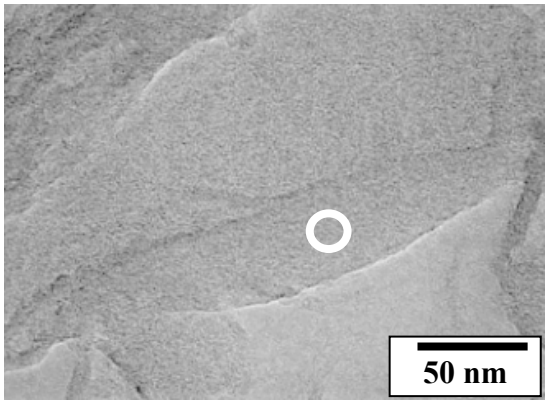

Fig.1.12. High magnification TEM photograph of a nanotube.

Chapter 1

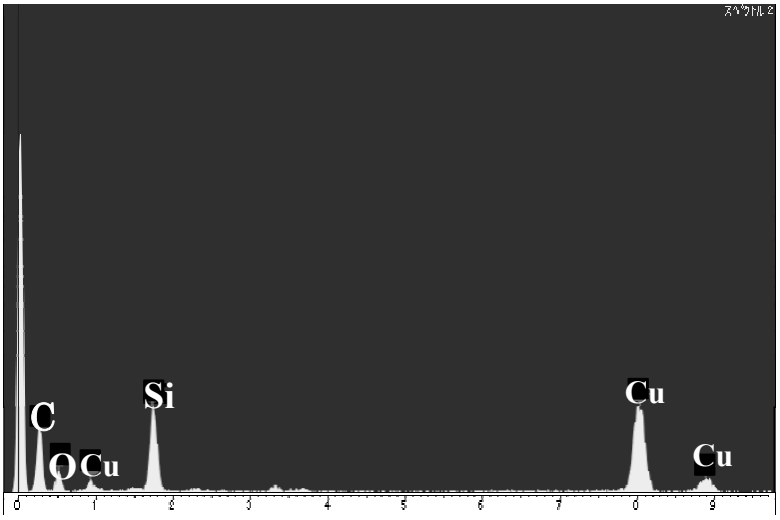

Fig.1.13. EDS profile of the nanotube from Figure 1.12.

Table 1. Elemental analysis of PDMSVA after heating at 1000 °C, PCS filament heated at 850 °C and Nicalon used as references.

Materials	Si (at.%)	C (at.%)	O (at.%)
PDMSVA heated at 1000 °C	21.8	66.5	11.7
PCS filaments heated at 850 °C [35]	35.0	44.0	20.0
Nicalon fiber heated at 1200 °C [35]	38.0	49.0	13.0

The silicon and oxygen contents of PDMSVA are lower compared to the PCS filament and Nicalon, but the carbon content of PDMSVA after heating was higher than the others. If the composition of PDMSVA heated at 1000 °C is assumed 15.95 SiC + 5.85 SiO_2 + 50.55 C and for Nicalon 31.5 SiC + 6.5 SiO_2 + 17.5 C, the excess carbon is more evident for the PDMSVA compared to Nicalon. Excess carbon leads to oxidation that results in lowering of the mechanical properties at higher temperatures.

The fibers or nanofibers from silicon carbide precursor polymers may be called as “silicon carbide-based nanofiber”, but “silicon carbide nanofiber” is used in the text to avoid confusing.

The low yield of the ceramic product can be related with the non-stoichiometric character of the silicon carbide precursor PDMSVA, in which the C:Si ratio is 6:1 compared to polycarbosilane as Nicalon precursor (C:Si, 2:1). The structure of PCS derived from polydimethylsilane is shown in Figure 1.14.

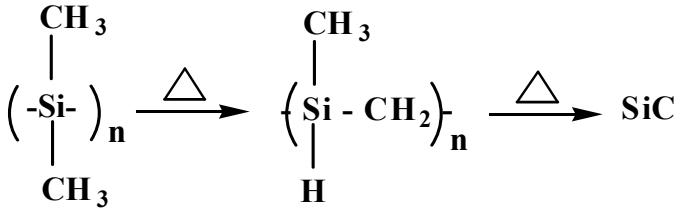

Fig.1.14. Formation process of Nicalon fiber from polydimethylsilane.

1.4. Conclusions

As explained above, the possibility to prepare nanotubes from PDMSVA by using polymer blend and wet-spinning techniques coupled with stretching was shown. The key step in the preparation is the stabilization process (the formation of cross-linkages) for the silicon carbide precursor polymer, PDMSVA. A silicon carbide precursor must be as near as the stoichiometric (Si:C, 1:1) in order to increase the ceramic yield in the resulting material.

Chapter 2

Preparation of nanotubes from poly(methyl methacrylate)/polycarbosilane and poly(methyl methacrylate)/polyacrylonitrile/polycarbosilane core/shell particles by using polymer blend and wet-spinning techniques

2.1. Introduction

The first polymer as a precursor of silicon carbide was developed by Yajima and co-workers. That is polycarbosilane (PCS) which is prepared by heating dimethyldichlorosilane in an autoclave [4]. The structure of PCS is shown in Figure 2.1. PCS is now used to produce commercially silicon carbide fibers named as Nicalon.

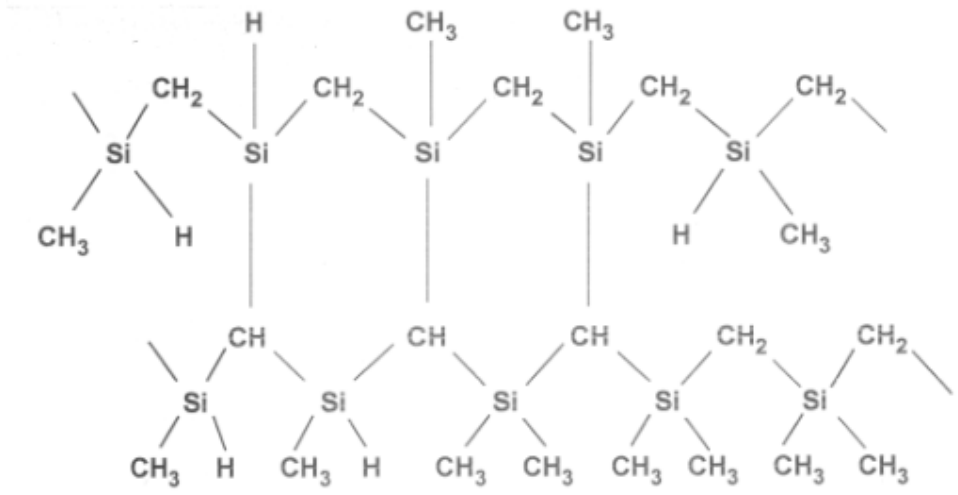

Fig.2.1. Structure of polycarbosilane as a SiC precursor.

In chapter 1, PDMSVA was used as a silicon carbide precursor. However, in view of the molecular structure, PCS seems to be a more suitable precursor to prepare

silicon carbide nanotubes, because PCS has a nearer stoichiometric structure to SiC than PDMSVA, and many data on stabilization treatment and thermal behaviors have been accumulated for PCS. A serious problem is that PCS can't be prepared by an emulsion polymerization, in other words, high purity core/shell particles consisting of PCS shell can't be prepared. A main interest of the present author, however, is to make clear the possibility to prepare silicon carbide nanotube by using polymer blend technique. Therefore, the author decided to use PCS instead of PDMSVA as a silicon carbide precursor.

Also the author is interested to prepare a hybrid nanotube with a layer consisting of two kinds of materials, a nanotube consisting of inner carbon and outer silicon carbide layer. Polymer blend technique was used in this attempt, too.

2. 2. Experimental

2.2.1 Materials

Polycarbosilane type A (PCS-A) with a molecular weight of 1400 and a softening point of 230 ^{o}C was purchased from Nippon Carbon Co. Ltd. and used in this work. Methyl methacrylate (MMA) and acrylonitrile (AN) monomers were purchased from Wako Pure Chemical Industries Ltd. The molecular structures are shown in Figure 2.2.

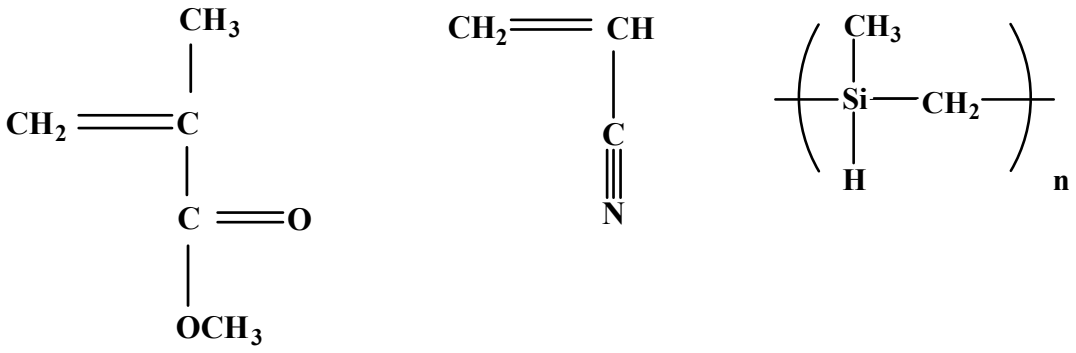

Methyl methacrylate **(MMA)** Acrylonitrile **(AN)** Polycarbosilane **(PCS)**

Fig.2.2. Molecular structures of methyl methacrylate, acrylonitrile and polycarbosilane.

2.2.2. Preparation Procedure

Core/shell particles were prepared by using a similar process as used in chapter 1. Poly(methyl methacrylate) (PMMA) and PCS were used as a thermally decomposable polymer and a SiC precursor polymer, respectively. The core/shell particles were prepared by soap-free emulsion polymerization. The PMMA core microspheres were synthesized by polymerizing 35 ml of methyl methacrylate (MMA) in 350 ml of water using a small amount of potassium persulfate (KPS) as a radical initiator. The solution was kept with stirring at 70-80 ^{o}C for 8 h in a flow of nitrogen. The resulting PMMA particles were suspended in hexane solution 10% of PCS by using a sonicator. The suspension was subjected to spray-drying to prepare the core/shell polymer particles consisting of PMMA core and PCS shell. The spray-drying was carried out in Shibata Kagaku Co. Ltd. The resulting particles were used to prepare silicon carbide nanotubes.

Another core shell polymer particles prepared has a structure of PMMA/PAN/PCS. The PMMA core particles were coated with polyacrylonitrile (PAN) by using two-step soap-free polymerization method as shown in Figure 2.3 [36]. The resulting core/shell polymer particles were coated with PCS by using spray-drying method as stated above and served for an attempt to prepare the hybrid nanotubes with double layer, one of carbon and another of silicon carbide. It is of course that PMMA/PAN particles were subjected to spray-drying for an attempt to prepare the hybrid SiC nanotubes. The structures of two kinds of core/shell polymer particles are shown in Figure 2.4 schematically.

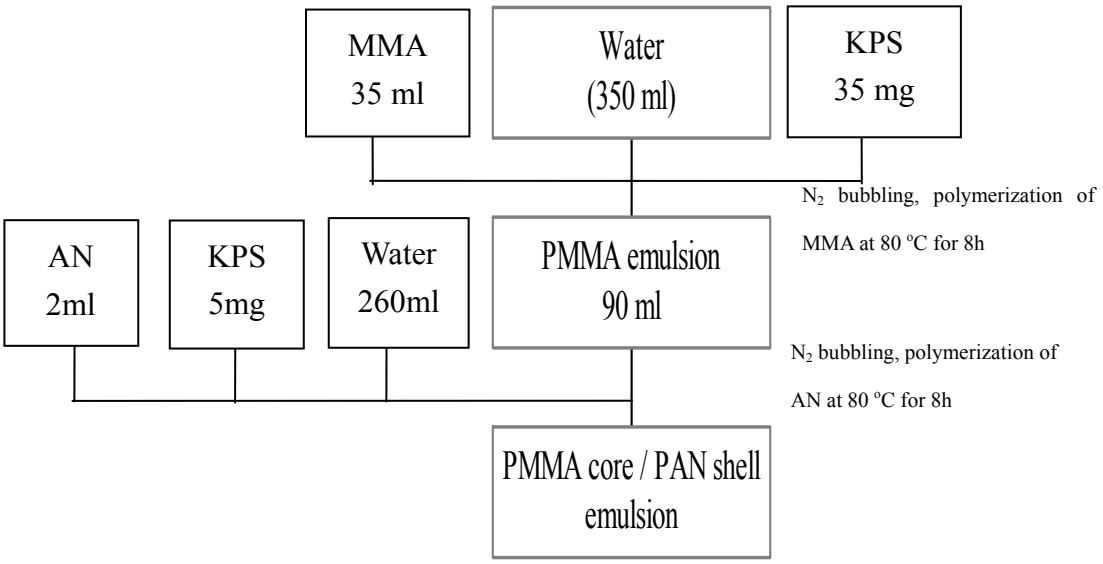

Fig.2.3. Preparation process of the core/shell (PMMA/PAN) particles by soap-free emulsion polymerization.

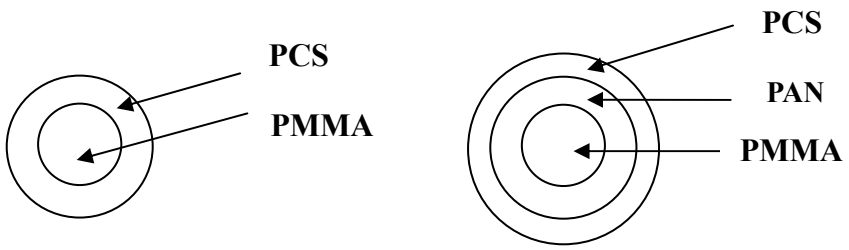

Fig.2.4. Structure of the core/shell particles.

Here the spray-drying method is explained briefly by using a typical apparatus shown in Figure 2.5. Heated gas source is introduced into a cylindrical chamber together with the atomized hexane solution of PCS containing the suspended particles as a feed in Figure 2.5. The ratio of PCS in the solution against PMMA or PMMA/PAN particles was 6:4 by weight. Hexane is evaporated instantly to leave the particles coated with PCS, that is, PMMA/PCS or PMMA/PAN/PCS core/shell particles are obtained. At this process, fine PCS particles are thought to be form in addition to the PCS-coated particles, but any fine particles were not observed in this work.

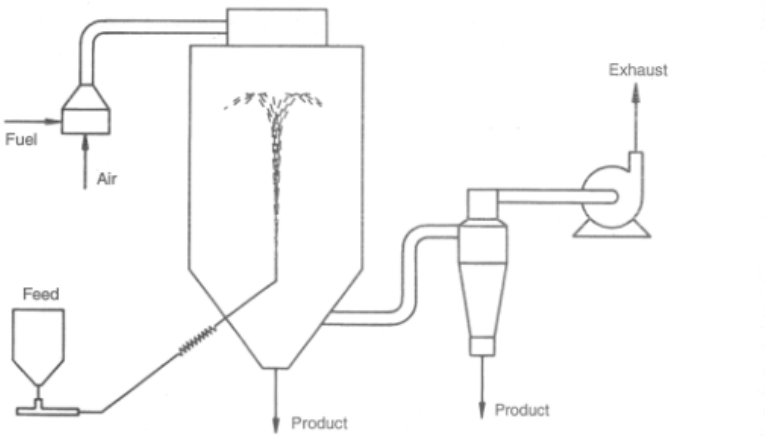

Fig.2.5. Schematic of a typical spray-drying system.

The core/shell polymer particles after spray-drying were treated according to the processes used in chapter 1. The core/shell polymer particles were initially suspended in poly (vinyl alcohol) (PVA) aqueous solution and subjected to wet-spinning. The resulting PVA fibers including the polymer particles were stretched mechanically to six times their original length at 140 °C. The fibers were washed with hot water to remove the PVA matrix and the elongated particles were collected by filtration. The particles were stabilized (cured) in air at 220 °C for 6 hours and finally heat-treated in a nitrogen atmosphere at 1000 °C for 1 hour.

2.2.3 Measurements

The FT-IR measurement of the core/shell particles (PMMA/PAN/PCS), stabilized and heat-treated samples and the chemical analysis of the stained sample (OsO_4) and the nanotubes derived from the core/shell particles (PMMA/PAN/PCS) were carried out by using the apparatuses described in chapter 1.

2.2.3.1. Field emission scanning electron microscopic (FE-SEM) analysis.

The core/shell particles (PMMA/PCS and PMMA/PAN/PCS), the samples after removal of PVA and after stabilization were observed by a JEOL JSM-6700FS field emission scanning electron microscope.

2.2.3.2. Transmission electron microscopic (TEM) analysis.

A transmission electron microscope JEOL JEM-2010 was used to observe the

morphology of the material after heat treatment. The structure of the core/shell particles (PMMA/PAN/PCS) was observed after cutting a 60 nm film (Reichert Supernova Ultramicrotome) of the sample embedded in an epoxy resin and stained with osmium (OsO_4 vapor).

2.3. Results and Discussion

Figure 2.6 shows FE-SEM photographs of the pristine PMMA/PCS and PMMA/PAN/PCS particles. As can be seen, the isolated and the coagulated particles were observed and their size was about 400 nm in both samples. Figure 2.7 shows the FE-SEM photographs of the two samples after the elongation and the washing out of PVA. In the sample of the PMMA/PCS particles shown in Figure 2.7 (a), the particles were fused seriously each other (arrowed by 3) or were not elongated (arrowed by 2). Fibrous materials were observed very rarely (arrowed by 1). In the PMMA/PAN/PCS particles, on the other hand, the fibrous materials were observed more frequently than in the PMMA/PCS particles as can be seen in Figure 2.7 (b) but they are fused together (arrowed by 1). Coalesced particles are also observed (arrowed by 2).

Figure 2.8 shows FE-SEM photographs of the samples after the stabilization. A few elongated particles with different size (arrowed by 1) and the coagulated particles (arrowed by 2) were observed for the PMMA/PCS sample (Figure 2.8 (a)). The elongated particles can be also seen in Figure 2.8 (b) for the PMMA/PAN/PCS sample. The thick elongated particles were possibly derived from the coagulated particles shown in Figure 2.6 (b).

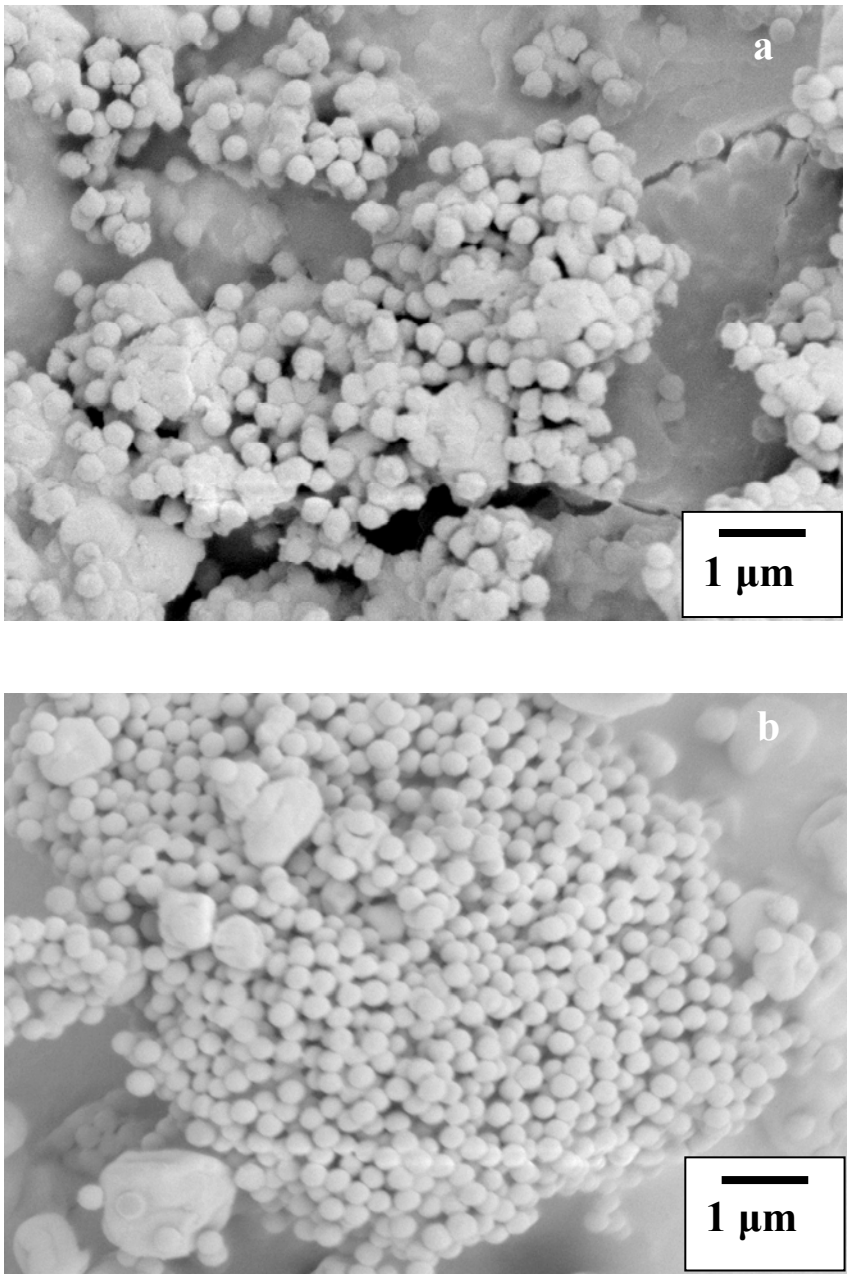

Fig.2.6. FE-SEM photographs of the core/shell particles a) PMMA/PCS and b) PMMA/PAN/PCS.

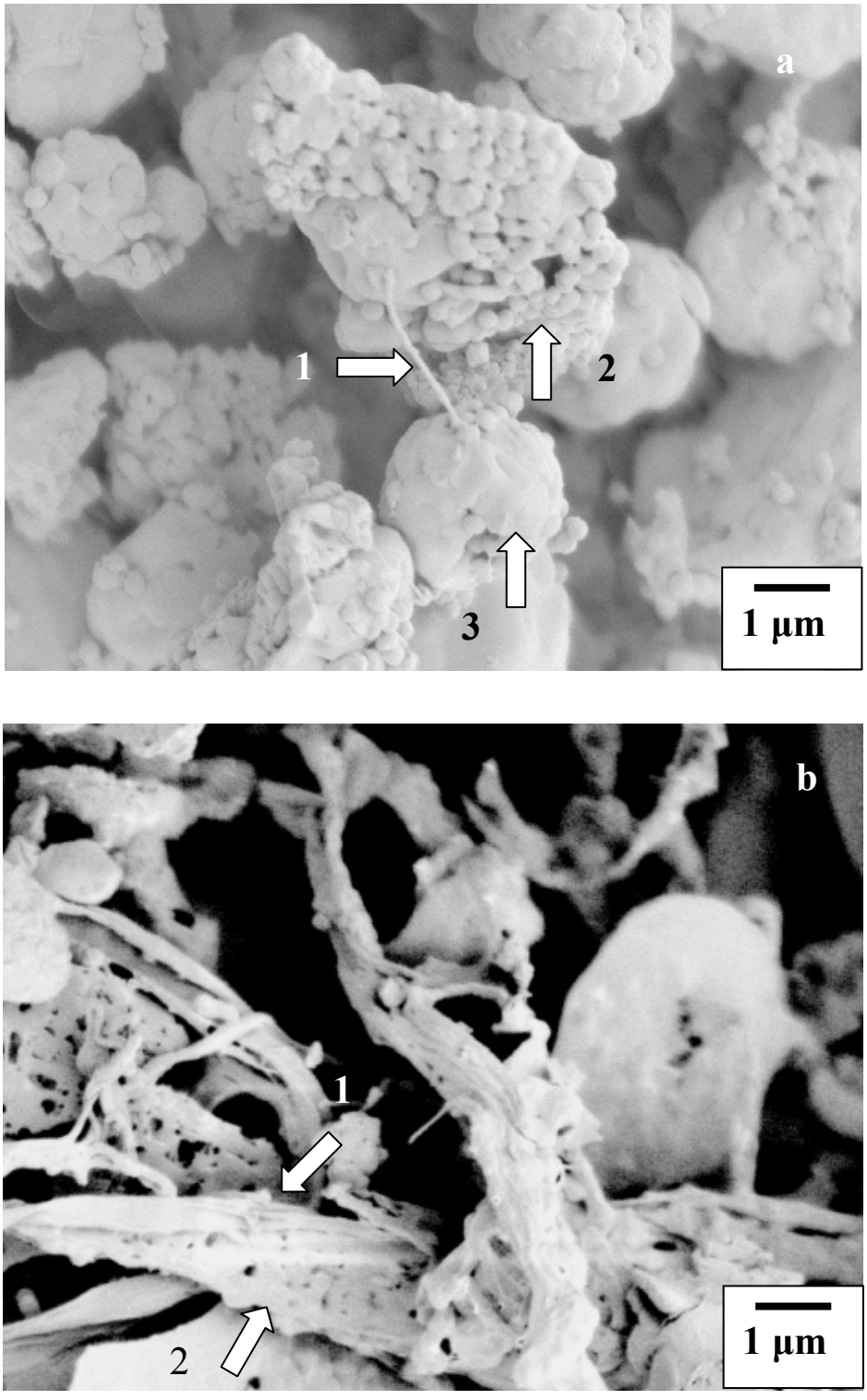

Fig.2.7. FE-SEM photographs of the sample after removal of PVA: a) PMMA/PCS and b) PMMA/PAN/PCS.

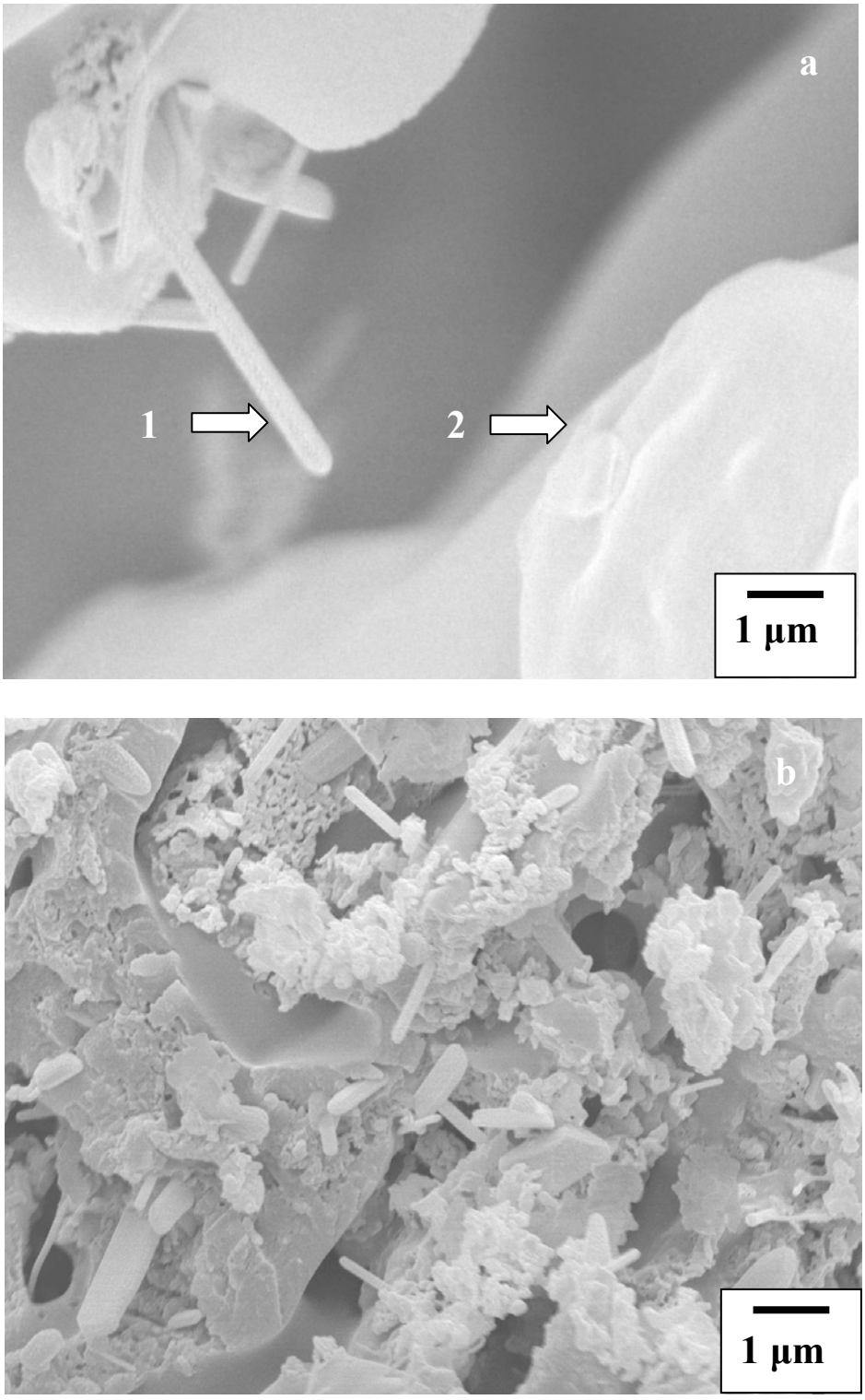

Fig.2.8. FE-SEM photographs of the sample after stabilization: a) PMMA/PCS and b) PMMA/PAN/PCS.

Figure 2.9 shows TEM photographs of the PMMA/PCS sample after the heat treatment. A tube-like structure was observed very rarely as seen in Figure 2.9 (a), but a large part of the sample consists of coalesced nanospheres as seen in Figure 2.9 (b). They must be derived from the coagulated particles seen Figure 2.7 (a). An isolated and the coalesced spheres were also observed in the PMMA/PAN/PCS sample as shown in Figure 2.10. Through the careful observation, some nanotubes were found in the PMMA/PAN/PCS sample as can be seen in Figure 2.11. The nanotubes seen in Figures 2.11 (a) and (b) have irregular shapes. The nanotube shown in Figure 2.11 (c) comprises a very thin wall and a large inner diameter. The site indicated by an arrow possibly result from an explosion of gas evolving from PMMA during heat treatment at 1000 ^{o}C. The shell must be stabilized before the core was completely decomposed. For this nanotube because the wall is very thin maybe it was not strong enough or was insufficiently stabilized to resist the gas explosion during removal of the PMMA core. The nanotube with a most regular shape is shown in Figure 2.11 (d). The nanotube tip is closed as indicated by the arrow. The elongated particles shown in Figure 2.8 (b) could lead to the formation of the nanotubes shown in Figure 2.11 after the heat treatment.

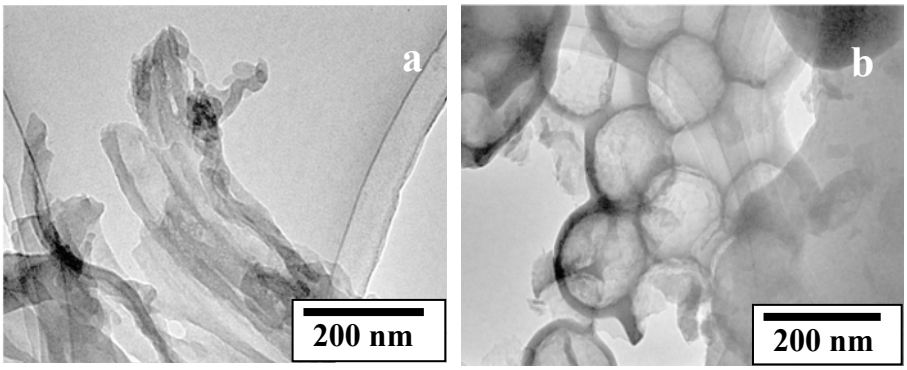

Fig. 2.9. TEM photographs of the sample derived from PMMA/PCS particles after heat treatment.

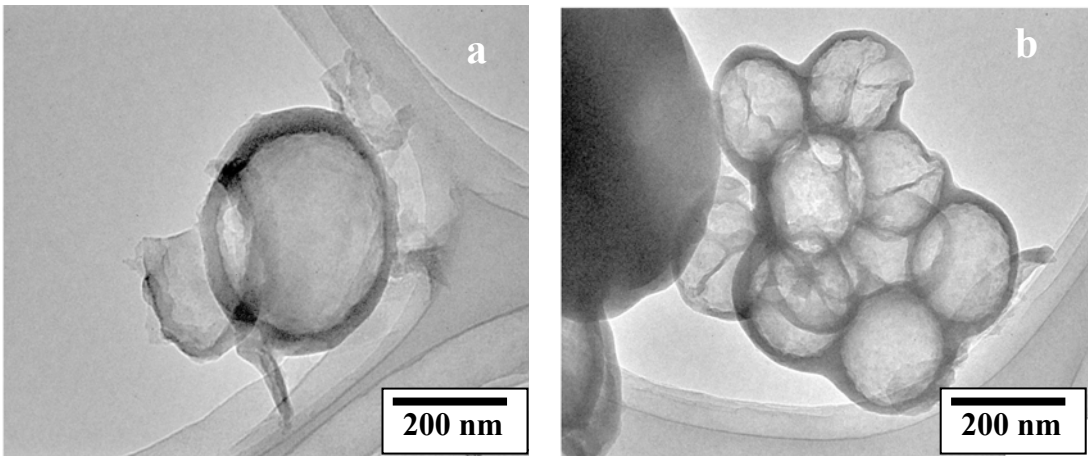

Fig.2.10. TEM photographs of the sample derived from PMMA/PAN/PCS particles after heat treatment.

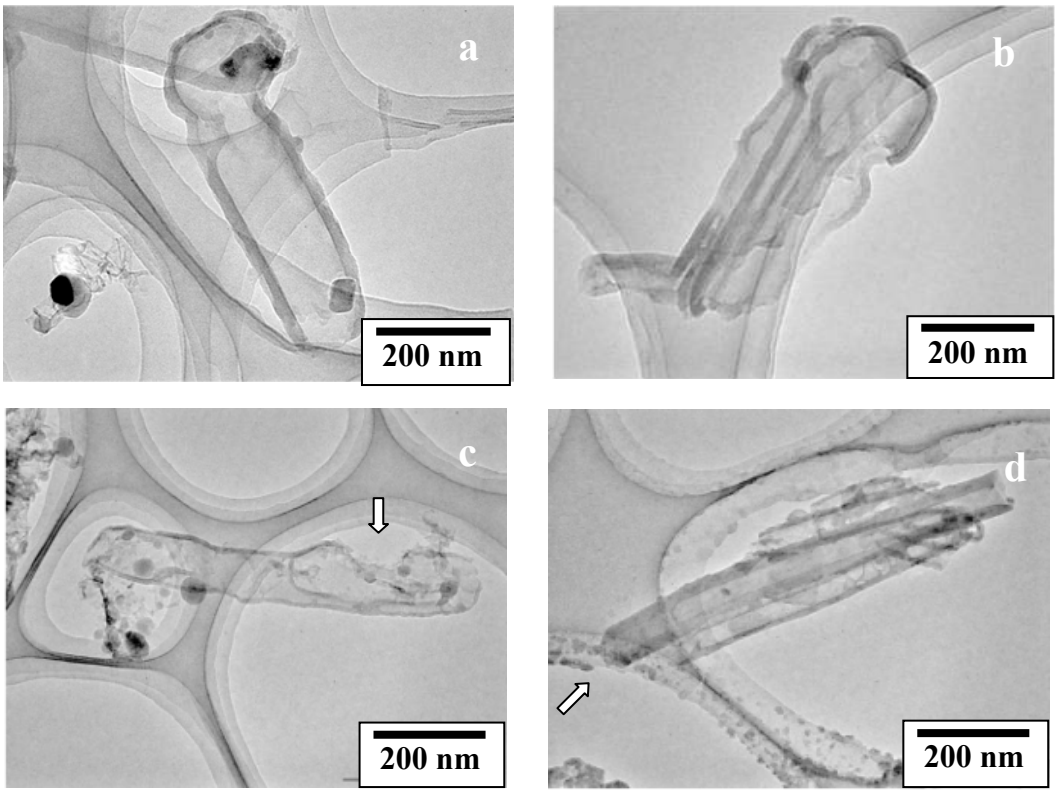

Fig.2.11.TEM photographs of nanotubes derived from the PMMA/PAN/PCS particles after heat treatment.

A higher magnification TEM photograph of the nanotube in Figure 2.11 (d) is shown in Fig.2.12. The diameter is ca. 100 nm and the wall thickness 30 nm. The shell thickness of the nanotubes must be derived from the six times stretching of the core/shell particles. Assuming theoretically the length of the nanotube after six times stretching, the calculated thickness is ca. 33 nm, which is in agreement with the wall thickness of the nanotube shown in Figure 2.12. Therefore, the nanotubes must be derived from the core/shell particles.

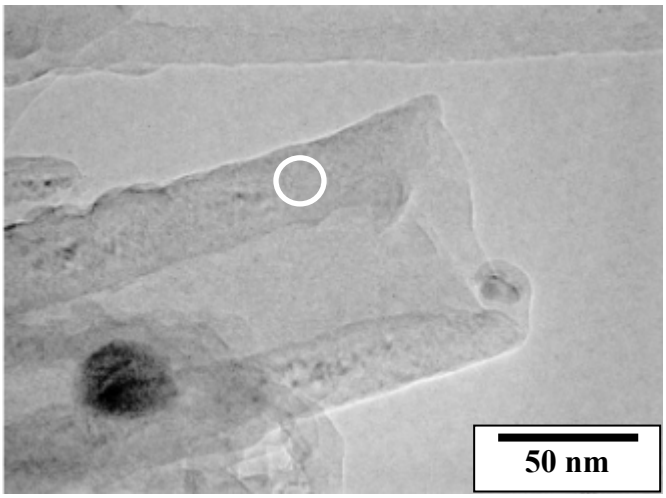

Fig.2.12. High magnification TEM photograph of the nanotube from Figure 2.11 (d).

The elemental composition of the nanotube shown in Figure 2.12 was examined by EDS. The EDS profile is shown in Figure 2.13. The elemental composition was C (57.2 at. %), Si (8.1 at.%) and O (17.1 at. %). Cu (15.3 at. %) is from a copper grid used for TEM observation. Na of 2.3 at.% must be a contaminant. The tube wall must be consistent of inner carbon layer and outer silicon carbide layer

derived from the PAN layer and PCS layer of the pristine core/shell particles, which will be discussed later.

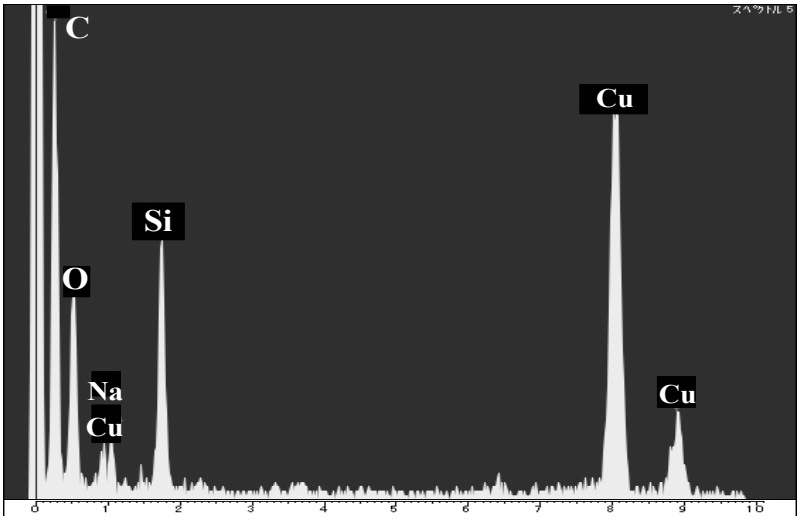

Fig. 2.13. EDS profile of the nanotube from Fig. 2.12

Bouillon *et al*. reported the elemental composition of PCS filaments after stabilization in oxygen at 160 ^{o}C and pyrolysis at 850 ^{o}C. The compositions are C (44 at. %), Si (35 at. %) and O (20 at. %) [35]. The silicon content of the present sample is low compared to the PCS filaments. After carbonization PMMA was removed. The higher carbon content of the present nanotube can be attributed to the carbon layer derived from PAN.

Figure 2.14 shows TEM photographs of a cross-section for a PMMA/PAN/PCS particle, after staining the PAN layer with OsO_4. The sites labeled 1 and 2 were examined by EDS. The profiles were shown in Figure 2.15. Table 1 shows the elemental compositions resulted from Figure 2.15. Both sites contain carbon and oxygen, but silicon was found only in site (2). The inner site (1) in Figure 2.14 consists

of a PAN layer and the outer site (2) of a PCS layer. The nanotube was derived from particles with the same structure as shown in Figure 2.14. After heat treatment the hybrid nanotube will result in an inner carbon layer and an outer silicon carbide-based layer. The wall of the nanotube was very thin to perform EDS analysis in order to identify the two layers.

As stated above, the PMMA/PAN/PCS particle results in the nanotube preferably than the PMMA/PCS particle. In the present work, PS was also used as a TDP but the core/shell (PS/PCS) particles were not elongated and after carbonization most of the sample was fused. Therefore for the double-layered core/shell particles, possibly PAN is stabilized more easily than PCS and keeps a morphology of elongated core/shell. PCS is decomposed on the stabilized PAN to result in the hybrid layer consisting of carbon and silicon carbide.

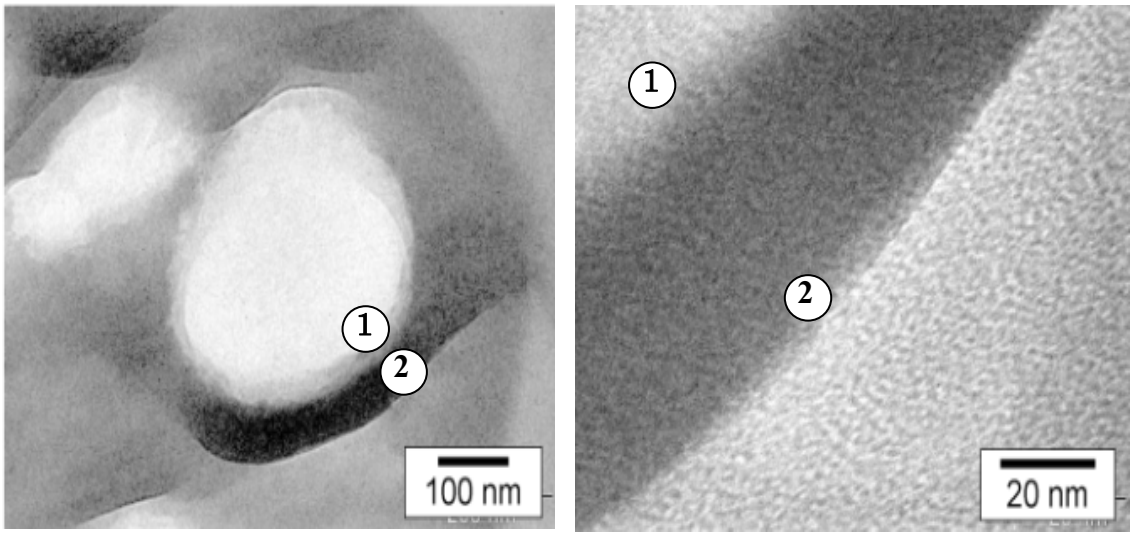

Fig.2.14. TEM photographs of PMMA/PAN/PCS particle after OsO_4 vapor dyeing: 1 and 2 are the sites were EDS analysis was performed.

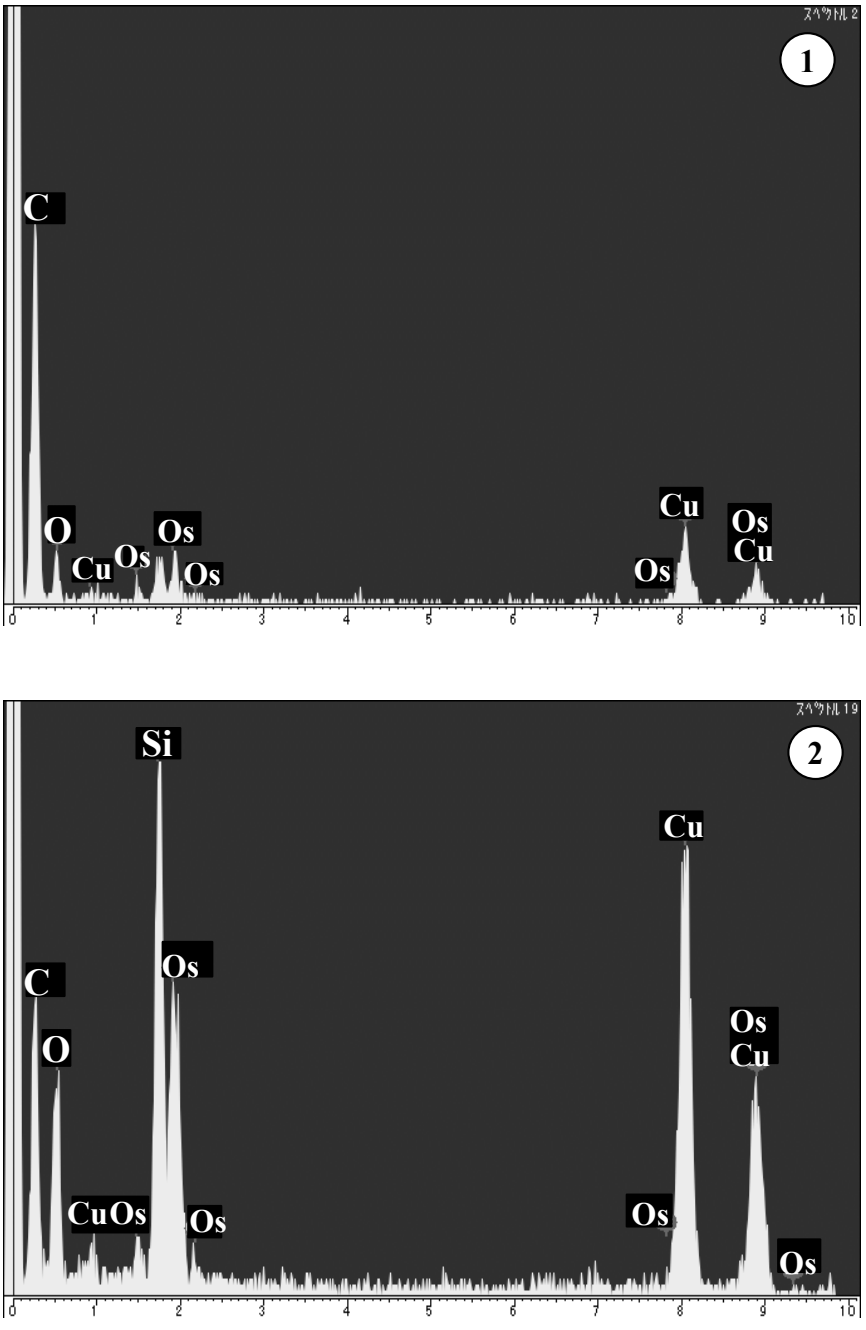

Fig.2.15. EDS profiles (sites 1 and 2) from Fig. 2.14

Table 1. Elemental compositions of sites 1 (inner) and 2 (outer) from Figure 2.14 for the PMMA/PAN/PCS core/shell particles after OsO_4 vapor dyeing.

Element	Inner (1)		Outer (2)	
	Wt %	At %	Wt %	At %
C	65.0	89.4	15.1	39.3
O	3.7	3.9	9.6	18.8
Si	-	-	18.7	20.8
Os	8.2	0.7	20.5	3.4
Cu	23.1	6.0	36.1	17.7

Finally the chemical change of PMMA/PAN/PCS sample by the treatments was examined by using FT-IR. The spectra of the core/shell particles, stabilized and heat-treated sample derived from PMMA/PAN/PCS is shown in Figure 2.16. The stabilization decreased intensities of the bands at 2100 cm^{-1} due to Si-H stretching, at 1250 cm^{-1} due to Si-CH_3 deformation and at 820 cm^{-1} due to Si-CH_3 rocking and Si-C stretching. The band at 1710 cm^{-1} assigned to C=O is also weakened. These results suggest that Si-H is oxidized to change into Si-OH. Subsequently, the Si-OH forms cross-linkages of Si-O-Si and Si-O-C by dehydrogenation reaction. The siloxane band (Si-O) at 1100 cm^{-1} was strengthened after the heat-treatment in spite of using an inert atmosphere. Possibly the survived radials react with oxygen in air after the sample was taken out from the furnace. The absorption band at 820 cm^{-1} assigned to Si-C stretching, is small.

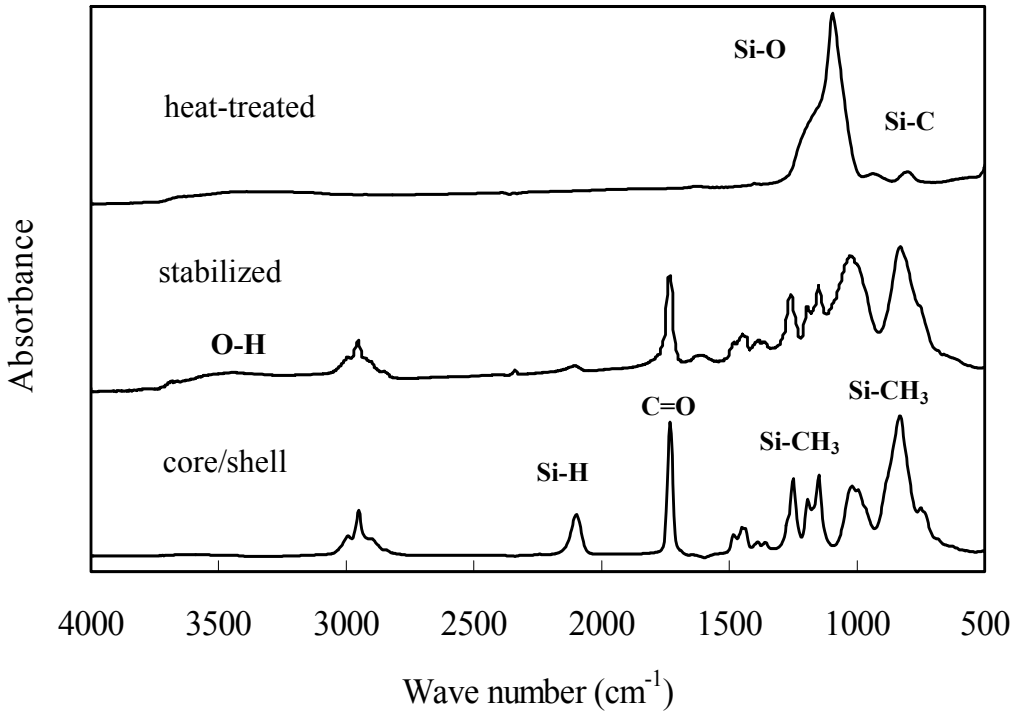

Fig.2.16. Infrared spectra of core/shell particles, stabilized and heat-treated sample derived from PMMA/PAN/PCS particles.

In order to increase the nanotube yield, the present method must be improved. From the experimental results, it is clear that the stretching technique was not efficient to elongate all the core/shell particles. A factor to be considered is the compatibility of the components of the core/shell particles that will influence the behavior during elongation. For example, if the components are compatible, the elongation should be between the two components, but if the blend is not compatible, the elongation will be influenced by the majority component.

After the stabilization process, coalesced particles were observed as indicative that the materials were insufficiently stabilized. The oxidizing agent, the temperature

and the residence time [37] are the most important factors in order to set the optimum conditions for the stabilization process. As stated before, the oxygen content of the present nanotubes was high. In the present work another techniques as electron beam, ozone and ozone-air curing were attempted in order to reduce the amount of oxygen introduced during the stabilization process but none of them were successful, the sample was insufficiently stabilized and fused during heat treatment. These aforementioned factors must be reconsidered.

2.4. Conclusions

Few SiC nanotubes were obtained from PMMA/PAN/PCS core/shell particles after heat treatment because not all core/shell particles were elongated during the stretching process. The elemental composition of one of the nanotubes prepared from the PMMA/PAN/PCS core/shell particles revealed that the ceramic yield was low. Improvement of the stretching process must be sought in order to obtain silicon carbide or hybrid (carbon/silicon carbide) nanotubes from elongated core/shell particles.

Chapter 3

Preparation of nanofibers from polycarbosilane by using polymer blend technique and their oxidation behavior

3.1. Introduction

The most popular composite materials are fiber-reinforced plastics (FRP) in which various kinds of fibers are used [38]. Particularly carbon fiber is used preferentially in advanced composite materials on the basis of high mechanical performance and lightness [39]. Novel composites materials using ceramics and metals as a matrix have become of interest in recent years. However, for these matrices carbon fiber can't be used, because carbon fiber reacts with metals or ceramics at a high temperature, leading to loosing reinforcement effect by the degradation [38]. For these matrices, ceramic fibers are used instead of carbon fibers. Various kinds of ceramic fibers are now commercially available. Among them, silicon carbide fiber is thought to be the most promising filler, in particular for light metal matrices such as aluminum [40].

The author's group joined to a challenging national project in which a target is to develop metal templates with μm size. Conventional metals can't be used here, because crystals in metal disturb fine molding or shaping. An amorphous metal with no crystals must be used instead. However, modulus of an amorphous metal is relatively low so that the template deforms easily, in other words, life time of the template is very short. In order to extend the life, an amorphous metal must be reinforced with fibers. Of

course, the fibers used must be nanofibers and in addition, have a high oxidation resistance. Silicon carbide nanofiber is one of the stronger candidates.

Silicon carbide fiber was developed by S. Yajima by using polycarbosilane as a precursor polymer and later commercialized by Nippon Carbon Co. as a trade name of Nicalon [4]. However, a commercially available silicon carbide nanofiber has not been developed until now without silicon carbide whisker [31,32]. The whisker is very expensive because of the difficulty of mass-production. This is why the present author is interested in the development of a new preparation method of silicon carbide nanofiber.

In this chapter, an attempt to prepare silicon carbide nanofiber from polycarbosilane by using polymer blend technique is described. The oxidation behavior of the resulting silicon carbide nanofibers is also shown. It is noted that the resulting nanofiber from polycarbosilane after heating is not silicon carbide stoichiometrically.

3.2. Experimental

3.2.1 Materials

Polycarbosilane (PCS) Type-L with chemical formula $[-SiH(CH_3)CH_2-]_n$ was purchased from Nippon Carbon Co. Ltd. and used as a silicon carbide precursor in this work. The number average molecular weight and the softening point are 800 and 80 ºC, respectively. Novolac-type phenol-formaldehyde resin (PF) with a softening point of 100 ^oC was supplied by Gun-ei Chemical Ind. Co. Ltd., and used as a carbon precursor. The molecular structure is shown in Figure 3.1.

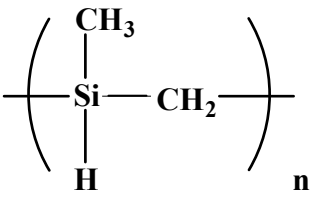

Polycarbosilane **(PCS)**

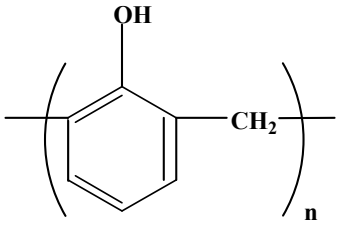

Novolac-type phenol-formaldehyde resin **(PF)**

Fig. 3.1. Molecular structures of polycarbosilane and novolac-type phenol-formaldehyde resin.

3.2.2. Preparation procedure

PCS and PF with a ratio of 3:7 by weight were dissolved into tetrahydrofuran (THF) with an ultrasonic generator. THF was removed by using a rotary evaporator and the residue was dried under vacuum at 60 ^{o}C for 24 h. The resulting polymer blend was melt-spun at 110 °C under an argon atmosphere. Figure 3.2 shows an assembly of the continuous melt-spinning apparatus. The polymer blend fibers were soaked in an acid solution containing hydrochloric acid and formaldehyde as main components for 16 hours at 100 °C in order to stabilize (cure) the PF matrix. A possible structure of the stabilized PF is shown in Figure 3.3 [41].

The stabilized polymer blend fibers were neutralized with aqueous ammonia, washed with water repeatedly, dried in a conventional furnace at 60 ^{o}C for 12 h and heat-treated at 1000 ^{o}C under a nitrogen atmosphere. The heating rate and the holding time were 100 ^{o}C/h and 1h, respectively. Finally, the heat-treated fibers were kept in a

60% nitric acid solution with stirring at 170-180 ^{o}C to remove the matrix carbon. In order to characterize the oxidation behavior during the nitric acid treatment, aliquots were taken after 30 min, 1 h, 2 h, 4 h, 8 h, 14 h, 24 h and 36 h. The released nanofibers were recovered by use of a membrane filter of 5 μm. A part of the nanofibers was further heated in a graphite tube resistance furnace at 1500 ^{o}C for 1 h under vacuum. Figure 3.4 shows the schematic flow of the preparation process of nanofibers.

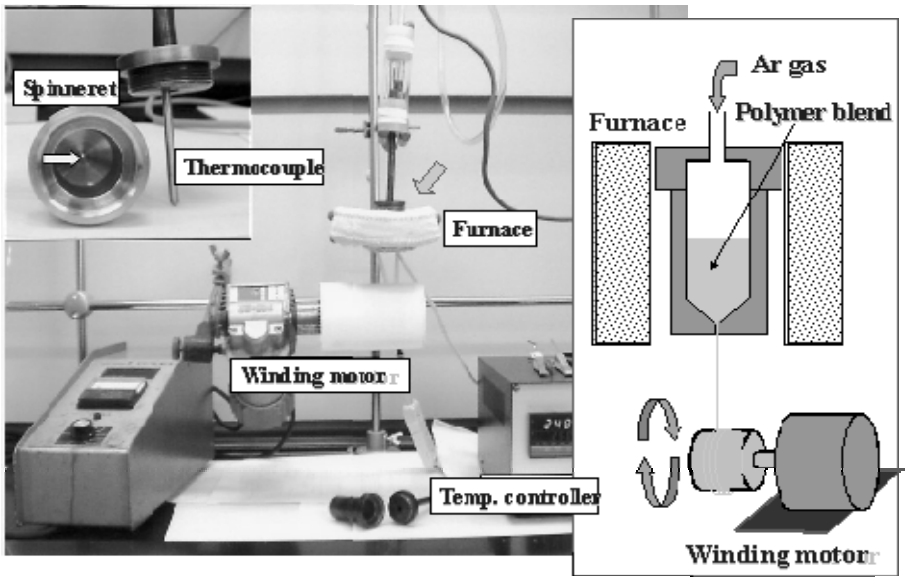

Fig.3.2. Melt-spinning apparatus.

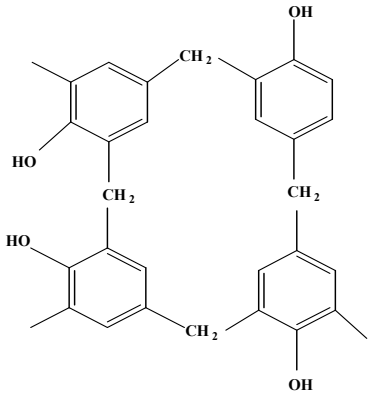

Fig.3.3. Novolac-type phenolic resin network after curing with HCl and formaldehyde .

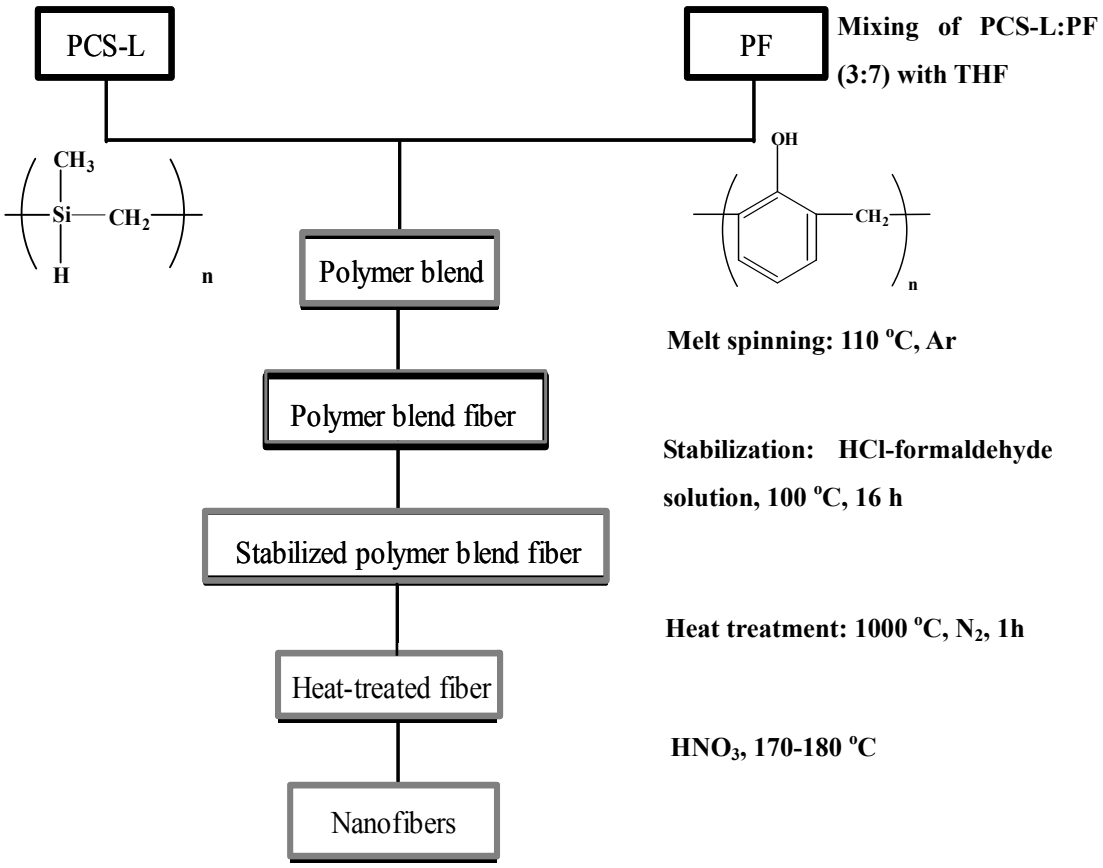

Fig.3.4. Schematic flow chart of the nanofibers preparation process by using polymer blend and melt spinning techniques.

3.2.3 Measurements

The polymer blend fibers, the stabilized polymer blend fibers and the heat-treated fibers were characterized by use of SEM. The surface morphology of the nanofibers was observed by using SEM and FE-SEM. The apparatuses were previously described in chapters 1 and 2.

3.2.3.1. X-ray photoelectron spectroscopic(XPS) analysis.

The XPS analysis for heat-treated fibers and nanofibers was performed by using a Perkin Elmer PHI-5600 apparatus with a monochromatic radiation AlKα and X-ray source with acceleration voltage 15 kV and anode power 40 W.

3.2.3.2. X-ray diffraction (XRD) analysis.

The nanofibers were subjected to X-ray diffraction analysis by using a Rigaku RINT2000/PC apparatus under acceleration voltage of 40 kV and current of 40 mA.

3.2.3.3. N_2 absorption/desorption measurement.

The specific surface area of the heat-treated fibers and the nanofibers was calculated from N_2-absorption/desorption isotherms measured at 77K. The apparatus was BELSORP 28SA (Japan Bell Corporation). Before the measurement, the samples were dried at 200 °C for 3 h.

3.3. Results and discussion

Figure 3.5 shows SEM photographs of the polymer blend fiber, the stabilized polymer blend fiber and the heat-treated fiber. As suggested from smooth surface of the polymer blend fiber in Figure 3.5 (a), the polymer blend showed a high spinnability. A cross-section of the stabilized fiber is shown in Figure 3.5 (b), in which the fine particles of about 1 μm or less (arrowed by 1) are seen together with elongated PCS

particles (arrowed by 2) pulled out from the PF matrix. Figure 3.5 (c) shows the fiber after the heat-treatment at 1000 ^{o}C. The smooth surface of the polymer blend fiber was somewhat changed after the heat treatment as seen in Fig.3.5 (c).

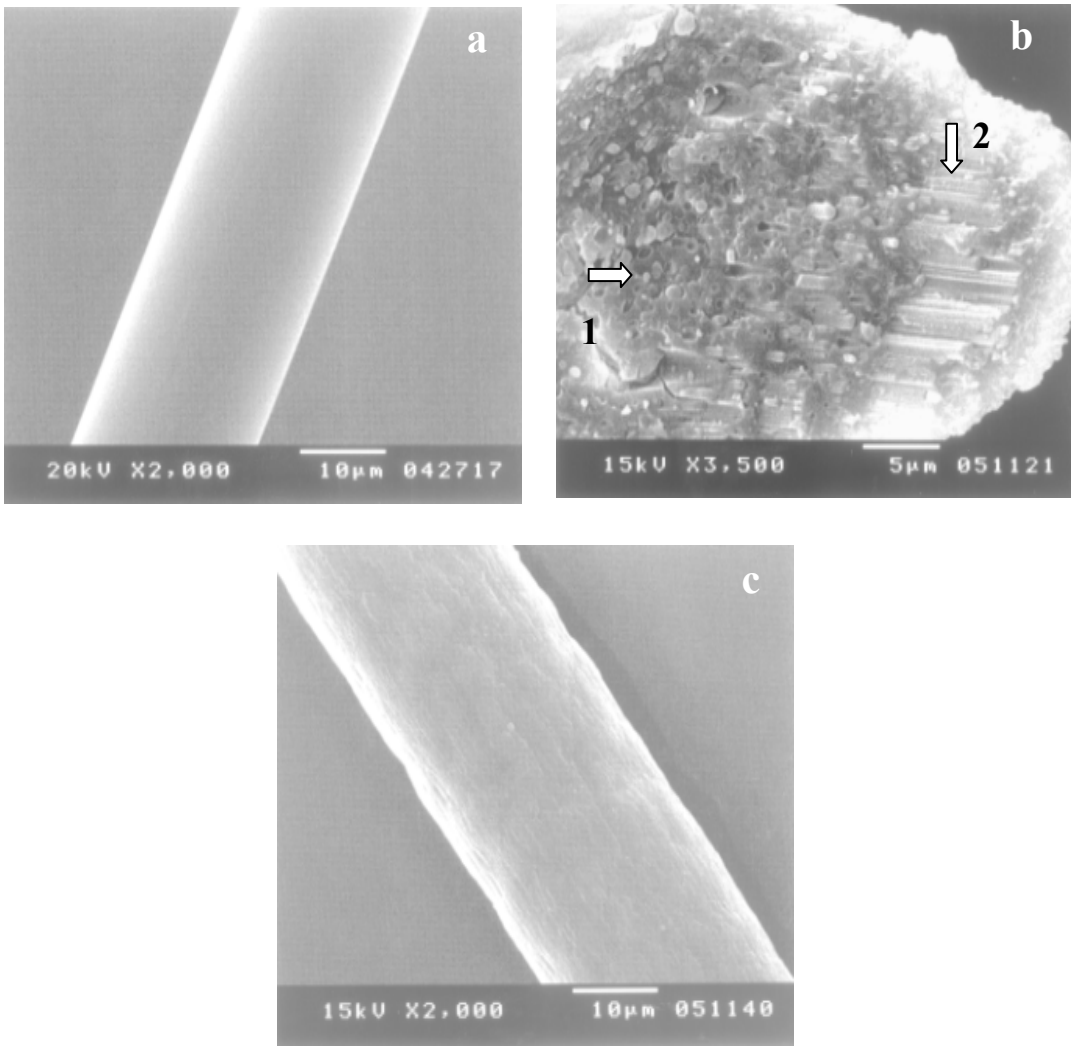

Fig.3.5. SEM photographs of a) the polymer blend fiber, b) stabilized polymer blend fiber and c) heat-treated fiber.

Figure 3.6 (a) and (b) show the cross-sections of relatively thin and thick blend fibers after the stabilization. They were further heated at 1000 ^{o}C and then treated with the nitric acid for 14 h. Figures 3.6 (c) and (d) shows thin and the thick fibers after the treatment, respectively. As seen in Figure 3.6 (c), the thin fibers resulted in a bundle of nanofibers. However, both nanofibers and fine particles were obtained from the thick fibers as seen in Figure 3.6 (d). They were formed at the periphery and the center regions of the thick fiber, respectively.

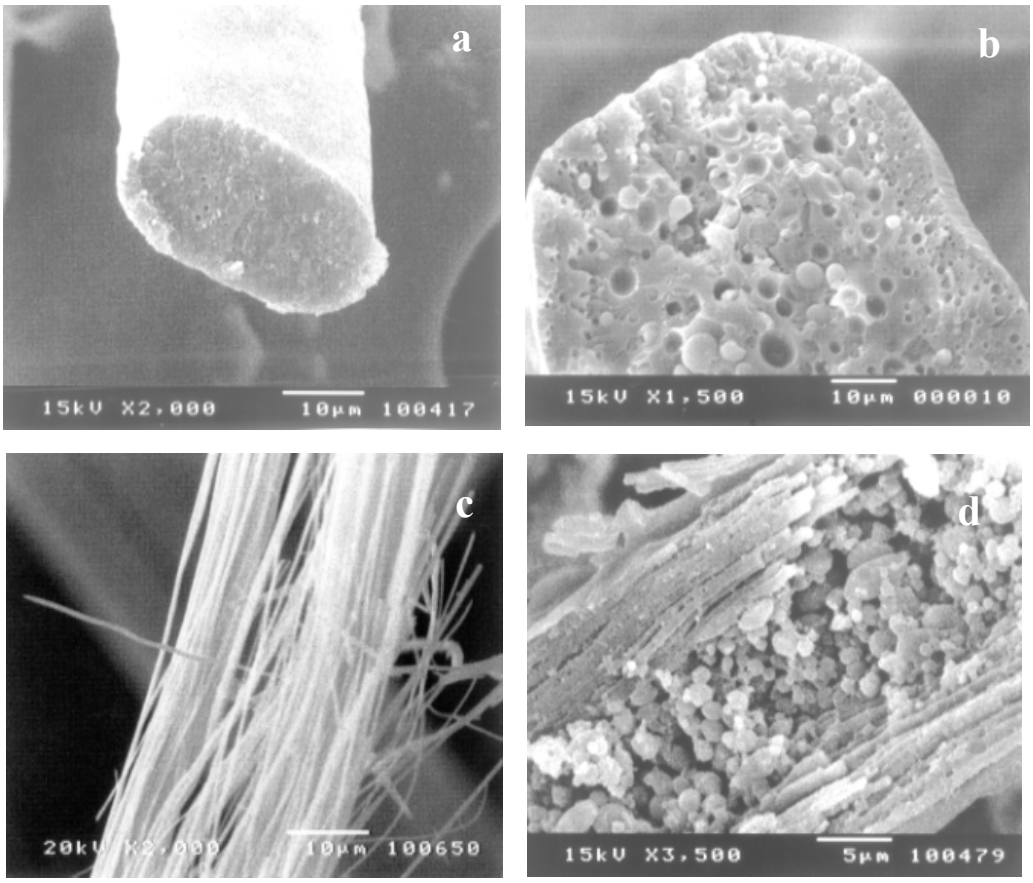

Fig.3.6. SEM photographs of a) thin and b) thick stabilized polymer blend fibers and c) and d) nanofibers after nitric acid treatment.

There are two possible reasons to explain the formation of the fine particles. One is that the center of thick fibers is subjected to less shear stress at the spinning process, leading to no elongation. This idea is shown in Figure 3.7 schematically. Another idea is that since the elongated PCS particles in the PF matrix were stabilized insufficiently, particularly in the center of the thick fibers, they rolled up by fusing during the heat treatment. To prepare high purity nanofibers, thinner polymer blend fibers must be spun.

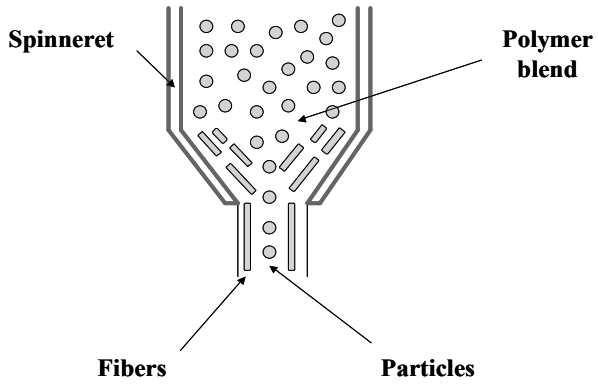

Fig.3.7. Possible cause of the formation of the fine particles.

In order to spin thin polymer blend fibers to avoid the formation of particles, the winding speed at spinning must be increased. Figure 3.8 shows the thin blend fibers spun under a high winding speed, from which the nanofibers shown in Figure 3.9 were obtained after the carbonization at 1000 ^{o}C and the nitric acid treatment for 14 h. Another way is to use other types of spinning apparatus. In particular, a melt-blown spinning apparatus is useful to spin thin fibers with several μm in diameter.

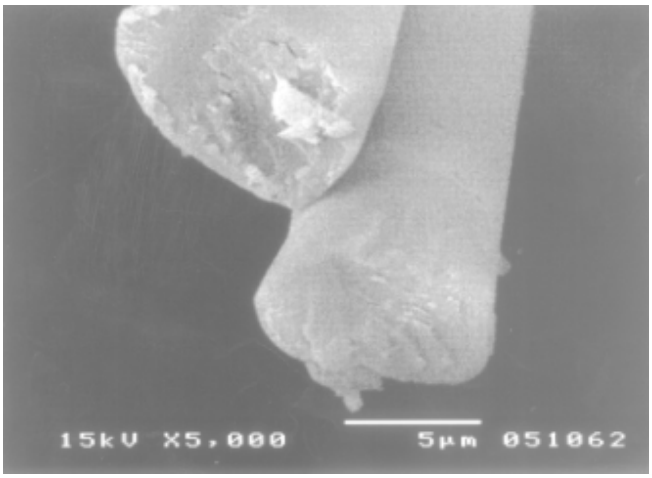

Fig.3.8. SEM photograph of polymer blend fibers using higher winding speed.

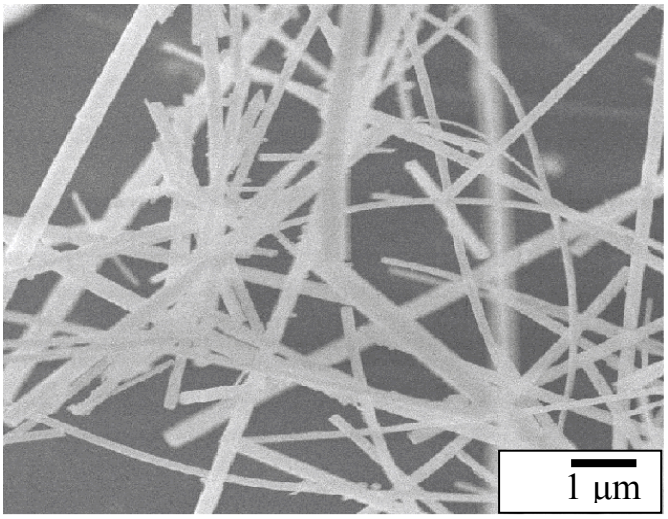

Fig.3.9. FE-SEM photograph of nanofibers after nitric acid treatment using higher melt-spinning winding speed.

Next, in order to make clear the oxidation behavior of nanofibers, the heat-treated blend fibers were soaked in the nitric acid and aliquots were taken out after soaking for 30 min, 1 h, 2 h, 4 h, 8 h, 14 h, 24 h and 36 h. Figures 3.10 and 3.11 show the SEM photographs of the samples after the nitric acid treatment for the various times.

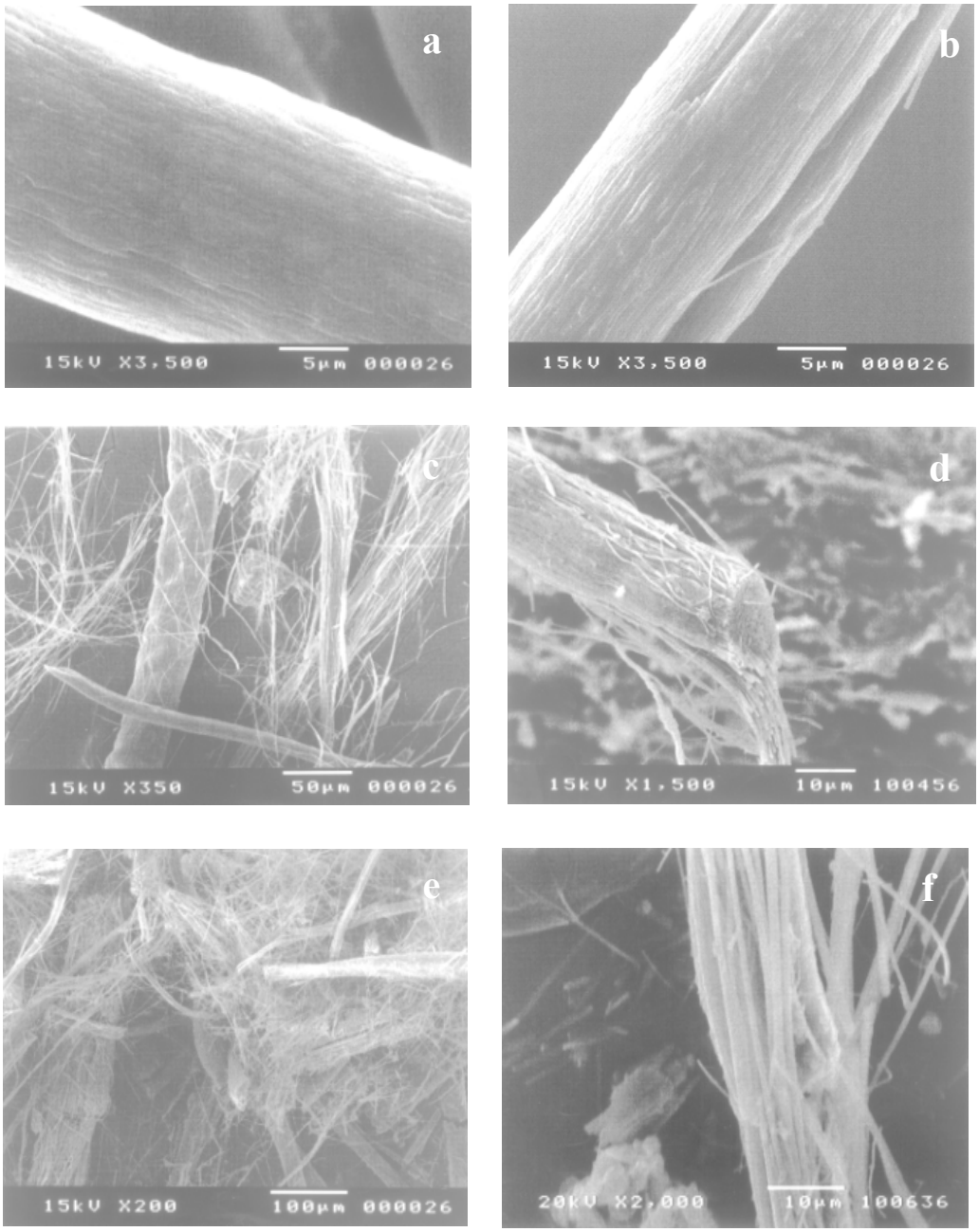

Fig.3.10. SEM photographs of the release of nanofibers after nitric acid treatment for the oxidation times of a) 30 min, b) 1 h, c) and d) 2 h, and e) and f) 4 h.

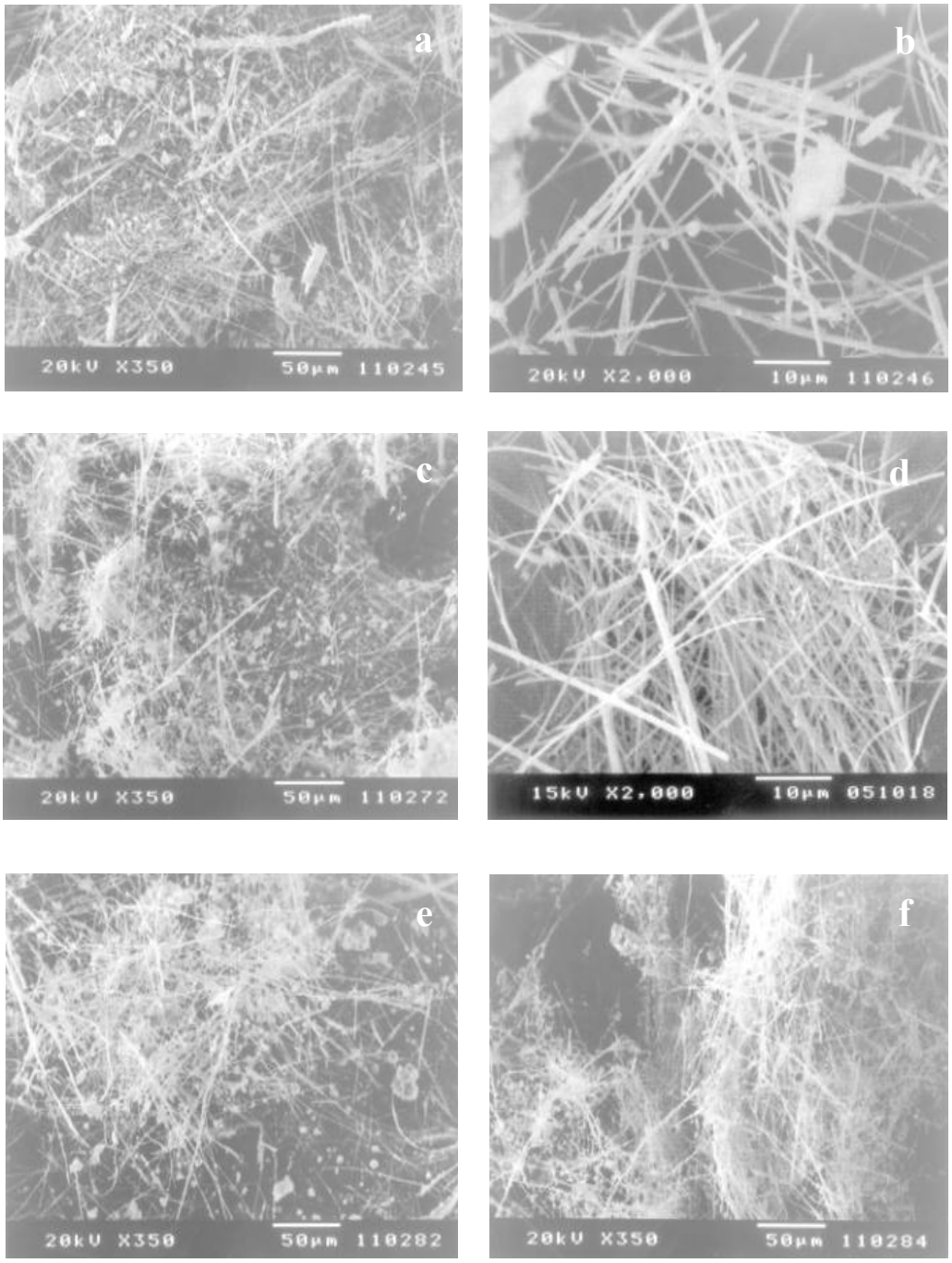

Fig.3.11. SEM photographs of the release of nanofibers after nitric acid treatment for the oxidation times of a) and b) 8 h, c) and d) 14 h, e) 24 h and f) 36 h.

No effect was observed after the nitric acid treatment for 30 min, because the surfaces in Figure 3.10 (a) and Figure 3.5 (c) are quite similar each other. After the treatment of 1 h, the nanofibers hardly appeared on the fiber surface but were not separated from the matrix carbon (Figure 3.10 (b)). As the treatment time is extended, the matrix carbon is removed gradually and the nanofibers were released as shown in Figures 3.10 (c)-(f). Just a small amount of the matrix carbon remained after the treatment for 4 h.

Figure 3.11 shows the nanofibers obtained after the nitric acid treatments of 8 h to 36 h. The nanofiber diameter showed some scatter as seen in Figure 3.11(b) and also they seem to be gradually broken with the extension of the treatment time. The nitric acid treatment (oxidation) is thought to generate micropores in the nanofibers. Therefore, the BET specific surface area (SSA) was measured.

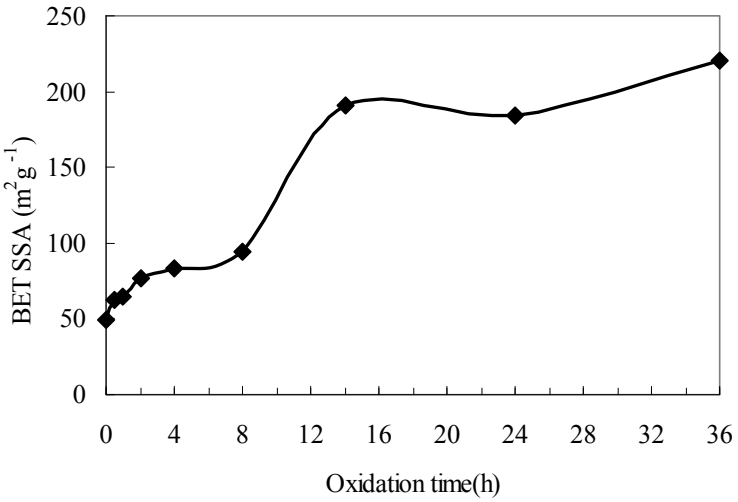

Fig.3.12. BET specific surface area vs. oxidation time for the heat-treated fibers and nanofibers.

Figure 3.12 shows changes of BET-SSA with increasing of the oxidation. The BET specific surface area increased from 50 m^2 g^{-1} for the pristine heat-treated fiber to 200 m^2 g^{-1} for the nanofibers obtained after the 14 h oxidation time. The most significant change occurred between 8 h and 14 h. Few change was observed by further extension of the oxidation time. The surface area will be increased by two factors: first, the release of the nanofibers after the removal of the matrix carbon, and second, the formation of micropores by nitric acid in the nanofibers. The value of the theoretical surface area calculated assuming the length and diameter of the nanofibers from the FE-SEM photographs is ca. 8.3 m^2 g^{-1}. Therefore, the formation of micropores in the nanofibers is the most important factor to consider.

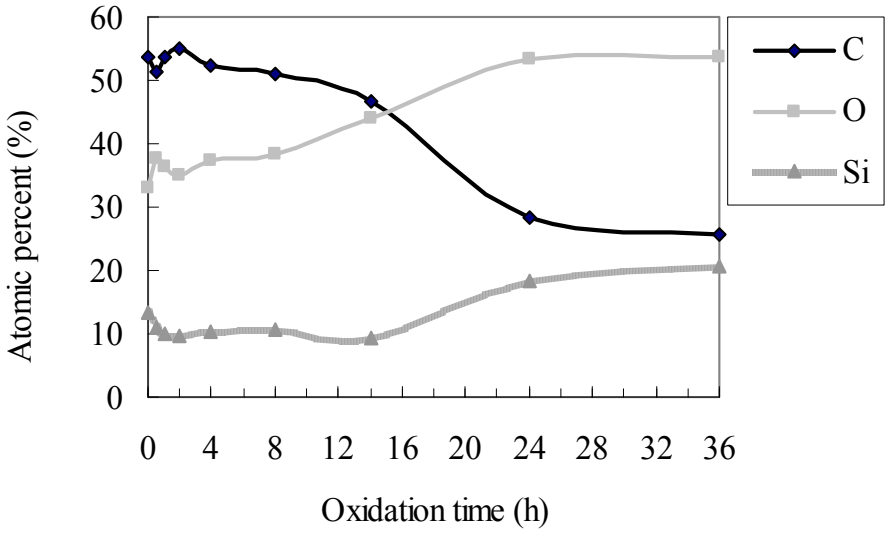

Fig.3.13. XPS analysis of the heat-treated fibers and nanofibers with oxidation time.

The oxygen content in the nanofibers is very important, because the oxygen results in a lowering of the mechanical properties of silicon carbide fiber, particularly at higher temperature [42]. Figure 3.13 shows changes of elemental compositions (atomic %) with increasing of the oxidation time. Mild changes of the compositions were observed at shorter oxidation time than 8 h. Of course, the carbon content must be decrease because the matrix carbon is removed gradually as the oxidation time is increased as shown in Figures 3.10 and 3.11, but the changes seem too little in view of the removal of matrix carbon. Drastic change occurred between 8 h and 24 h of the oxidation time, and no changes were observed with extending of the oxidation time.

According to the SEM photographs from Figures 3.10 and 3.11, the nanofibers are completely released from the matrix carbon between 8 and 14 h of the oxidation time. It is important to consider the relationship between the increase of surface area due to separation of the nanofibers after removal of the matrix carbon and formation of micropores. The oxygen content increased from 38 at. % to 43 at.% between 8 h and 14 h, and reached to more than 50 at.% at 36 h. In order to release completely the nanofibers with a less amount of oxygen as possible, the oxidation time between 8 h and 14 h is required. Therefore, 10 h was selected as the optimum time.

On the basis of the results, the polymer blend was spun with a high winding speed and the resulted heat-treated blend fibers were oxidized for 10 h with the nitric acid. Figure 3.14 shows the SEM photographs of the resulting nanofibers. The nanofibers are separated and particles are scarcely observed. Although the nanofibers were completely separated and the particles were not observed the oxygen content was

very high, 49 at.%. How to decrease the oxygen in the present nanofibers is the main problem to be solved. In order to avoid the use of a strong oxidizing agent, a new matrix polymer with the requirements of allow an efficient stabilization of PCS and at the same time be stable toward re-melting on heat treatment must be sought.

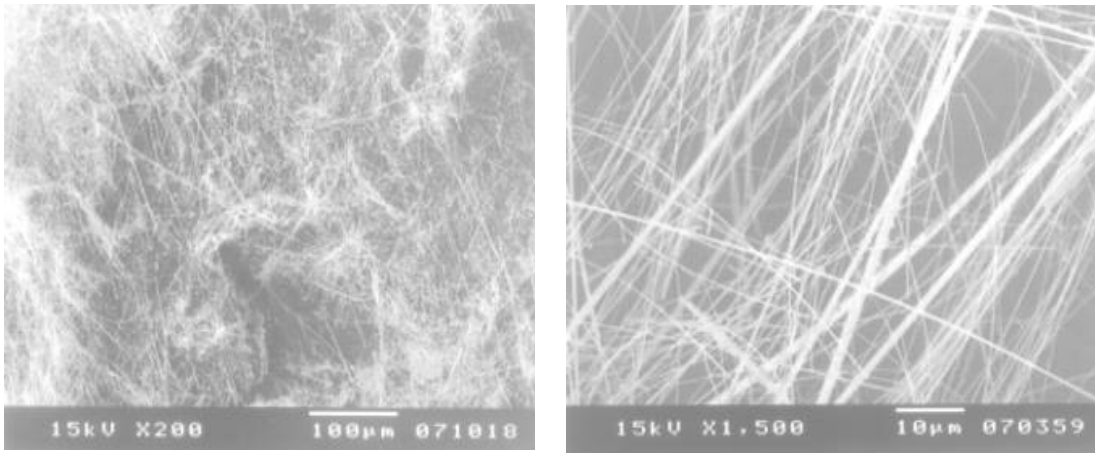

Fig.3.14. SEM photographs of the nanofibers after 10 h nitric acid treatment and higher winding speed.

Finally, the microstructural change of the nanofibers with increasing the heat treatment temperature was characterized by XRD analysis. Figure 3.15 includes XRD profiles of Nicalon fiber and β-SiC as references. The nanofibers heat-treated at 1000 ^{o}C are amorphous and changed into β-SiC after heat treatment at 1500 ^{o}C, analogous to Nicalon fibers [34].

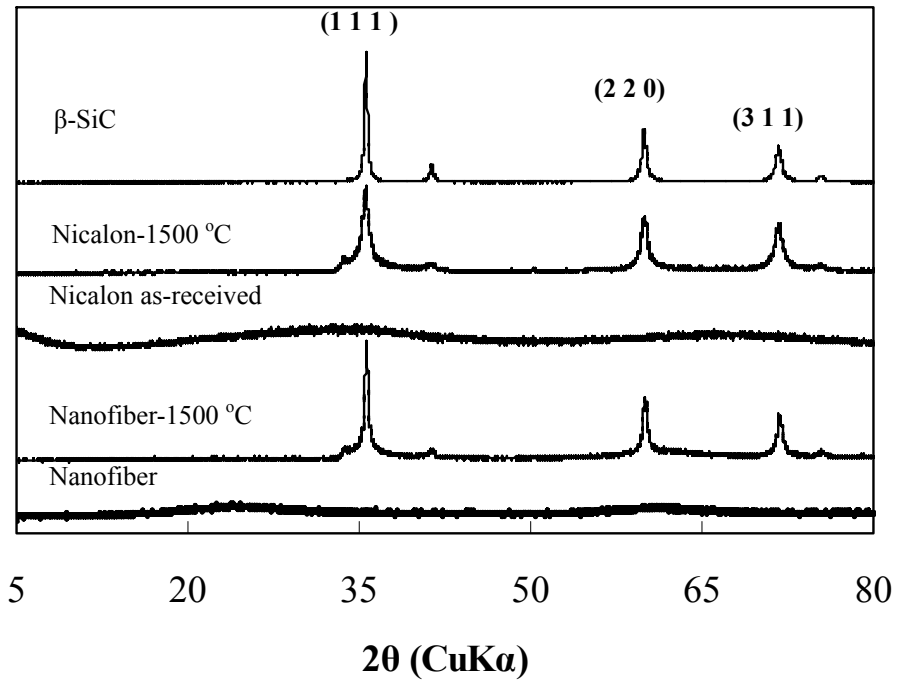

Fig.3.15. XRD profiles of the nanofibers and references.

3.4. Conclusions

Nanofibers of several 100 nm in diameter and more than 100 μm in length were prepared from polycarbosilane by using polymer blend technique. However, fine particles were observed in the center of thick fibers after stabilization and after nitric acid treatment, in addition to the nanofibers. The formation of the particles was suppressed by spinning thin blend fibers with a high winding speed. Highly purity nanofibers were obtained by oxidizing the heat-treated blend fibers with the nitric acid for 10 h. However the oxygen content was high. The resulting nanofibers were amorphous and changed into β-SiC after heating at 1500 °C.

Chapter 4

Microstructural analysis of nanofibers prepared from polycarbosilane by using of polymer blend and melt-spinning techniques

4.1. Introduction

As noted in the previous chapter silicon carbide fiber named as Nicalon is produced commercially from polycarbosilane by Nippon Carbon Co. Ltd. Nicalon is expected to be used as a filler in metal- and ceramic-based composites. Carbon fiber can't be used for these matrices, because it reacts with these matrices to degrade and looses its high reinforcement effect [39].

Polycarbosilane is conventionally stabilized (cured) by oxidizing in air. Therefore, Nicalon shows relatively large oxygen content more than 10% as an unstable oxycarbide phase. When the oxycarbide is heated to a higher temperature more than 1000 ^{o}C, it decomposes into β-SiC and gases of SiO and CO, leading to damage into the fiber. As a result, the mechanical properties are lowered. Also if Nicalon is heated to a temperature higher than 1350 ^{o}C, β-SiC crystal deposits and grows, which lowers the mechanical properties drastically. Therefore how to decrease the oxygen content is a key to develop silicon carbide fiber with high mechanical properties at high temperature [43].

As shown in the previous chapter, the silicon carbide-based nanofibers, though with high oxygen content, were prepared but their microstructures were not made clear. It is sure that the microstructure of the nanofiber relates intimately with its mechanical

and other properties. Therefore, the microstructure must be revealed in order to improve properties of the nanofibers.

In this chapter, the microstructures of the nanofibers after heating at 1000 ^{o}C and 1200 ^{o}C were examined in detail by use of microscopy, XRD, N_2-absorption/desorption isotherms, XPS and the TG mass spectroscopy.

4.2. Experimental

4.2.1. Materials

Polycarbosilane (PCS) Type-L with chemical formula of $[-SiH(CH_3)CH_2-]_n$ was used in this work. The number average molecular weight and the softening point are 800 and 80 ºC, respectively. Novolac-type phenol-formaldehyde resin (PF) with a softening point of 100 ^{o}C was kindly supplied by Gun-ei Chemical Ind. Co. Ltd. and used as a carbon precursor. The structures of both polymers are shown in Figure 4.1.

Polycarbosilane **(PCS)** Novolac-type phenol-formaldehyde resin **(PF)**

Fig. 4.1. Molecular structures of polycarbosilane and Novolac-type phenol-formaldehyde resin.

4.2.2. Preparation procedure

PCS and PF with a ratio of 3:7 by weight were dissolved in tetrahydrofuran (THF) by using an ultrasonicator. THF was removed and the resulting polymer blend was dried under vacuum at 60 ^{o}C for 12 h. The polymer blend was melt-spun continuously at 110 °C under an argon atmosphere. The polymer blend fibers were soaked in an acid solution containing hydrochloric acid and formaldehyde as main components at 100 °C for 16 h. The stabilized polymer blend fibers were neutralized with aqueous ammonia, washed with de-ionized water repeatedly and dried. The fibers were heated at 1000 ^{o}C and 1200 ^{o}C under a nitrogen atmosphere with a heating rate of 100 ^{o}C/h and a holding time of 1h. Finally the heat-treated fibers were soaked in 60% nitric acid solution at 170-180 ^{o}C for 10 h with stirring to remove the matrix carbon, and released nanofibers were recovered by using a membrane filter of 5 μm.

4.2.3 Measurements

FE-SEM, TEM, XRD and the absorption/desorption measurement for the nanofibers were performed using the same apparatuses described in the previous chapters.

4.2.3.1. X-ray photoelectron spectroscopic(XPS) analysis.

Elemental compositions of filaments of the nanofibers were measured by an X-ray photoelectron spectrometer (XPS), Thermo Electron Theta Probe, with a

monochromatic radiation AlKα. The filaments were etched by Ar^+ and the final etching time was 2500 sec. The etching rate of 0.18 nm/sec for SiO_2 film was used as a reference. The peak deconvolution was made by addition of Gaussian–Lorentzian components. The measurement was performed by Sumika Chemical Analysis Service.

4.2.3.2. Thermogravimetric (TG) mass spectra analysis.

TG mass analysis was carried out by using a Rigaku Thermo plus TG8120 apparatus coupled with a Hewlett Packard 5973 mass selective detector and a Hewlett Packard HP 6890 gas chromatograph. The heating rate and the He gas flow rate were 30 ^oC /min and 400 ml/min, respectively.

4.3 Results and discussion

Figure 4.2 shows FE-SEM photographs of the nanofibers obtained from blend fibers heat-treated at 1000 ^oC and 1200 ^oC, respectively. In the present chapter they are referred as 1000 ^oC-nanofibers and 1200 ^oC-nanofibers. The average diameter of the nanofibers was below 1 μm, although some scatter was seen in the diameters of both the nanofibers. The 1000 ^oC-nanofibers (Figure 4.2 (a)) were shorter than the 1200 ^oC-nanofibers (Figure 4.2 (b)), because the former seemed to be fragile and were broken during the stirring in nitric acid. It should be noted that the nanofibers, particularly the 1200 ^oC-nanofibers, were straight and very long.

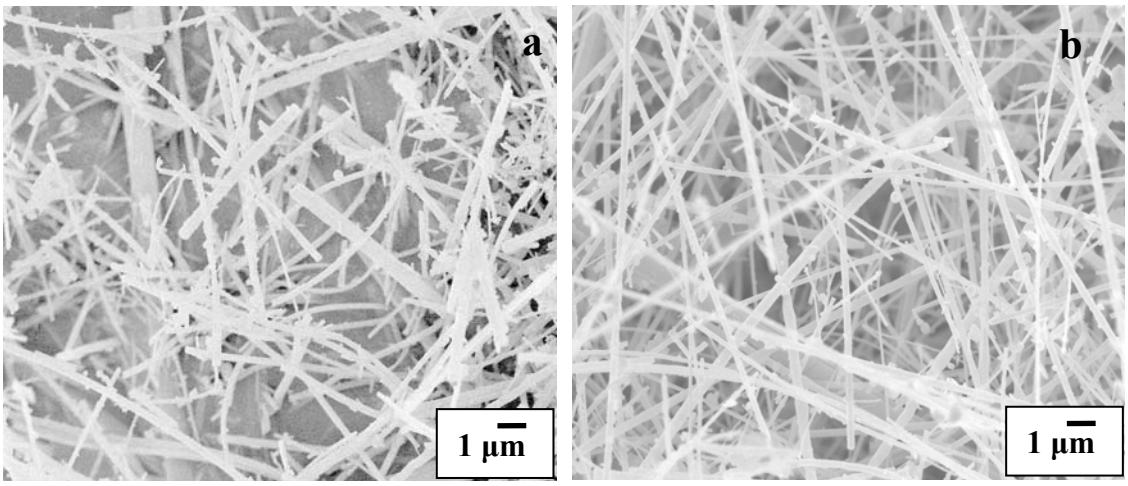

Fig.4.2. FE-SEM photographs of the a) 1000 ^{o}C-nanofibers and b) 1200 ^{o}C-nanofibers.

Figure 4.3 show FE-SEM photographs of a 1000 ^{o}C-nanofiber and a 1200 ^{o}C-nanofiber. There was some difference in the appearance of these nanofibers, but on the whole, the 1200 ^{o}C-nanofiber showed a smoother surface than did the 1000 ^{o}C-nanofiber.

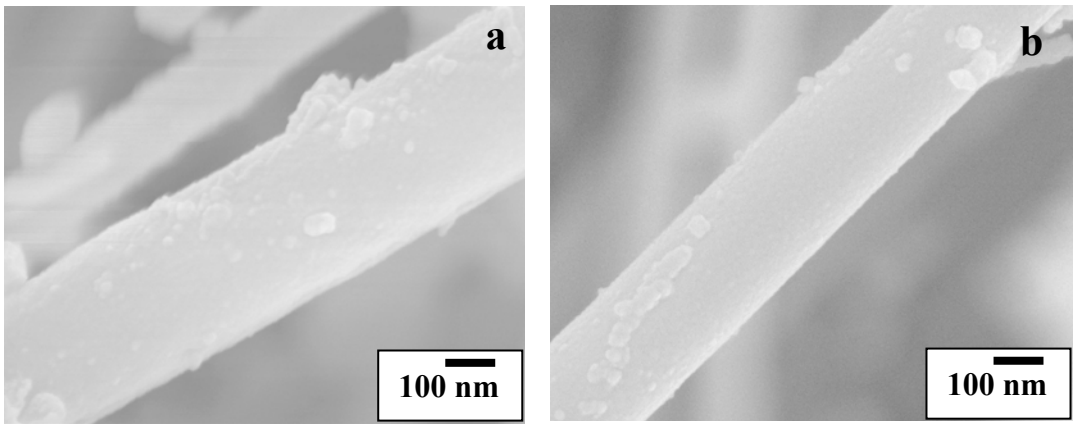

Fig.4.3. FE-SEM photographs of a) 1000 ^{o}C-nanofiber and b) 1200 ^{o}C-nanofiber.

Figure 4.4 shows TEM photographs of a 1000 ^{o}C-nanofiber and a 1200 ^{o}C-nanofiber. As evidenced from Figure 4.4 (a) the surface of the 1000 ^{o}C-nanofiber was very rough, possibly because of severe oxidation by nitric acid [44]. The surface of the 1200 ^{o}C-nanofiber was far smoother, compared with that of the 1000 ^{o}C-nanofiber.

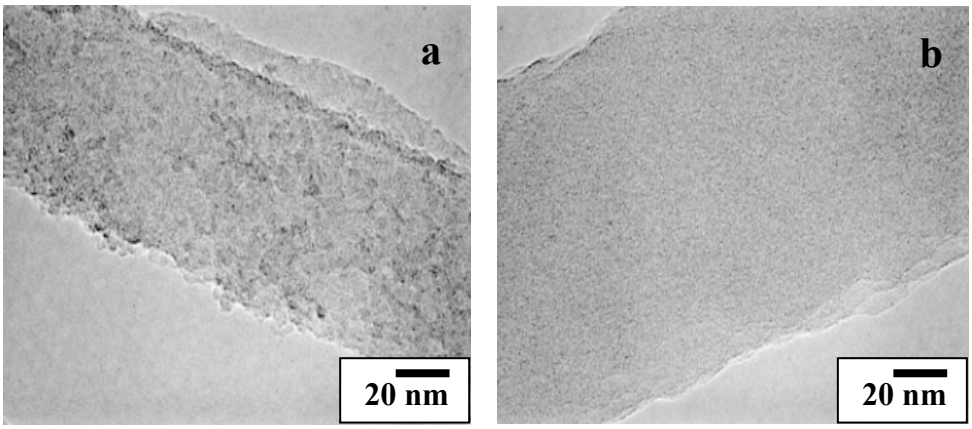

Fig.4.4. TEM photographs of a) 1000 ^{o}C-nanofiber and b) 1200 ^{o}C-nanofiber.

XPS analysis was performed to determine the chemical structures of the 1000 ^{o}C-nanofibers and 1200 ^{o}C-nanofibers. The XPS wide scan spectrum of the 1000 ^{o}C-nanofibers without etching is shown in Figure 4.5. The spectrum revealed the existence of Si, C and O in the nanofibers. A similar spectrum observed for the 1200 ^{o}C-nanofibers is shown in Figure 4.6.

As mentioned above, a major concern of the author was the oxygen introduced in the present in the nanofibers. Figures 4.7 and 4.8 show changes in the elemental composition of 1000 ^{o}C-nanofibers and 1200 ^{o}C-nanofibers as a function of increasing

the etching time (i.e., distance from the surface). An etching time of 2500 sec corresponded to a depth of 450 nm for SiO_2 film. The 1000 ^{o}C-nanofibers contained a large amount of oxygen and just a slight amount of carbon as one would expect based on the rough surface seen in the TEM photograph (Figure 4.4 (a)). The elemental composition remained unchanged in the filaments interior. Figure 4.8 suggests that the 1200 ^{o}C-nanofibers were more oxidation resistant than the 1000 ^{o}C-nanofibers. The at. % oxygen decreased gradually from the surface to the interior and reached ca. 30 at. % at 2500 sec. The carbon and silicon contents showed opposite behaviors, and the filaments interior contained a roughly constant C:Si:O atomic ratio of 1:1:1.

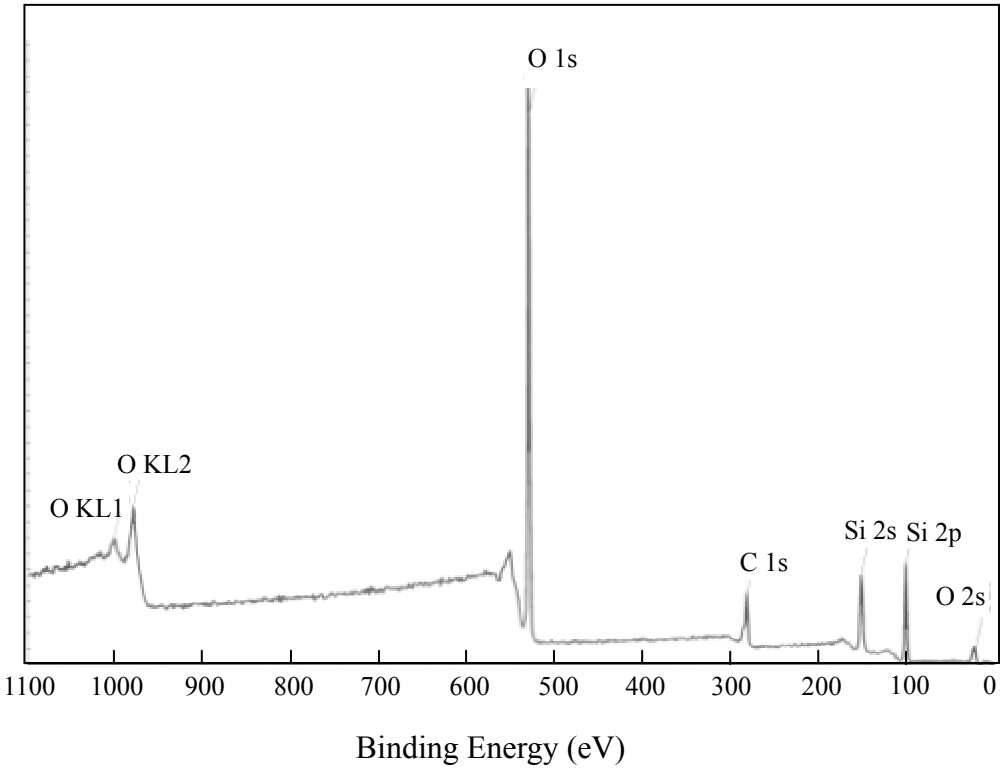

Fig.4.5. XPS wide scan spectra for the 1000 ^{o}C-nanofibers.

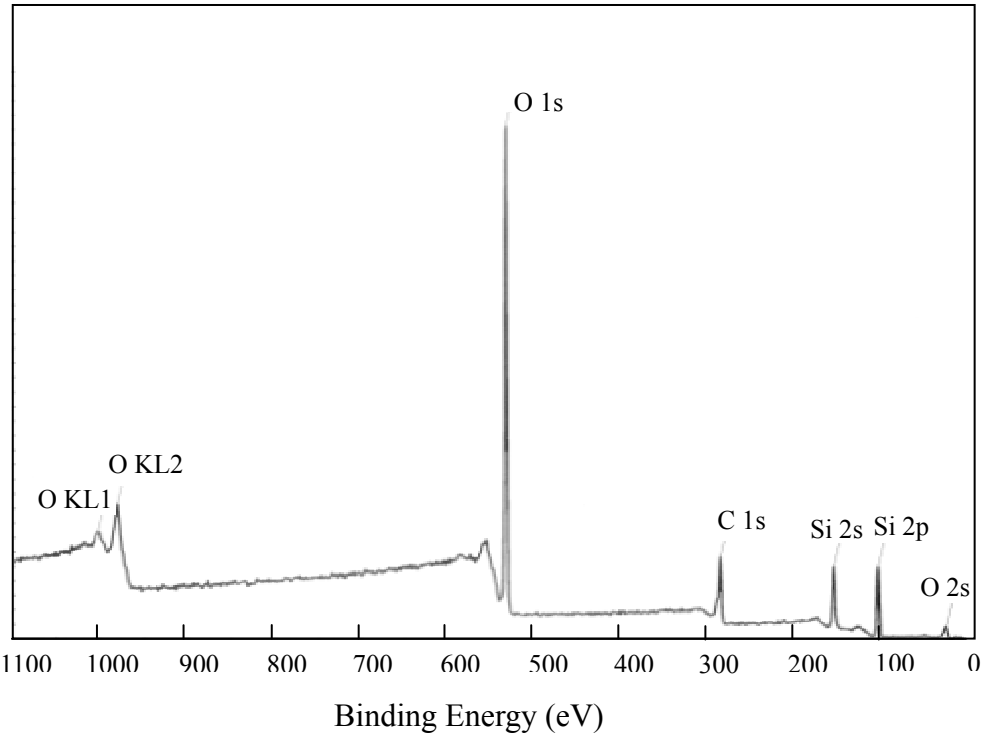

Fig.4.6. XPS wide scan spectra for the 1200 °C-nanofibers.

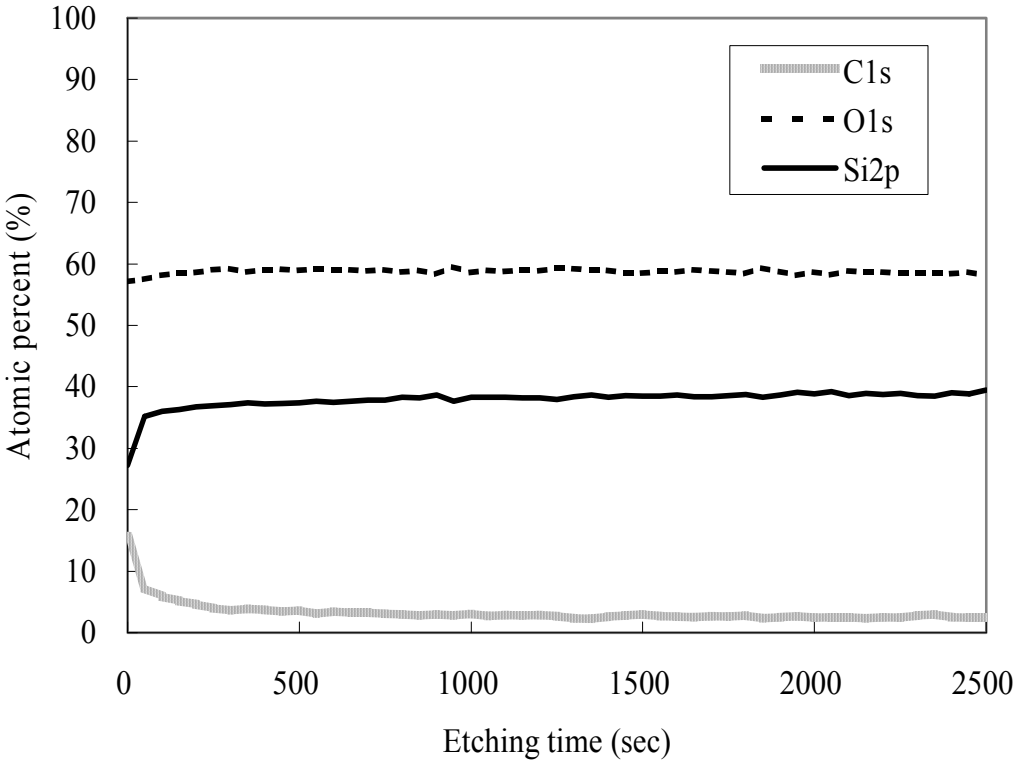

Fig.4.7. Depth profile of the 1000 °C-nanofibers as function of the etching time.

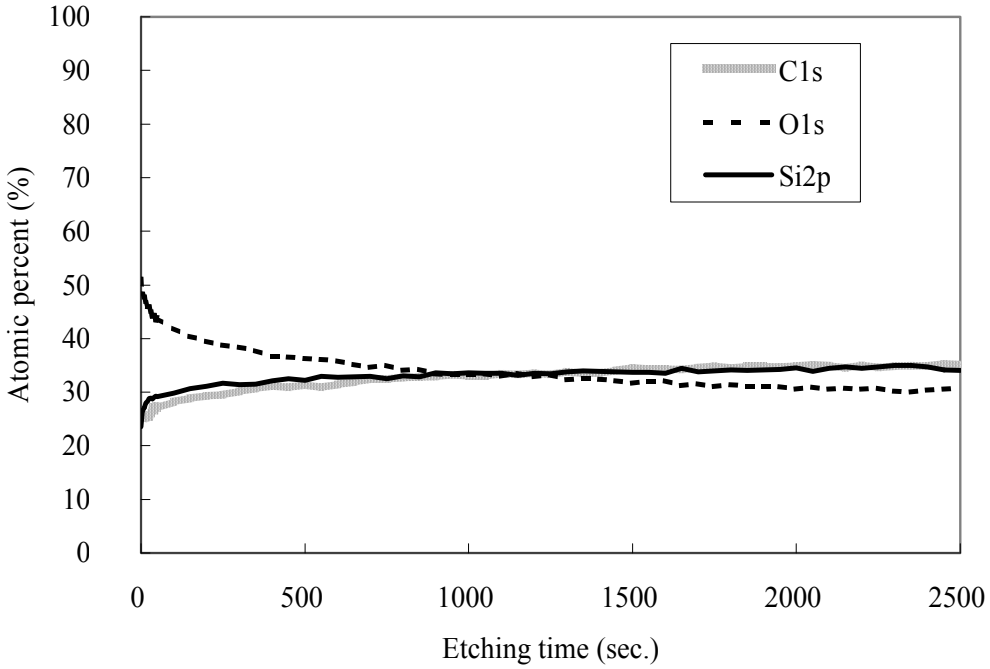

Fig.4.8. Depth profile of the 1200 ^{o}C-nanofibers as function of the etching time.

Table 1 shows the analysis of the chemical bonds and the attributions of the Gaussian-Lorentzian components for C 1s, O 1s and Si 2p of the 1000 ^{o}C-nanofibers after 2500 sec of etching time. Figures 4.9 and 4.10 show the C 1s core-level spectra and the Si 2p core-level spectra for the 1000 ^{o}C-nanofibers after 2500 sec of etching time, respectively. These data showed that the 1000 ^{o}C-nanofibers mainly consist of a silicon oxide phase (SiO_2).

Table 2 shows the analysis of the chemical bonds and the attributions of the Gaussian-Lorentzian components for C 1s, O 1s and Si 2p of the 1200 ^{o}C-nanofibers before and after 2500 sec of etching time. Figure 4.11 shows C 1s core-level spectra of the 1200 ^{o}C-nanofibers and Figure 4.12 shows the Si 2p core-level spectra of the same nanofibers. The surface of the 1200 ^{o}C-filaments consist of carbon in C-C or C-H,

C=O and silicon dioxide (SiO_2). The oxidized carbon disappeared after the etching. The interior is composed of a silicon oxycarbide phase (SiC_xO_y).

Table 1. Analysis of the chemical bonds from the XPS experiments and attributions of the Gaussian-Lorentzian components for the 1000 ^oC-nanofibers after 2500 sec of etching time.

	1000 ˚C after etching BE (eV)	At. %	Attribution
C 1s	284.4	2	C-C, C-H
	285.7	0.5	C-O
O 1s	533.4	57	SiO_2
Si 2p	101.0	2	SiC_xO_y
	103.5	38	SiO_2

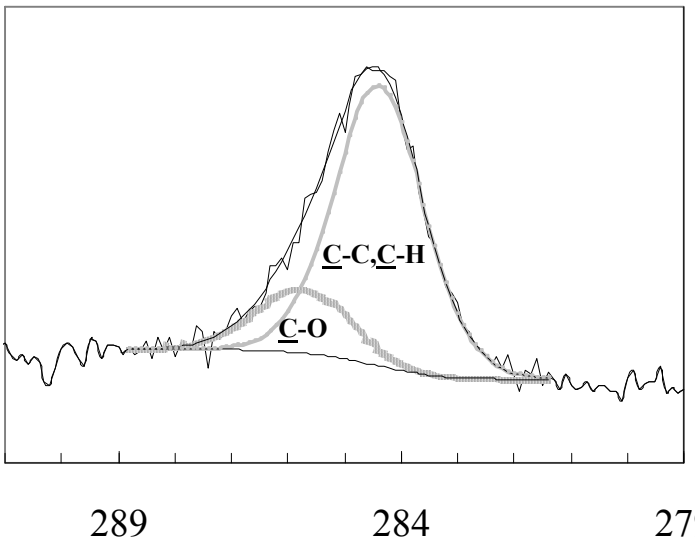

Fig. 4.9. C 1s core-level spectra of the 1000 ^oC-nanofibers after 2500 sec of etching time.

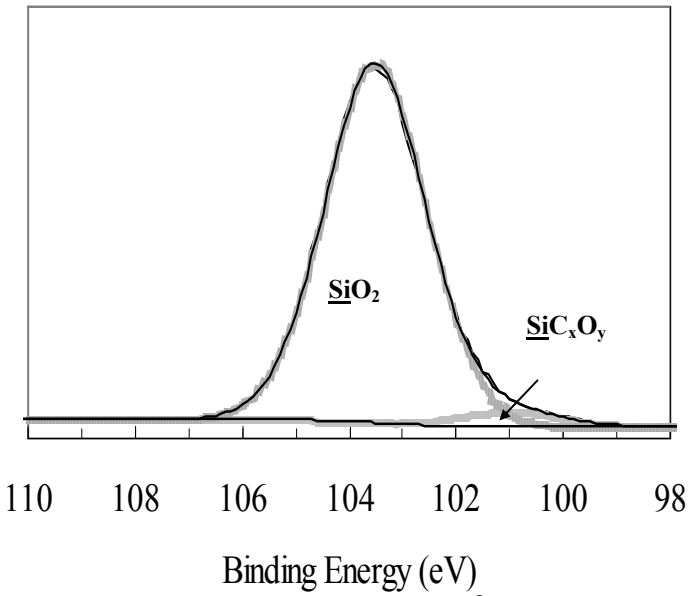

Fig. 4.10. Si 2p core-level spectra of the 1000 °C-nanofibers after 2500 sec of etching time.

Table 2. Analysis of the chemical bonds from the XPS experiments and attribution of the Gaussian-Lorentzian components for the 1200 °C-nanofibers before and after 2500 sec of etching time.

	1200 ˚C before etching BE (eV)	At. %	1200 ˚C after etching BE (eV)	At. %	Attribution
C 1s	-		283.8	36[a]	$Si\underline{C}_xO_y$
	285.0	18	285.6		$\underline{C}$-C, $\underline{C}$-H
	286.9	2	-		$\underline{C}$=O
	289.1	5	-		-$\underline{C}O_3$
O 1s	-		532.1	29	$SiC_x\underline{O}_y$
	532.9	51[b]			$Si\underline{O}_2$
	534.4				-$C\underline{O}_3$
Si 2p	-		101.3	35	$\underline{Si}C_xO_y$
	103.2	24	-		$\underline{Si}O_2$

[a] ($Si\underline{C}_xO_y$ + $\underline{C}$-C, $\underline{C}$-H) , [b] ($Si\underline{O}_2$ + -$C\underline{O}_3$)

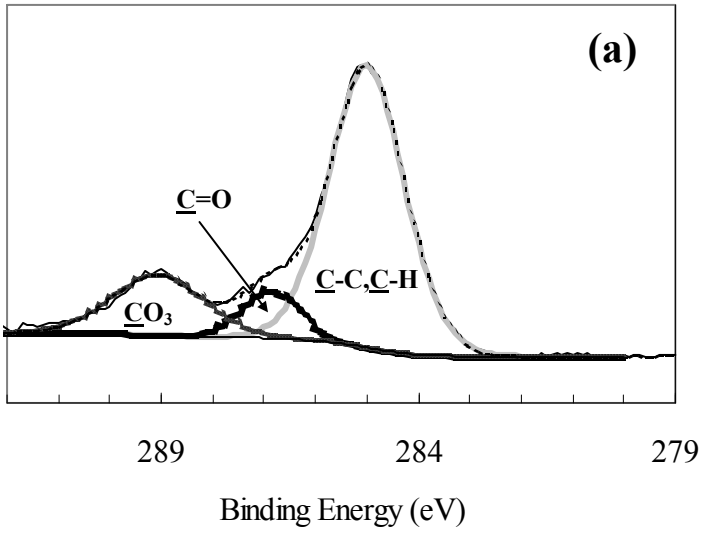

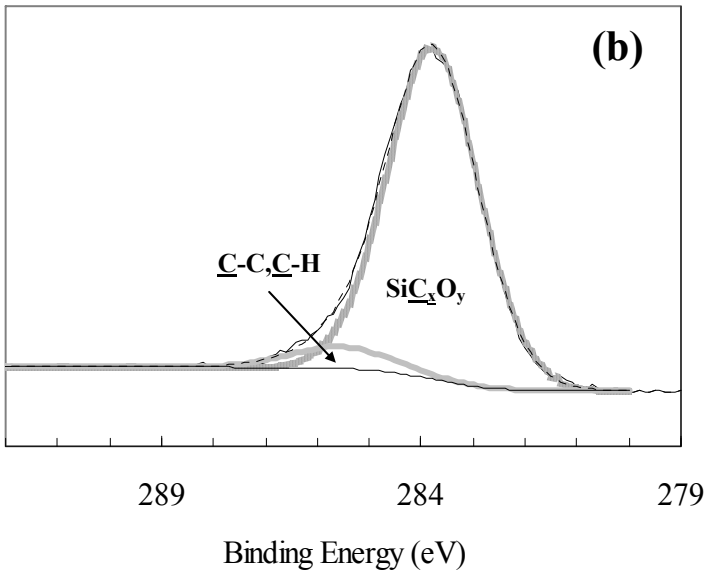

Fig. 4.11. C 1s core-level spectra the 1200 ^{o}C-nanofibers a) before and b) after 2500 sec of etching time.

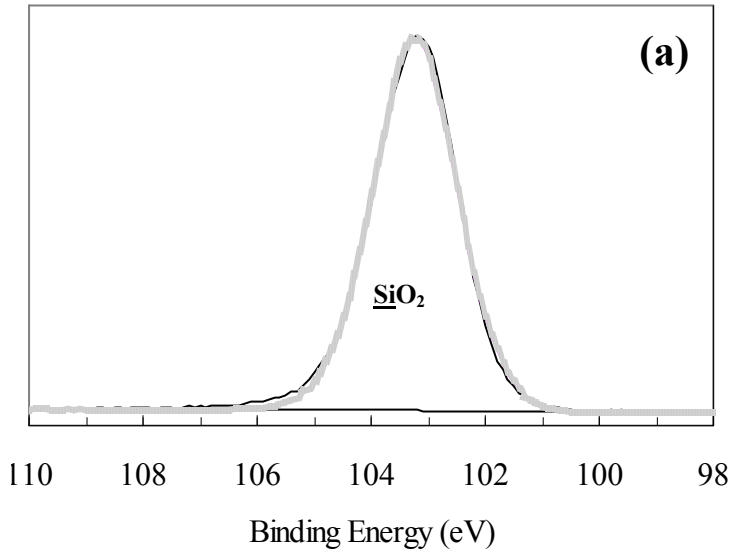

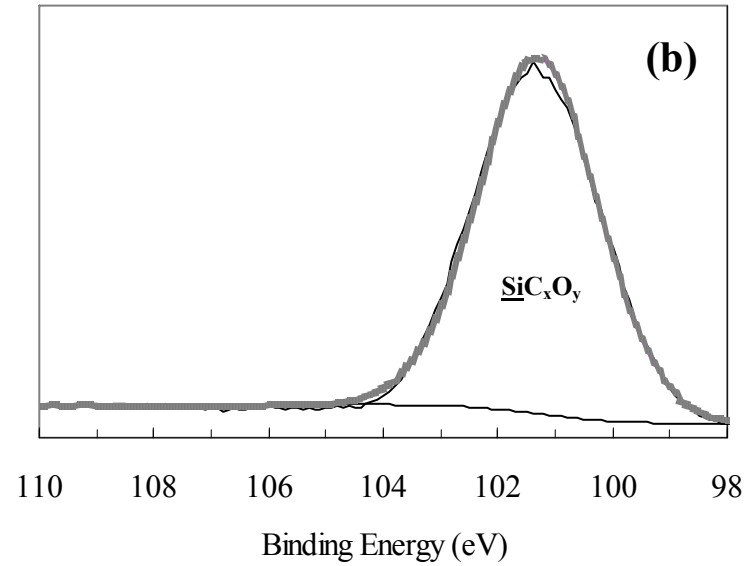

Fig. 4.12. Si 2p core-level spectra of the 1200 ^{o}C-nanofibers a) before and b) after 2500 sec of etching time.

Figure 4.13 shows XRD profiles of the nanofibers. Both the nanofibers showed very broad bands. The 1000 ^{o}C-nanofibers were expected to consist primarily of amorphous silicon dioxide, from Figure 4.7. It was not easy to deduce the structure of the 1200 ^{o}C-nanofibers, but the elemental composition shown in Figure 4.8 corresponded to an amorphous silicon oxycarbide.

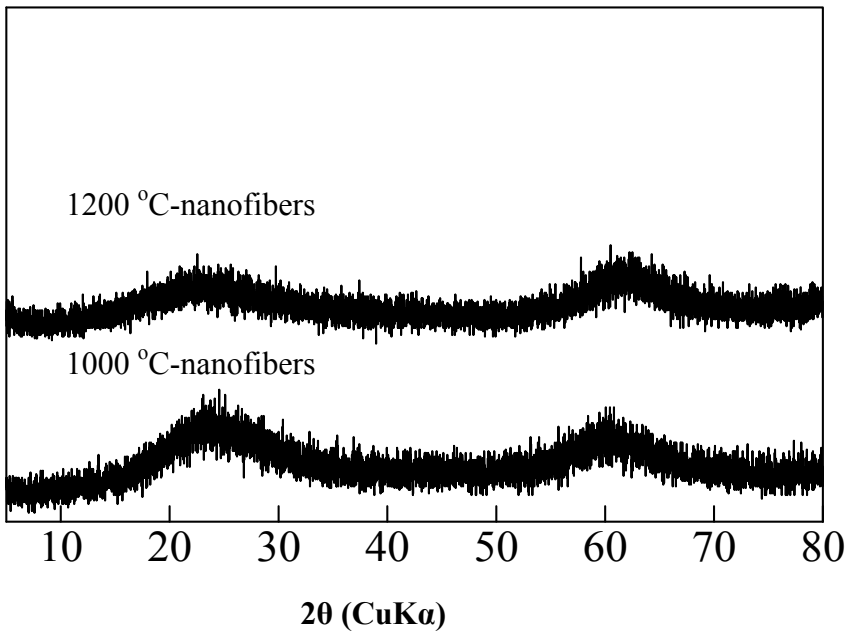

Fig. 4.13. XRD profiles of the 1000 ^{o}C-nanofibers and 1200 ^{o}C-nanofibers.

As stated above, the nanofibers were oxidized severely by nitric acid. It was quite reasonable to assume that pores were generated by this oxidation process. Figure 4.14 shows the adsorption/desorption isotherms for both types of nanofibers. Several important points were deduced from the isotherms. Micropores were formed in the 1000 ^{o}C-nanofibers more abundantly than in the 1200 ^{o}C-nanofibers. Both nanofibers

showed an increase in the adsorbed amount of nitrogen at high P/P_o, suggesting the presence of macropores. Minor hysteresis was observed between adsorption and desorption isotherms for these nanofibers. The specific surface areas (SSA), which are substantially dependent on micropore volume, were 288 m^2/g and 44 m^2/g for the 1000 ^oC-nanofibers and 1200 ^oC-nanofibers, respectively.

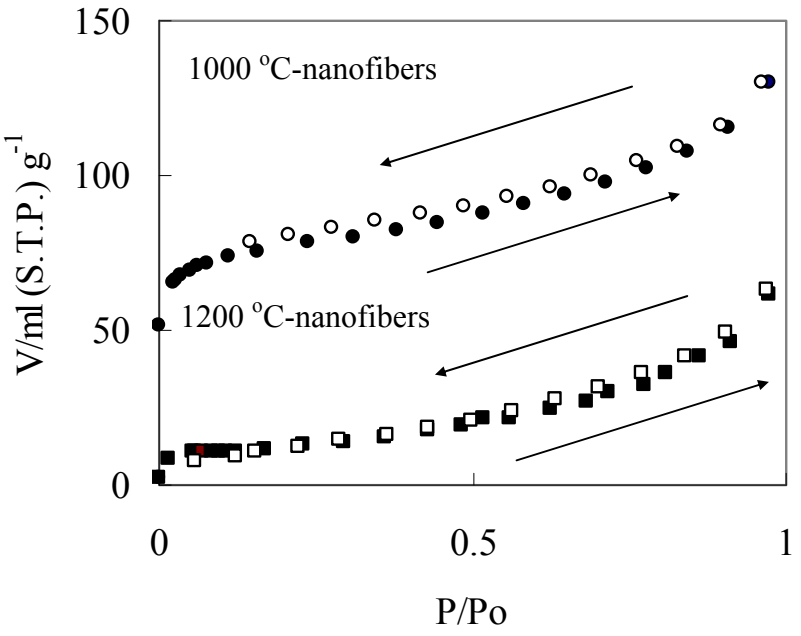

Fig. 4.14. N_2-absorption/desorption isotherms of the 1000 ^oC-nanofibers and 1200 ^oC-nanofibers.

The chemical compositions of the two different nanofibers were shown in Figures 4.7 and 4.8. Here the following point should be noted. As may be easily supposed, nanofibers in the vicinity of the blend fiber surface were likely released before those in the interior. The former nanofibers would therefore have been oxidized

for longer than the latter. Thus, the samples examined doubtless included nanofibers oxidized to varying degrees. It is difficult to evaluate from Figures 4.7 and 4.8 how severely the filaments were oxidized. Nevertheless, the significance of the temperature at which the blend fibers were heated was clear, as discussed below. The nanofibers will be evaluated from two points of view, namely with respect to defects and elemental composition. Defects will be discussed initially.

There were two kinds of defects in these nanofibers. One was the surface roughness of the nanofibers, easily recognized in the FE-SEM and the TEM photographs. It was clear from the photographs that nanofibers obtained from the blend fiber heated at 1200 ^{o}C had fewer defects and a smoother surface. Another defect was nitric acid-induced pores, which could be evaluated based on the SSA obtained by the adsorption/desorption isotherms. The nanofibers prepared from blend fibers heated at 1200 ^{o}C also had the smaller SSA. However, it is known that the high mechanical strength of commercially available PCS-derived Nicalon fiber is drastically reduced upon crystallization induced by heating to temperatures possibly higher than around 1350 ^{o}C [45]. This behavior would also be expected of the nanofibers in this study. It could be concluded, therefore, that in order to prepare high quality nanofibers by the present method, the blend fiber needed to be heated at the highest temperature possible without inducing crystallization, because PCS is transformed more completely to an inorganic material at higher temperature. In the present work, the optimum temperature for the heat treatment was settled as 1200 ^{o}C.

The next factor is the elemental composition of the nanofibers. The compounds

formed in PCS upon heating have been discussed in detail on the basis of XPS data. As stated above, however, the nanofibers prepared in the present work were individually subjected to varying degrees of oxidation, and it was impossible to know how severely the nanofibers shown in Figures 4.7 and 4.8 were oxidized. Consequently, only differences in elemental composition between the 1000 ^{o}C-nanofibers and the 1200 ^{o}C-nanofibers will be briefly discussed.

The 1000 ^{o}C-filaments shown in Figure 4.7 were severely oxidized, although the higher carbon content on the surface compared to the interior was curious, and the carbon content of just several % remained unchanged within the filaments interior. The elemental composition in Figure 4.7 suggested the existence of an amorphous compound with a composition relatively close to that of silicon dioxide. It is known that the oxygen in Nicalon fiber impairs mechanical properties at high temperature, because the oxygen is removed as CO gas, resulting in defects in the fiber [46].

In contrast to the above, the oxygen content in the 1200 ^{o}C-filaments decreased gradually from the surface to the interior. The C:Si:O ratio was 1:1:1, corresponding to silicon oxycarbide. The composition was unchanged above ca. 800 sec of etching time (corresponding to 144 nm for SiO_2). The oxygen content in the 1200 ^{o}C-nanofibers was far higher than the 13 atom% for Nicalon heated at 1200 ^{o}C [35]. Thus, decreasing the oxygen content in the present nanofibers is the major problem yet to be solved. Other open questions are why the elemental composition within filaments is constant and whether the carbon within the nanofibers can survive further oxidation. The results shown in Figures 4.7 and 4.8 clearly indicated that the blend fiber had to be heated to

the highest temperature to prepare nanofibers with high carbon content, by more complete transformation of PCS into oxidation-resistant inorganic material.

It is important to study the thermal stability of the nanofibers and the abundance of the gaseous species that evolved from the nanofibers on heating, in order to use them in composite materials for applications at high temperatures. To characterize the thermal behavior of the nanofibers, TG mass spectrum was recorded by heating up to 1000 ^{o}C in He. The TG curves are shown in Figures 4.15 and 4.16. The weight losses are 14.82 wt.% and 4.23 wt.% for the 1000 ^{o}C-nanofibers and 1200 ^{o}C-nanofibers, respectively. The weight loss was higher for the 1000 ^{o}C-nanofibers because of the higher porosity (Figure 4.14).

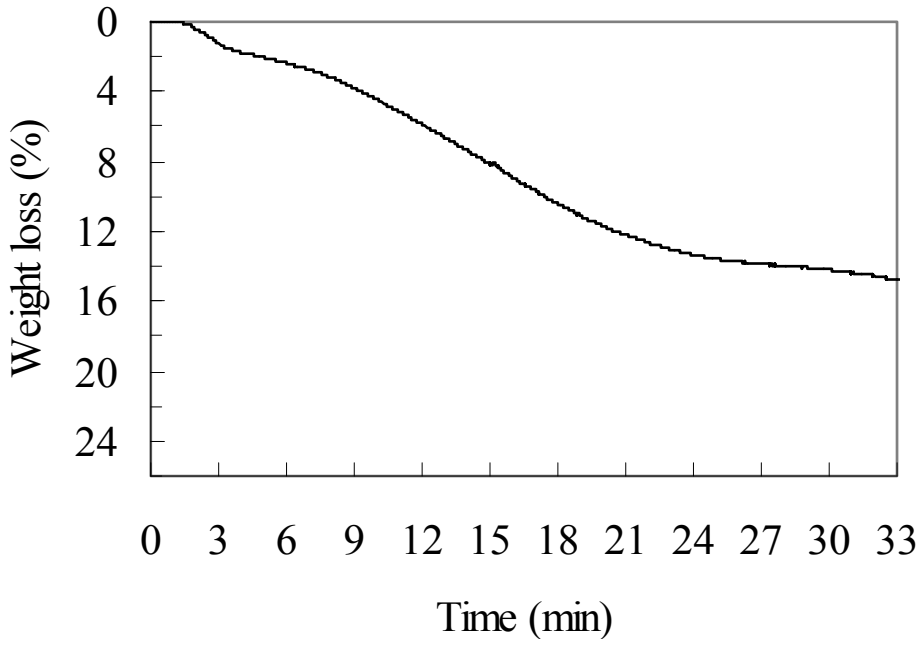

Fig. 4.15. TG curve of the 1000 ^{o}C-nanofibers in He.

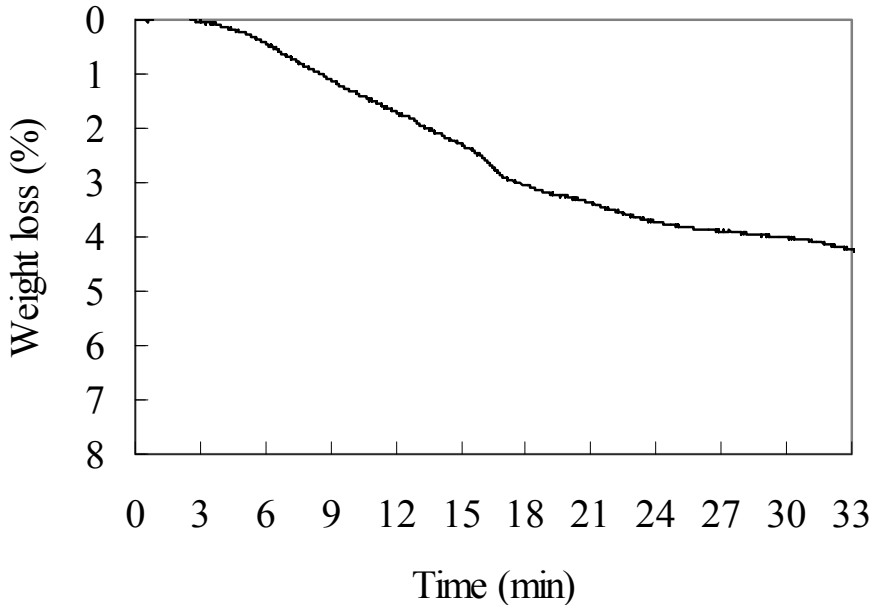

Fig. 4.16. TG curve of 1200 ^{o}C-nanofibers in He.

Figures 4.17 and 4.18 show the selected ion chromatograms (abundance vs. time) of the 1000 ^{o}C-nanofibers and 1200 ^{o}C-nanofibers. The main species identified are water (H_2O), carbon monoxide (CO) and carbon dioxide (CO_2), for both nanofibers.

The TG curve in Figure 4.15 for the 1000 ^{o}C-nanofibers shows a small weight loss up to 4 min due to evolution of water (120 ^{o}C) and then a weight loss is observed between 8 and 24 min (240-720 ^{o}C) due to evolution of CO and CO_2 as seen from Figure 4.17. The TG curve for the 1200 ^{o}C-nanofibers is shown in Figure 4.16. The TG curve showed a gradual weight loss up to 14 min due to evolution of water, CO and CO_2. A weight loss corresponding to CO_2 gas evolution is observed between 15 and 18 min (450-540 ^{o}C). This result is in agreement with the peak observed in the selected ion chromatograph in Figure 4.18.

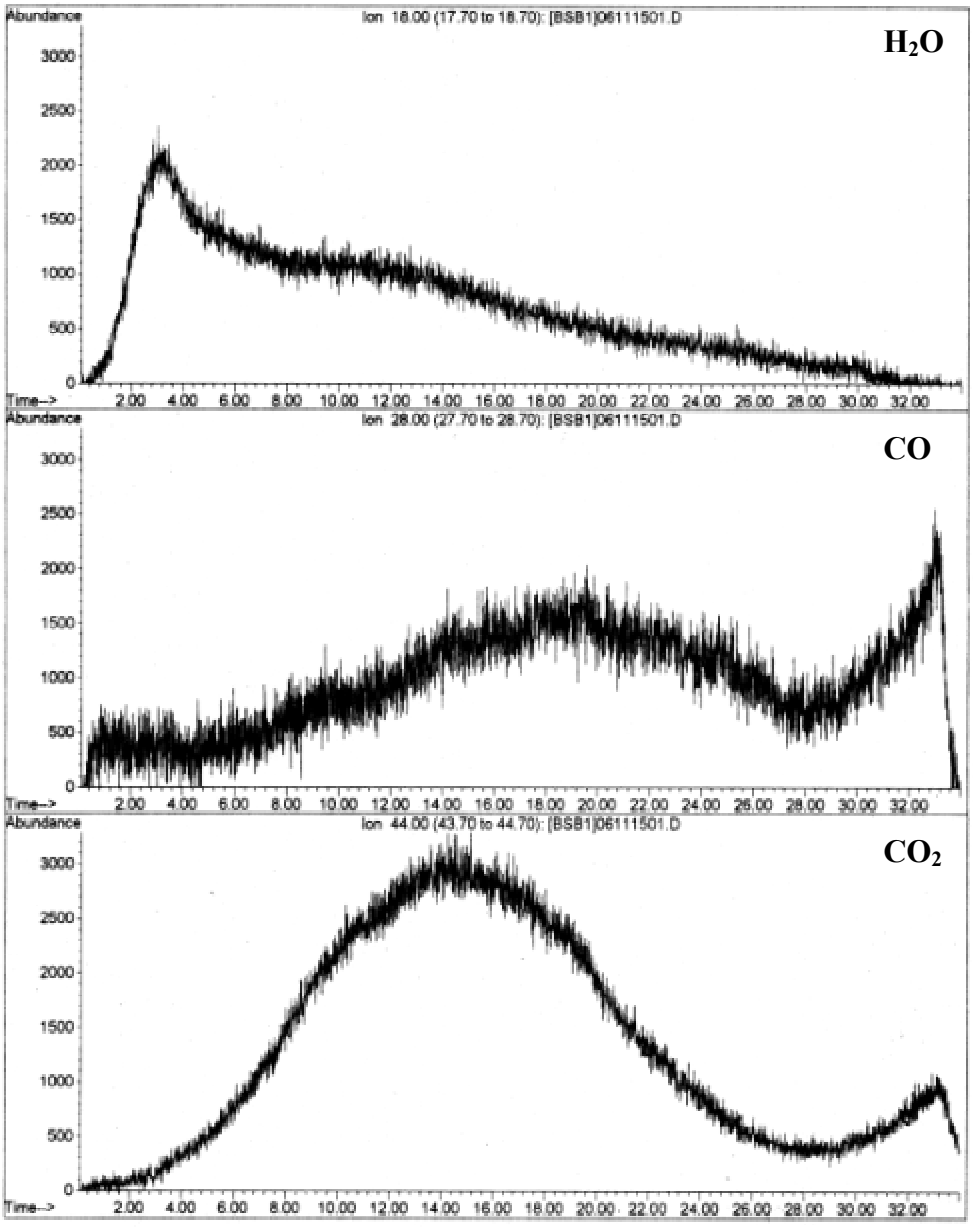

Fig.4.17. Ion chromatograms of the 1000 ^{o}C-nanofibers.

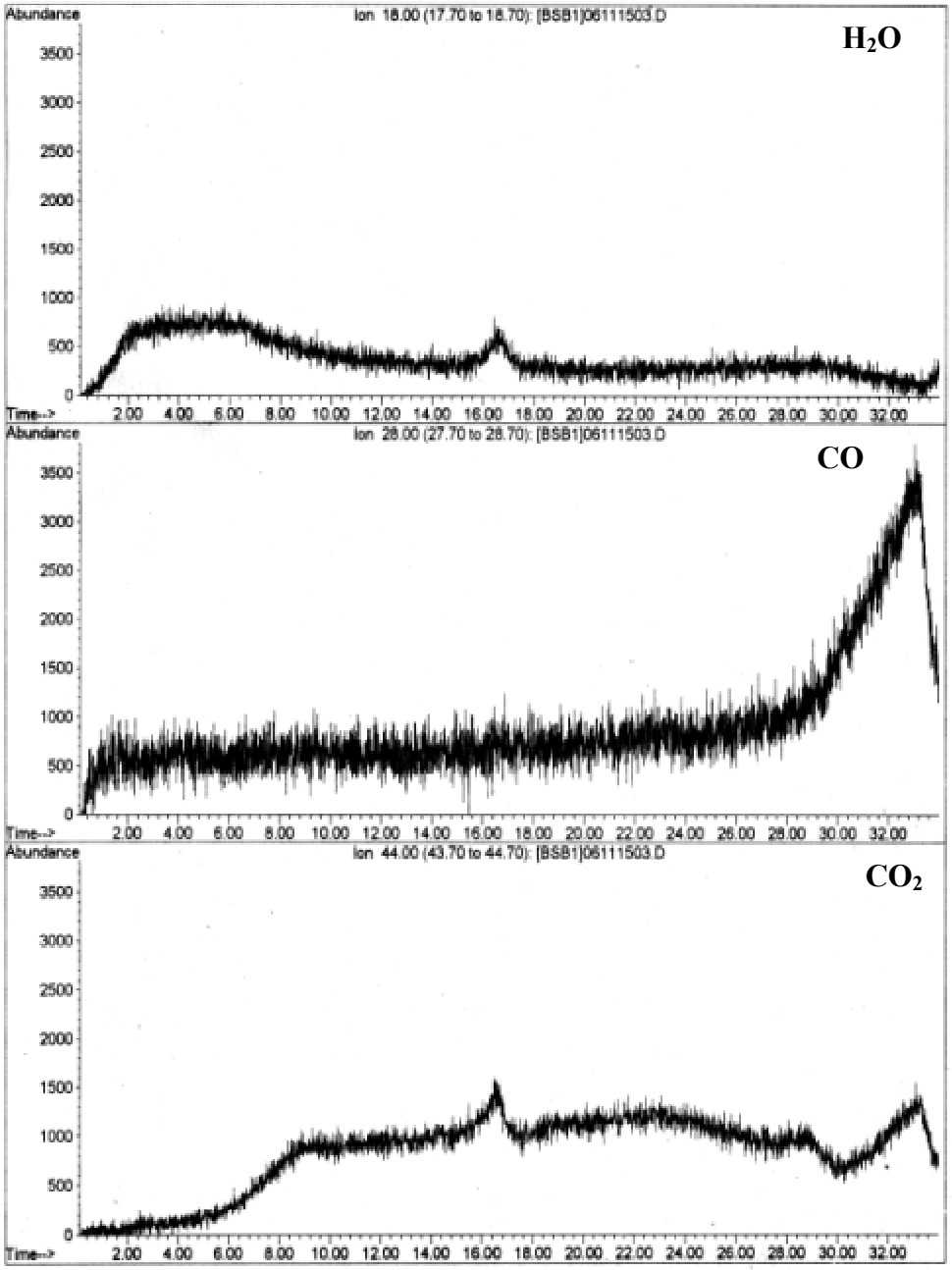

Fig.4.18. Ion chromatograms of the 1200 ^{o}C-nanofibers.

Gases species results from broken organic bonds. Carboxyl functional groups (C=O) in the surface of the nanofibers (evidenced in the XPS analysis) were released as CO or CO_2 on heating during the TG measurement. These groups were created during nitric acid treatment.

As stated above, the 1000 ^{o}C-nanofibers retained more the organic character of the PCS precursor polymer and some Si-CH_3 groups could still remain in the nanofibers. Small emissions of CH_4 were detected from the 1000 ^{o}C-nanofibers. The selected ion cromatogram is shown in Figure 4.19. The possible mechanism of methane gas generation is shown below.

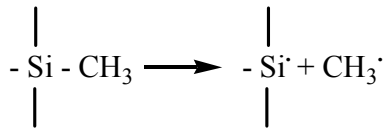

(1)

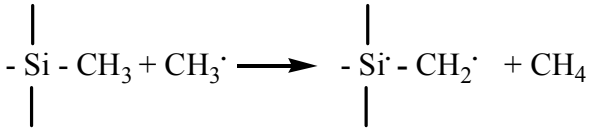

(2)

The elemental compositions were evaluated for the present nanofibers after nitric acid treatment but it will be interesting to examine the compositions of the nanofibers before the oxidation process in order to know the degree of conversion from the organic to the inorganic. Etching of the heat-treated fiber will revealed the details of the composition of the nanofibers before oxidation, but the time required for this measurement could be long.

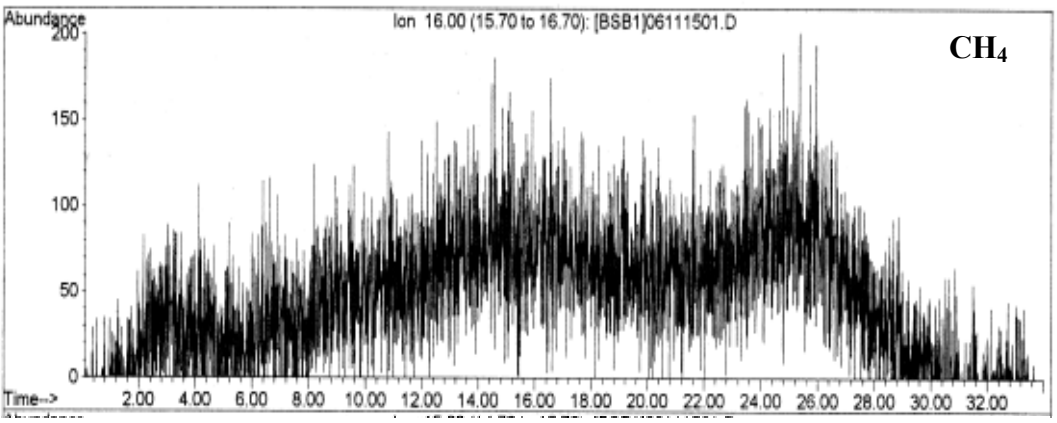

Fig.4.19. Ion chromatogram of the 1000 ^{o}C-nanofibers for CH_4.

4.4. Conclusions

Phenolic resin containing fine polycarbosilane particles was spun, stabilized and heat-treated at 1000 ^{o}C or 1200 ^{o}C in an inert atmosphere, followed by oxidation using nitric acid to remove the matrix carbon. The nanofibers thus formed were recovered and their structures were examined, focusing in particular on the effects of temperature during the heat treatment step. The 1200 ^{o}C-nanofibers showed higher oxidation resistance, and had a smoother fiber surface than did the 1000 ^{o}C-nanofibers. The high oxidation resistance of the 1200 ^{o}C-nanofibers gave rise to a smaller specific surface area of 44 m^2/g against 288 m^2/g for the 1000 ^{o}C-nanofibers. Quantitative elemental analysis using XPS showed that the 1200 ^{o}C-filaments contained about 30 at. % carbon, whereas the carbon content of 1000 ^{o}C-filaments were just a few %. High-temperature heating was required to prepare highly oxidation resistant nanofibers.

The preparation of nanotubes from two different silicon carbide polymer precursors, PDMSVA and PCS, was attempted in chapters 1 and 2. The stretching technique and the stabilization process must be improved in order to increase the nanotube yield. The polymer blend technique was used and therefore seems to be a good candidate for mass-scale production of nanostructures.

In chapters 3 and 4, nanofibers of several 100 nm in diameter and more than 100 μm in length were prepared. However, a large amount of oxygen was incorporated in their structure. The nanofibers must be heat-treated at the highest temperature without crystallization in order to have higher resistance to oxidation by nitric acid. However, decreasing the oxygen content of the nanofibers is the most important problem to be solved.

References

[1] J. Huheey, R. Keiter and E. Keiter. *Inorganic Chemistry. Principles of Structures and Reactivity*, Harper Collins College Publishers, New York, USA, A-30 (1993)

[2] S. Pawlenko. *Organosilicon Chemistry*, Walter de Gruyter & Co., Berlin, Germany, p. 7-8 (1986)

[3] A. W. Weimer. *Carbide, Nitride and Boride Materials. Synthesis and Processing*, Chapman & Hall, London, UK, p. 14-15, 46, 436, 525-526 (1997)

[4] S. Yajima, Y. Hasegawa, J. Hayshi and M. Iimura, *J. Mater. Sci.* **13**, 2569-2576 (1978)

[5] R. Jones, W. Ando and J. Chojnowski. *Silicon-Containing Polymers. The Science and Technology of Their Synthesis and Applications*, Kluwer Academic Publishers, Dordrecht, The Neetherlands, p.247-248, 267-268 (2000)

[6] S. Iijima, *Nature* **354**, 56-58 (1991)

[7] N. Chopra, R. Luyken, K. Cherry, M. Cohen, S. Louie and A. Zettl, *Science* **269**, 966-967 (1995)

[8] A. Loiseau, F. Willaime, N. Demoncy, G. Hug and H. Pascard, *Phys. Rev. Lett.* **76**, 4737-4740 (1996)

[9] D. Goldberg, Y. Bando, W. Ahn, K. Kurashima and T. Sato, *Chem. Phys. Lett.* **308**, 337-342 (1999)

[10] C. Pham-Huu, N. Keller, G. Ehret and M. Ledoux, *J. Catal.* **200**, 400-410 (2001)

[11] N. Keller, C. Pham-Huu, G. Ehret, V. Keller and M. Ledoux, *Carbon* **41**, 2131-2139 (2003)

[12] X. Sun, C. Li, W. Wong, N. Wong, C. Lee, S. Lee and B. Teo, *J. Am. Chem. Soc.* **124,** 14464-14471 (2002)

[13] M. Rümmeli, E. Borowiak-Palen, T. Gemming, M. Knupfer, K. Biedermann, R. Kalenczuk and T. Pichler, *Appl. Phys. A* **80**, 1653-1656 (2005)

[14] Silicon Carbide Nanotube Synthesized, http://www.grc.nasa.gov

[15] Q. Cheng, L. Interrante, M. Lienhard, Q. Shen and Z. Wu, *J. Eur. Ceram. Soc.* **25,** 233-241 (2005)

[16] G. Mpourmpakis, G. Froudakis, G. Lithoxoos and J. Samios, *Nano Lett.* **6**, 1581-1583 (2006)

[17] Y. Morisada and Y. Miyamoto, *Mat. Sci. and Eng. A* **381**, 57-61 (2004)

[18] J. Hulteen and C. Martin, *J. Mater. Chem.* **7**, 1075-1087 (1997)

[19] Y. Hasegawa, M. Iimura and S. Yajima, *J. Mater. Sci.* **15**, 720-728 (1980)

[20] H. Ichikawa and M. Takeda, Invited Lecture, *9th Cimtec-World Forum on New Materials,* Symphosium V-Advanced Structural Fiber Composites. Techna Srl (1999)

[21] G. Chollon, M. Czerniak, R. Pailler, X. Bourrat, R. Naslain, J. Pillot and R. Cannet, *J. Mater. Sci.* **32**, 893-911 (1997)

[22] S. Honda, Y. Baek, T. Ikuno, H. Kohara, M. Katayama, K. Oura and T. Hirao, *Appl. Surf. Sci.* **212-213**, 378-382 (2003)

[23] A. Huczko, M. Bystrzejewski, H. Lange, A. Fabianowska, S. Cudzilo, A. Panas and M. Szala, *J. Phys. Chem. B* **109**, 16244-16251 (2005)

[24] V. Raman, G. Bathia, S. Bhardwaj, A. Srivastva and K. Sood, *J. Mater. Sci.* **40**, 1521-1527 (2005)

[25] Y. Hao, G. Jin, X. Han and X. Guo, *Mater. Lett.* **60**, 1334-1337 (2006)

[26] K. Tenmoku, Master's Thesis, Gunma University (2003)

[27] W. Han, S. Fan, Q. Li, W. Liang, B. Gu and D. Yu, *Chem. Phys. Lett.* **265**, 374-378 (1997)

[28] H. Lai, N. Wong, X. Zhou, F. Au, N. Wang, I. Bello, C. Lee and S. Lee, *Appl. Phys. Lett.* **76**, 294-296 (2000)

[29] M. Tello, R. Garcia, J. Martin-Gago, N. Martinez, M. Martin-Gonzalez, L. Aballe, A. Baranov and L. Gregoratti, *Adv. Mater*.**17**, 1480-1483 (2005)

[30] H. Ye, N. Titchenal, Y. Gogotsi and F. Ko, *Adv. Mater*.**17**, 1531-1535(2005)

[31] D. Zhou and S. Seraphin, *Chem. Phys. Lett.* **222**, 233-238 (1994)

[32] X. Li, L. Liu, Y. Zhang, Sh.D. Shen, Sh. Ge and L. Ling, *Carbon* **39**, 159-165 (2001)

[33] D. Hulikova, K. Hosoi, S. Kuroda, H. Abe and A. Oya, *Adv. Mater.* **14**, 452-455 (2002)

[34] Y. Hasegawa, *J. Mater. Sci.* **24**, 1177-1190 (1989)

[35] E. Bouillon, D. Mocaer, J. Villeneuve, R. Pailler, R. Naslain, M. Monthioux, A. Oberlin, C. Guimon and G. Pfister, *J. Mater. Sci.* **26**, 1517-1530 (1991)

[36] D. Hulikova and A. Oya, *Carbon* **41**, 1443-1450 (2003)

[37] H. Ichikawa, F. Machino, S. Mitsuno, T. Ishikawa, K. Okamura and Y. Hasegawa, *J. Mater. Sci.* **21**, 4352-4358 (1986)

[38] J. Zeigler and F. Gordon. *Silicon-Based Polymer Science. A Comprehensive Resource*, American Chemical Society, Washington, USA, p. 48, 565, 570 (1990)

[39] F. Lamouroux, X. Bourrat, R. Naslain and J. Sevely, *Carbon* **31**, 1273-1288 (1993)

[40] A. Chapman, S. Bleay and V. Scott, *J. Mater. Sci.* **29**, 4523-4534 (1994)

[41] C. Fyfe, A. Rudin and W. Tchir, *Macromolecules* **13**, 1320-1322 (1980)

[42] L. Sawyer, M. Jamieson, D. Brikowski, M. Haider and R. Chen, *J. Amer. Ceram. Soc.* **70**, 798-810 (1987)

[43] T. Shimoo, I. Tsukada, M. Narisawa, T. Seguchi and K. Okamura, *J. Ceram. Soc. Japan* **105**, 559-563 (1997)

[44] J. Rubio, F. Rubio and J. Otelo, *J. Mater. Sci.* **26**, 2841-2845 (1991)

[45] N. Hochet, M. Berger and A. Bunsell, *J. of Microsc.* **185**, 243-258 (1997)

[46] T. Shimoo, H. Chen and K. Okamura, *J. Mater. Sci.* **29**, 456-463 (1994)

List of Publications and conferences proceedings

Publications

Z. Correa, T. Sandou, C. Ida and A. Oya. *Preparation of double-layered nanotubes consisting of an inner carbon layer and outer silicon carbide layer by elongation of core-shell polymer particles.* Tanso **225**, 336-339 (2006)

Z. Correa, H. Murata, T. Tomizawa, K. Tenmoku, A. Oya. *Preparation of SiC Nanofibers by Using the Polymer Blend Technique.* Advances in Science and Technology **51**, 60-63 (2006)

Z. Correa, C. Ida and A. Oya. *Structure of nanofibers derived from polycarbosilane using the polymer blend technique.* (Accepted for publication) Tanso **227** (2007)

Conferences Proceedings

Z. Correa, H. Murata, T. Tomizawa, A. Oya. *Preparation of SiC nanofibers by use of polymer blend technique (2).* Proceedings of 32th Japanese Carbon Society Conference, p. 52-53; Nagano, Japan, December 7-9 (2005)

Z. Correa, T. Hashimoto, K. Sunada, Y. Mashiko, A. Oya. *Silicon Carbide Nanotubes Based in Polymer Blend Technique.* Proceedings of 31th Japanese Carbon Society Conference, p. 362-363; Kochi, Japan, December 1-3 (2004)

Acknowledgements

This thesis is a result of much effort and contributions from many people who supported me□

First I would like to thank God for giving me strength and the power to believe in myself.

I am very thankful to my advisor, Professor Asao Oya, for his support and guidance.

Also I would like to express my gratitude to Associate Professors Jun-ichi Ozaki and Soshi Shiraishi for their kindness and help.

Special thanks to Mrs. Chiemi Ida who gave me invaluable help in the laboratory.

I am very grateful to Professor Barry Keith for his help regarding my English.

Thanks to all my lab-mates who always helped me when I needed assistance.

Special thanks to my mother, grandmother and aunt and my dear family for their support and their infinite love.

Finally, thank you to my dearest friends that always care about my studies and about my life in Japan.